LIGNIN AND CELLULOSE NANOFIBERS ENHANCED CORN-BASED

THERMOPLASTIC COMPOSITES

A Thesis
Submitted to the Graduate Faculty
of the
North Dakota State University
of Agriculture and Applied Science

By

Yanlin Chen

In Partial Fulfillment of the Requirements
for the Degree of
MASTER OF SCIENCE

Major Program:
Materials and Nanotechnology

July 2021

Fargo, North Dakota

North Dakota State University
Graduate School

Title

Lignin and Cellulose Nanofibers Enhanced Thermoplastic Corn-based Composites

By

Yanlin Chen

The Supervisory Committee certifies that this ***disquisition*** complies with North Dakota

State University's regulations and meets the accepted standards for the degree of

MASTER OF SCIENCE

SUPERVISORY COMMITTEE:

Dr. Long Jiang

Chair

Dr. Chad Ulven

Dr. Mohi Quadir

Approved:

07/22/2021	Dr. Erik Hobbie
Date	Department Chair

ABSTRACT

The goal of this project is to develop biobased thermoplastics and composites using corn as the main raw material. Corn contains mainly starch, zein, and oil. Thermoplastic starch/zein blends were prepared through internal mixing and extrusion. Lignin was used as a compatibilizer to refine the phase structure of the blend and increase the mechanical properties of the product. Scanning electron microscopy study showed that the incorporation of lignin significantly reduced the domain size of the zein phase in the blends. Modulus and tensile strength of the blend were increased greatly. Thermogravimetric analysis showed that the thermal stability of the blends was slightly improved after the incorporation of lignin. Cellulose nanofibrils (CNFs), a biobased nanomaterial, were also tested as a reinforcement for the blend. The incorporation of CNFs further enhanced the modulus and strength of the blends, suggesting a strong synergy between lignin and CNFs in reinforcing the corn-based thermoplastics.

ACKNOWLEDGEMENTS

TABLE OF CONTENTS

LIST OF TABLES

LIST OF FIGURES

LIST OF ABBREVIATIONS

G..Glycerol

EG ....EG

CA ....Citric acid

LP ....Lignin powder

LS..Lignin solution

SZ..Starch-zein

CM ....Cornmeal

DSL..Dynamic light scattering

SEM ....Scanning electron microscopy

XRD ....X-ray diffraction

FTIR..Fourier-transform infrared spectroscopy

TGA ....Thermogravimetric analysis

DTG ....Derivative thermogravimetry

PE..Polyethylene

PEO..Poly (ethylene oxide)

CNF..Cellulose nanofibril

PLA..Polylactic acid

TPS..Thermoplastic starch

KL ....Kraft lignin

LCNF ....Lignin-containing cellulose nanofibrils

AA..Adipic acid

AASM..Adipic acid modified starch

GO..Graphene oxide

TPZ ....Thermoplastic zein

LSS..Sodium lignosulfonate

AL ....Alkaline lignin

PEG..Polyethylene glycol

SPI..Soy protein isolate

WG...Wheat gluten

FDM...Fused deposition modeling

3D...Three dimensional

LO ....Organosolv lignin

LB ....Lignoboost® lignin

KLP ....Phosphorylated kraft lignin

UPe...Unsaturated polyester

KLP ....Phosphorylated kraft lignin

PVA..Polyvinyl alcohol

Ch...Chitosan

LNPs ....Lignin nanoparticles

EDS...Energy dispersive spectroscopy

GC...Glycerol system control sample

EGC...Ethylene glycol system control sample

CMC..Cornmeal control sample

SZC ....Starch-zein control sample

LIST OF SYMBOLS

NaOH ....Sodium hydroxide

Na_2S ....Sodium sulfuret

HSO^{3-} ....Hydrogen sulfite

SO_3^{2-} ....Sulfite

pH..potential of hydrogen

$ZnCl_2$ ....Zinc chloride

CO ....Carbon monoxide

CO_2..Carbon dioxide

Mw ....Molecular weight

LIST OF APPENDIX TABLES

LIST OF APPENDIX FIGURES

1. INTRODUCTION

1.1. Problem Statement and Research Motivation

The history of modern corn started at the beginning of human agriculture about 10,000 years ago in Mexico[1]. Over thousands of years' selective breeding, a broad variety of corn have been created and the crop has become a staple food in many parts of the world. In North America, more than 90 million acres of land are used to grow corn and most of them are in the Heartland region. 14.2 billion bushels of corn was produced in the US in 2020.[2] The two largest uses of corn in the US are for ethanol production and animal feed, accounting for 44% and 25% of the total corn consumption, respectively[3]. The supply-and-demand condition of corn in recent years has kept the crop at a low price - the monthly average corn price from 01/2015 to 01/2021 is $3.55 per bushel (USDA World Agricultural Supply and Demand Estimates, 5/28/2021).

Developing new uses for corn is an effective method to increase the consumption and the value of the crop. Large-scale new uses can significantly increase market demand for corn and potentially boost corn price and increase the income of corn producers. Currently, corn and corn products (i.e., starch and zein) only have a niche market in the plastic resin industry. The major drawbacks that prevent the materials from being a mainstream resin are the low mechanical strength and low water resistance of starch and zein. As a result, they are usually blended with other traditional resins to become a minor component in the blends, which greatly limits corn's usage. To increase the consumption of corn, new resin that consists of primarily of corn materials and possesses improved mechanical properties and water resistance needs to be developed.

An earlier study proved that thermoplastic starch–zein blends showed stronger water resistance than thermoplastic starch due to the insolubility of zein in water[4]. However, more

recent studies demonstrated that the starch–zein blends exhibited poor mechanical properties because of the incompatibility between the two phases, resulting in poor stability of the resulting material[5,6,7,8].

Cellulose and lignin are the two most abundant biopolymers on earth. Lignin's functional groups, including phenolic and aliphatic hydroxyl, carbonyl, carboxylic, and methoxyl groups, can interact with many polymer matrixes and lead to improved compatibility, interfacial bonding, and composite properties[9,10,11,12]. Cellulose nanofibrils (CNFs) exhibit high crystallinity, high aspect ratio, outstanding mechanical properties, low density, and a large number of surface functional groups[13,14,15]. They have been shown to be a highly effective reinforcement material for many polymers.

1.2. Research Objectives

The goal of this research is to develop a novel corn-based plastic resin in which corn materials including starch and zein are the major components. The hypothesis of this study is that lignin can function as a compatibilizer in the resin system to increase the compatibility between the components of the resin and CNFs are able to reinforce the resin as nanofibers, and the two materials act synergistically to improve the mechanical properties and water resistance of the resin. Three specific objectives are designed for this research to achieve the project goal.

- Develop starch-zein based plastics which is potentially biodegradable[16]
- Improve processability, phase morphology, and mechanical properties of the starch-zein composites with citric acid
- Develop low-cost cornmeal-based thermoplastics

This thesis consists of 5 chapters. Chapter 1 discusses the research motivation and research goal of this project. Chapter 2 provides background information in about the biopolymers used in the project including starch, zein, lignin, cellulose nanofibrils, and corn related composites. Chapter 3 details the development of starch-zein thermoplastic containing lignin and cellulose nanofibrils using an internal mixer. Chapter 4 explores water-free starch-zein thermoplastic using twin-screw extrusion. Citric acid was incorporated to improve the processability of the formulation. In Chapter 5 starch and zein were replaced with low-cost cornmeal to drive down the cost of the resin. Chapter 6 summarizes the findings and results from this research and recommends future research tasks.

2. BACKGROUND

In recent years, there has been an increased interest in producing renewable materials due to the significant environmental impacts of producing and disposing of petroleum-based polymers[17]. Corn-derived materials including starch, zein, and polylactic acid (PLA), can be attractive materials for applications such as food packaging, mulch, plant pots, utensils, and other household and industrial items. Their potential to replace some petroleum-based polymers has been recognized and has been widely studied[18,19,20,21,22,23,24]. According to USDA World Agricultural Supply and Demand Estimates (10 Jan 2021), corn production is estimated to be 13.692 billion bushels in 2021 and the total corn use is up to 14.070 billion bushels.

Corn kernels contain mainly starch (62%), zein (7.8%), oil (3.8%), ash (1.2%), and others. As shown in Figure 2.1, the major parts of the corn kernel are the endosperm and the germ. Most of the corn starch is presented in the endosperm, while most of the corn protein and oil are located in the kernel germ.
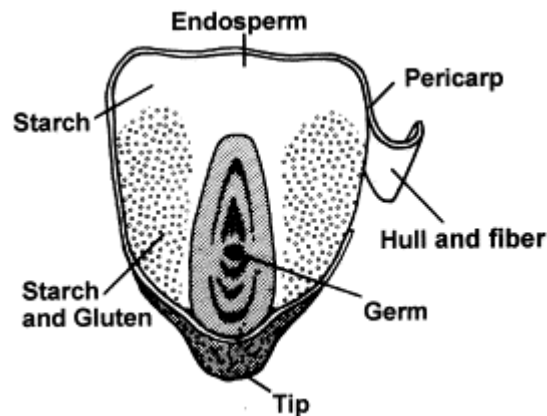
Figure 2.1. Cross-section of corn kernel showing location of major components[25].

2.1. Starch and Thermoplastic Starch

Starch, the second-largest biomass produced, is one of the most studied and used natural polymers. Starch has major applications in the food industry, packaging, adhesives, paper, and

biocomposites because of its renewability, sustainability, and low-cost[26,27,28,29,30]. Starch is the source of stored energy for many plants such as stalks, crop seeds, rice, corn, wheat, tapioca and potato[31]. Corn is the world's main source of starch, and its percentage is up to 82%[31]. Starch is a physical combination of branched and linear polymers, i.e., amylose and amylopectin, respectively. As shown in Table 2.1, the weight percentage of amylopectin varies between 65% and 83.3% from different starch sources and the amylose ranges from 16.7 to 35%.

Table 2.1. Amylose and amylopectin concentration of various starch source[32].

Source	Amylose (in %)	Amylopectin (in %)
Arrowroot	20.5	79.5
Banana	17	83
Cassava	18.6	81.4
Corn	28	72
Potato	17.8	82.2
Rice	35	65
Tapioca	16.7	83.3
Wheat	20	80

Amylose is defined as a linear molecule of (1→4) linked α-d-glucopyranosyl units, but it is today well established that some molecules are slightly branched by (1→6)-α-linkages. Amylopectin, the major component of most starches, is highly branched. It consists of a great number of shorter chains which is formed through chains of α-d-glucopyranosyl residues linked together mainly by (1→4) linkages but with 5–6% of (1→6) bonds at the branch points (Figure 2.2)[33,34].
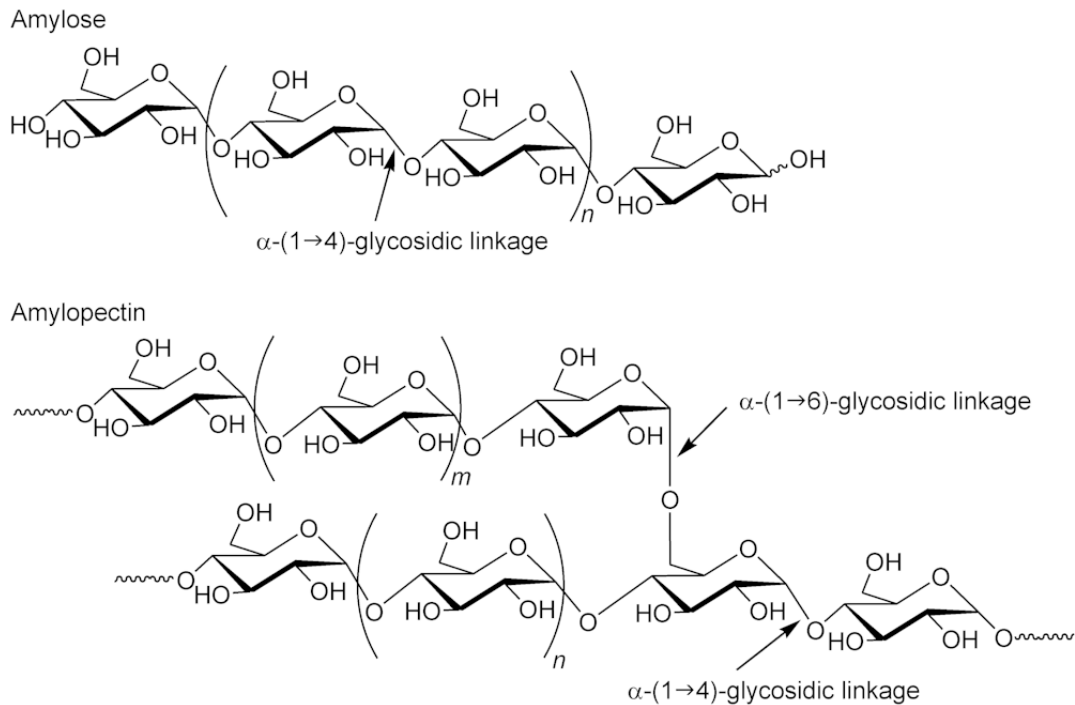
Figure 2.2. Structures of amylose and amylopectin[34].

Although there are still debates about the distribution of the ordered and unordered regions in starch granules and the contribution of amylose and amylopectin to starch crystallinity, Figure 2.3 shows a generally accepted structure of the starch granules[33,35].

In the presence of plasticizer, including water, polyols and chemicals containing amide groups (e.g. glycerol, glycol, sorbitol, formamide, acetamide and urea), the hydrogen bonds between the plasticizer and starch molecules can be formed under high temperature and shear, and the crystalline structure or the strong intermolecular and intramolecular hydrogen bonds in the starch granules are ruptured[36,37,38,39,40,41,42]. As a result, semi-crystalline starch behaves like a thermoplastic polymer, allowing the material (termed thermoplastic starch or TPS) to be processed through injection molding, extrusion, and blow molding, in ways similar to conventional synthetic thermoplastic polymers[17,36,43]. However, due to the hydrophilic property of starch, TPS is very sensitive to humidity and heat. Thus, TPS is rarely used alone because of its low mechanical properties and poor moisture resistance. It is often blended with hydrophobic

thermoplastic polymers, such as polyethylene, polypropylene, PLA, poly(ethylene-co-vinyl alcohol), and polyvinyl alcohol to improve its performance[21,44,45,46,47,48].
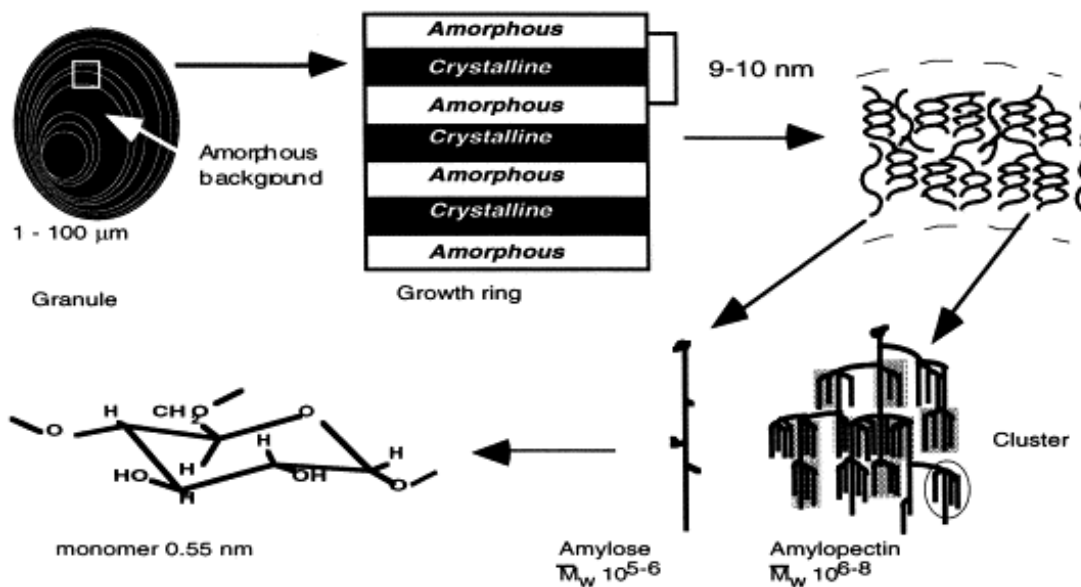
Figure 2.3. Schematic representation of the different structural levels of the starch granule and the involvement of amylose and amylopectin[33].

Corn starch has wide applications and can be used in many areas including medical applications, industrial uses, and baby care products (Figure 2.4). In the medical field, it can be used as anti-stick agent and wound dressing for relieving rashes and treating gastric dumping syndrome. Industrial uses include cleaning agent, fabric stiffer, organic pesticides, and fast absorbent polymers in water management facilities. In baby care products, starch is used as a safe alternative to talcum baby powder and the agent to relieves itchiness due to its non-toxicity.

In the plastic industry, corn starch is also combined with natural polymers (such as cellulose, chitosan, gelatin, polylactic acid, proteins, collagen, glycerol, etc.) using different methods such as extrusion, casting and melt electrospinning as a filler or TPS[50,51]. The corn starch-based composites are used in the packaging, biomedical, and agriculture fields (Table 2.2).
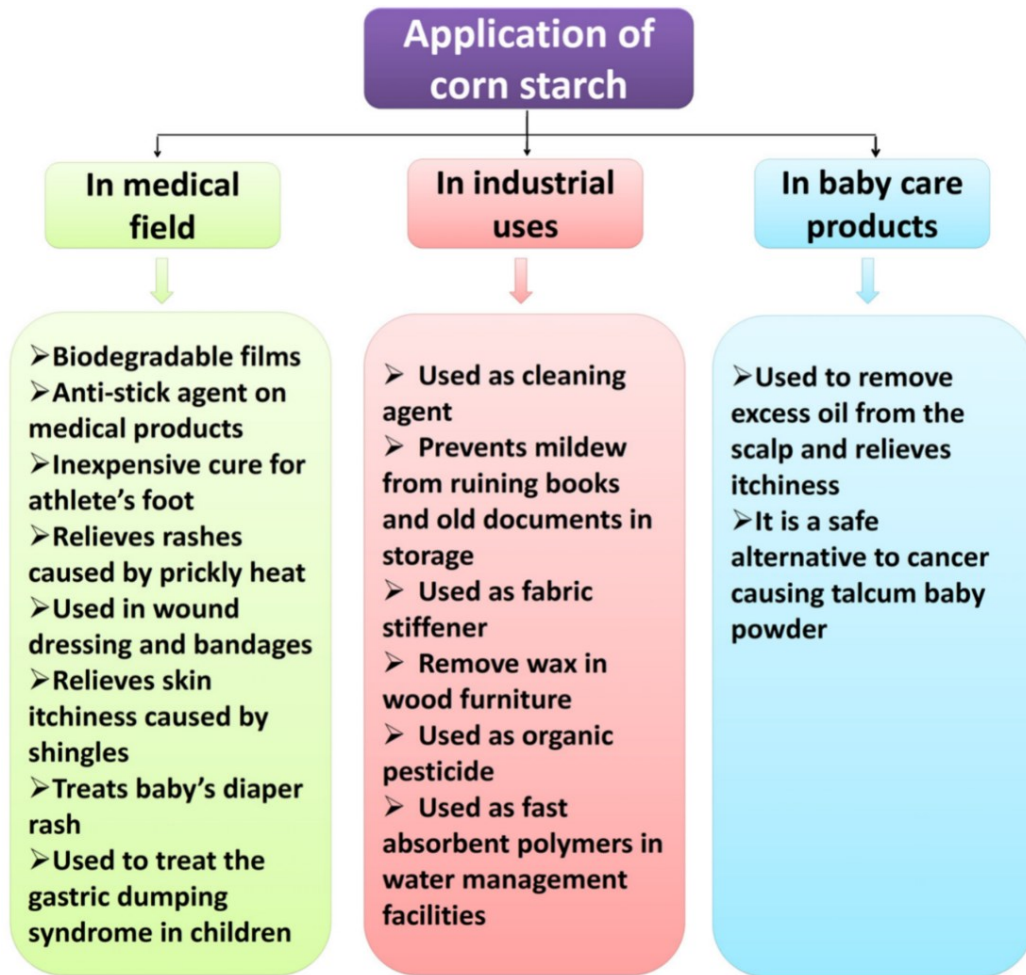
Figure 2.4. Different applications of corn starch[49].

Table 2.2. Combination of corn starch with natural polymers, method of preparation, and their applications[49].

No.	Corn Starch Combination with	Method of Preparation	Size of the Particles	Applications
1	Cellulose	Nanobiocomposite: Electrospun method	100 μm	Food packaging
		Biocomposite films	80 μm	Industrial relevance
		Biocomposite films	100 μm	Packaging applications
2	Chitosan	Biodegradable polymer blends: Extrusion	50 μm	Production of packaging materials
		Crosslinked microparticles	20 μm	Packaging materials
		Biocomposite films	10–20 μm	Food and pharmaceutical packaging applications
3	Gelatin	Nanobiocomposite	10 μm	Food and pharmaceutical applications
		Polymer matrix: Twin-screw extrusion and compression molding	20–50 μm	Food and pharmaceutical applications
		Biocomposite films	50 μm	Applications in edible food packaging
		Microcapsule composite: Glass-filament single droplet dying method	50 μm	Food and pharmaceutical applications
4	Alginate	Agglomerated beads by dripping method	100 μm	Biomedical applications: Control the structure and function of the engineered tissue
		Hydrogel beads: Peristaltic pump	100 μm	Protect and deliver yerba mate antioxidants into food products
		Microparticles: External ionic gelation technique	10–40 μm	Pharmaceutical applications
5	Polylactic acid	Nanocomposite Blends	50–200 μm	Applications in packaging, biomedical, and agriculture fields
		Nanocomposite microfibers: Melt electrospinning method	200–500 μm	Biomedical applications
		Nanocomposite blends: Extrusion molding	100 μm	Biomedical applications
		Bionanocomposite: Extrusion method	100 μm	Applications in packaging, biomedical, and agriculture field
6	Proteins	Bionanocomposite: Extrusion method	10–100 μm	Health and medicinal applications
		Cooled pastes	20 μm	Enhancing the quality of starch-based food products including buttermilk or salad dressings
		Biodegradable film blends: Extrusion	10–00 μm	Innovation for application as a packaging material
7	Collagen	Biodegradable film	20–50 μm	Applications in bioengineering and biomedicine fields
8	Fatty acid	Biodegradable film	10–60 μm	Application as a packaging material
9	Glycerol	Biodegradable paste	20–50 μm	Used as a thickener, gelling agent, bulking agent, and water retention agent
		Bionanocomposite: Reinforcing method	5–100 μm	Biomedical applications
10	Microalgae	Biodegradable film	20–100 μm	Biomedical applications
11	Seaweeds	Biodegradable film	50–100 μm	Biomedical applications

2.2. Zein

Zein is a major storage amphiphilic protein of corn and it comprises 45–50% of the

protein in corn. It has been investigated for uses other than foods and animal feed since the early

20th century after it showed potential as a polymer material. Gorham named the protein "zeine" after isolating it form corn[52]. Zein is a completely amorphous polymer and it belongs to the family of proteins known as prolamins[5,53]. It can be processed as a thermoplastic material in the presence of the plasticizers with high boiling point, such as glycerol, oleic acid, etc[21,52]. Similar to corn starch, zein is mostly present in the endosperm of corn[25]. The hardness of corn endosperm is determined by zein alone.

Four major classes of proteins in corn are defined primarily by their solubility in selected solvents. Albumins, globulins, glutelin and zein are soluble in water, salt, alkali and alcohol, respectively (Table 2.3). Almost all the albumins and globulins are present in the germ, whereas most of the zein is present in endosperm. Glutelin is distributed in both endosperm and germ.

Table 2.3. Distribution of protein fractions in corn (% dry basis)[25].

Protein	Solubility	Whole kernel	Endosperm	Germ
Albumins	Water	8	4	30
Globulins	Salt	9	4	30
Glutelin	Alkali	40	39	25
Zein	Alcohol	39	47	5
Protein	Solubility	Whole kernel	Endosperm	Germ

Zein is a mixture of different peptides[25]. According to their molecular weight and location in the protein body, zein can be further divided into four different classes: α-zein, β-zein, γ-zein and δ- zein. Due to their various amino acid sequences, they exhibit different solubility in solvents. α-zein makes up 75–85% of the total prolamine present in corn. Structural studies on zein have mainly focused on a-zein and g-zein, probably due to their high fractions in total zein mass[54]. Figure 2.5 represents four kinds of proposed 3-D structural models of a-zein, including cylindrical model, ribbon-like model, hairpin model and super helical structural model.
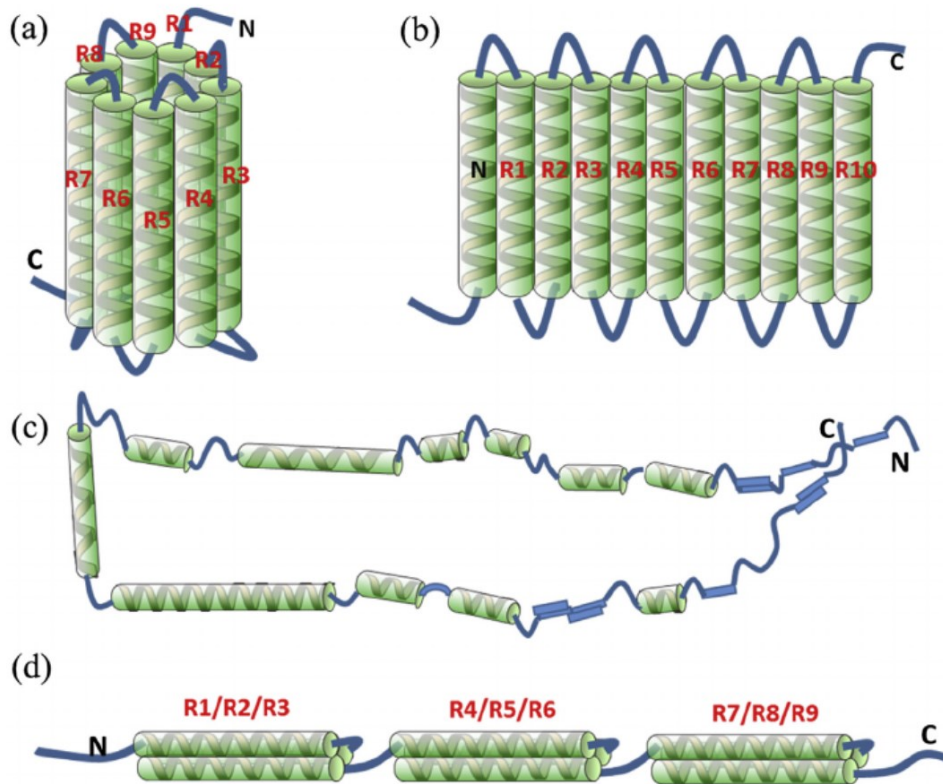
Figure 2.5. Proposed 3-D structural models of a-zein. (a) cylindrical model; (b) ribbon-like model; (c) hairpin model; and (d) super helical structural model. R means repeat unit[54].

2.3. Cellulose Nanofibrils and Lignin

Natural fibers can be classified into plant-based and animal-based fibers (Figure 2.6)[55]. Plant-based fiber can be divided into six main categories, such as bast, leaf, fruit, grass, straw and wood pulp. All plant-based fibers are lignocellulosic. Generally, lignocellulosic materials are mainly composed of cellulose, lignin, hemicellulose and others (e.g., pectin, resins, waxes, ashes, minerals, etc.) Among them, cellulose is a major component with its content ranging from 40% to 90%[56]. Figure 2.7 and Table 2.4 present the structure and compositions of cellulose, hemicellulose and lignin in a few lignocellulosic biomasses[57,58].
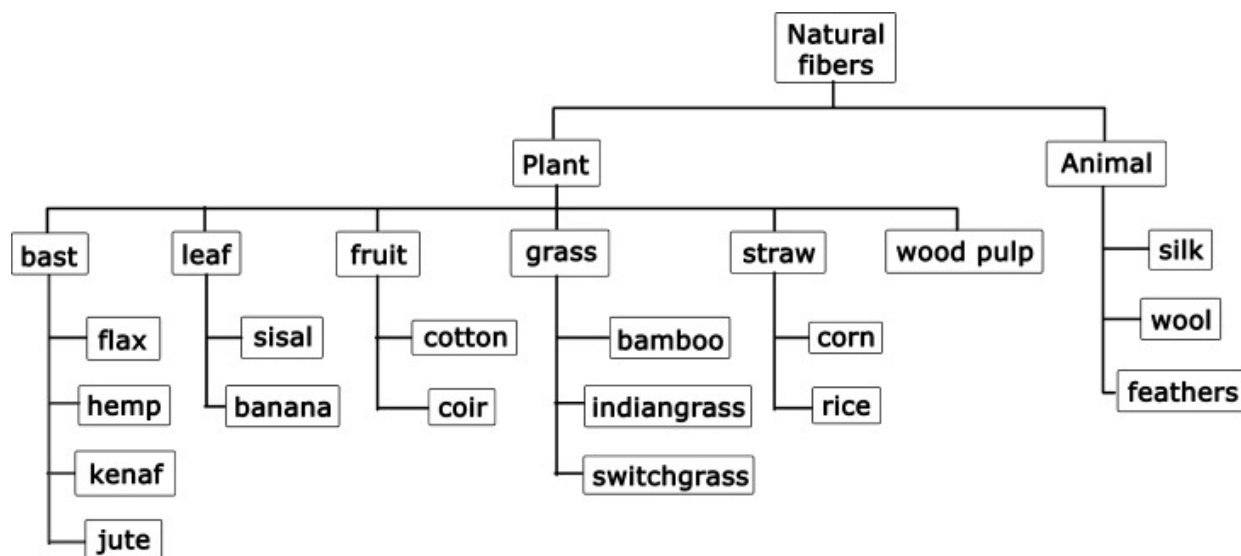
Figure 2.6. Classification of natural fibers[55].

Table 2.4. Chemical composition of some lignocellulosic fibers[57].

Fiber	Cellulose (wt %)	Hemicellulose (wt %)	Lignin (wt %)
Bagasse	55.2	16.8	25.3
Bamboo	26–43	30	21.0–31.0
Birch branches	33.3	23.4	20.8
Corn stalk	42.7	23.6	17.5
Flax	71	18.6–20.6	2.2
Kenaf	72	20.3	9
Hemp	68	15	10
Jute	41–48.0	21–24	18.0–22.0
Oil palm	65	-	29
Pine branches	32	32	21.5
Rice rusk	35.0–45.0	19.0–25.0	20
Rice straw	41.0–57.0	33	8.0–19.0
Sisal	65	12	9.9
Spruce branches	29	30	22.8
Switchgrass	34	27	17
Wheat straw	38.0–45.0	15.0–31.0	12.0–20.0
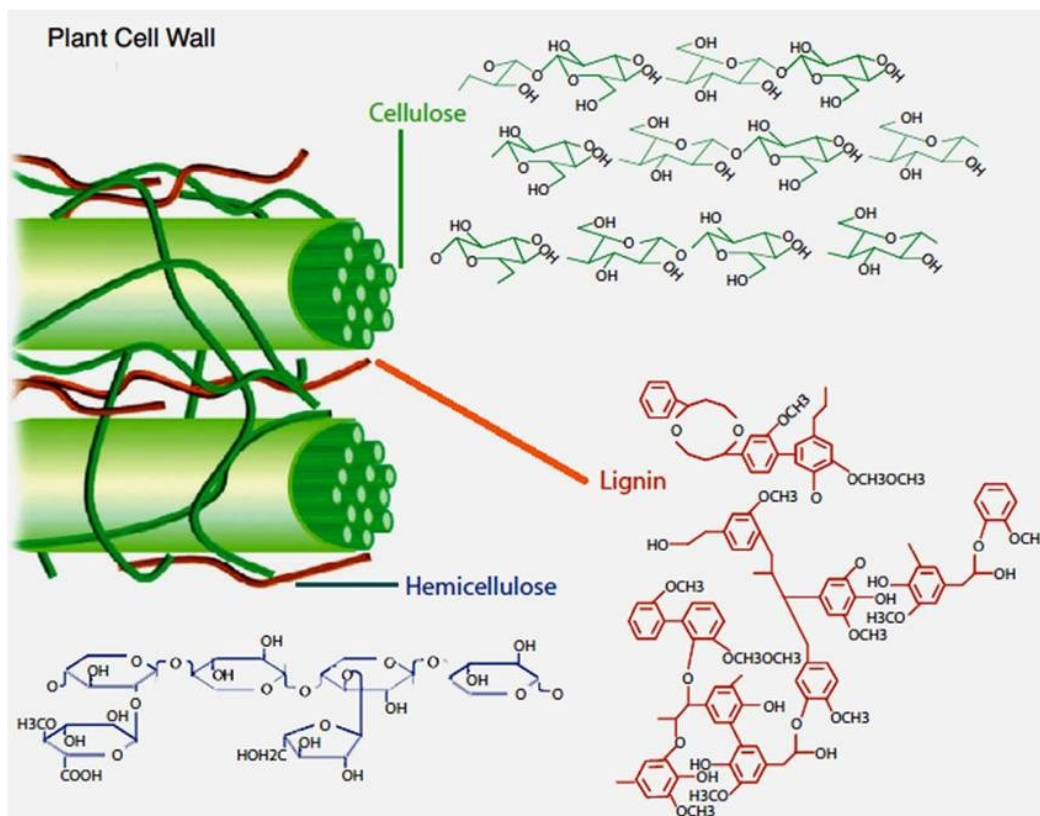
Figure 2.7. Structure of lignocellulosic biomass[58].

2.3.1. Cellulose nanofibrils

Cellulose is a linear biopolymer made up of 7000–15,000 β-1,4-glycosidic linked D-glucose monomers as presented in Figure [53,57]. The linear molecular chains bundle together to form cellulose nanofibrils (CNFs) through van der Waals forces, intramolecular and intermolecular hydrogen bonds between the hydroxyl groups of glucose, and crystallization[56,59]. CNFs have been extensively studied in recent years for many important applications including polymer nanocomposites[13]. Their high crystallinity, high aspect ratio, outstanding mechanical properties, low density, and surface functionalization have made them the most promising biobased nano-reinforcement materials[14,15].

2.3.2. Lignin

Lignin (and hemicellulose) acts as a glue to bundle cellulose fibers together to form cell wall. It provides the mechanical stability of the plant[56]. Lignin is an amorphous aromatic polymer and is one of the most abundant organic substances on earth. Currently, around 63 million tons of lignin is generated per year from the pulp and paper industries.

Lignin means wood in Latin and the term was first used in 1813 by A.P. Candolle. As one of the major components of lignocellulosic biomass, lignin improves the stiffness of the plant. The content of lignin in biomass varies by the type of plant. For example, in grass, lignin represents about 17-24 wt% of the total mass; in softwood, lignin represents about 18-25 wt% of the total mass; in hardwood, the content of lignin is 27–33 wt%[11,60]. Lignin as a polyphenolic macromolecule consists of three types of monomeric units, i.e., coniferyl alcohol (G), p-coumaryl alcohol (H), and sinapyl alcohol (S). The dominated monomeric unit and lignin chemical structure vary by the plant source. For example, in softwoods, hardwood and grasses, the dominated components of lignin are coniferyl alcohol, sinapyl alcohol and p-hydroxyphenyl alcohol, respectively[58]. Figure 2.8 shows the primary lignin monomers, generic lignin unit and major lignin structure units in the polymer.

a) predominant monomers (the hydroxycinnamyl alcohols)

MH — p-coumaryl alcohol
MG — coniferyl alcohol
MS — sinapyl alcohol

b) generic lignin units

General p-hydroxyphenyl unit (PH)
General guaiacyl unit (PG)
General syringyl unit (PS)

c) major structural units in the polymer

A — β-aryl ether [β-O-4]
B — phenylcoumaran [β-5 (α-O-4)]
C — resinol [β-β (γ-O-α)]
E — biphenyl ether [5-O-4]
D — biphenyl [5-5]
D2 — dibenzodioxocin [5-5/β-O-4 (α-O-4)]
X1 — cinnamyl alcohol

Figure 2.8. (a) Primary lignin monomers M, the monolignols. (b) Lignin polymer P units are denoted based on the methoxyl substitution on the aromatic ring as generic PH, PG, and PS units. (c) Major structural units in the polymer; the bolded bonds are the ones formed in the radical coupling reactions[62].

Lignin can be divided into two types based on their sulfur content: sulfur containing lignin and sulfur free lignin. The sulfur containing lignin including kraft lignin, lignosulfonates and hydrolyzed lignin. The sulfur content of kraft lignin, lignosulfonates and hydrolyzed lignin are 1.0-3.0%, 3.5-8.0% and 0-1.0% respectively[11,61]. Organosolv lignin, soda lignin, and lignin from second generation biorefinery process are known as sulfur free lignin[11]. Their structures vary based on the various extraction processes and the different functional groups, such as methoxyl, hydroxyl, carbonyl, carboxyl[57]. Kraft lignin and lignosulfonates which are produced by paper making industry are two principal categories of lignin. Table 2.5. shows chemical composition of the technical lignin[63].

Table 2.5. Chemical composition of the technical lignin[63].

Parameter	Soda Lignin	Kraft Lignin	Hydrolysis Lignin	Organosolv Lignin	Lignosul-phonates	Lonic Liquid Lignin
Ash, %	0.7-2.3	0.5-3.0	1.0-3.0	1.7	4.0-8.0	0.6-2.0
Moisture Content, %	2.5-5.0	3.0-6.0	4.0-9.0	7.5	5.8	-
Carbohydrates, %	1.5-3.0	1.0-2.3	10.0-22.4	1-3	-	0.1
Acid soluble lignin, %	1.0-11	1-4.9	2.9	1.9	-	-
Nitrogen, %	0.2-1.0	0.05	0.5-1.4	0-0.3	0.02	-
Sulphur, %	0	1.0-3.0	0-1.0	0	3.5-8.0	1.5
Molecular Weight, Mw	1000-3000(up to 15000)	1500-5000(up to 25000)	5000-10000	500-5000	1000-5000(up to 15000)	2000
Polydispersity	2.5-3.5	2.5-3.5	4.0-11.0	1.5	4.2-7.0	-

Kraft lignin (KL) is produced by Kraft pulping process[64]. Wood chips are cooked in NaOH and Na_2S solution to separate the lignin with hemicelluloses. The degraded lignin fragments with different molecular weight are dissolved in alkali solution and converts into black liquor while the celluloses are converted into pulp after cooking. The most popular process to isolate kraft lignin from black liquor in large scale is known as LignoBoost process. During LignoBoost process, acid solution is added to lower the pH (pH=1-2) of the black liquor which enable the precipitation of purified lignin from the inorganic cooking liquor. The obtain lignin contains increased amount of phenolic hydroxyl, carboxyl groups due to β-aryl bonds cleavage and oxidative conditions during several cooking condition. Its molecular weight is within the range 1500 to 25000[63].

Lignosulfonates is generated by sulfite process as by-product[63]. During sulphite cooking, wood is delignified by means of HSO_3^{-} and SO_3^{2-} ions. After sulfonation and hydrolysis of lignin, high amounts of sulfur are then incorporated with lignin structure, in the form of sulfonate groups (SO_3^{-}). The degree of sulfonation of lignosulphonates is 0.4 to 0.5 per phenylpropanoid unit. Lignosulphonates are water-soluble anionic polyelectrolytes with relatively high molecular weight, broad distribution of molecular weights. It contains various functional groups such as

phenolic hydroxyl groups, carboxylic groups, and sulphur containing groups which provide the

possibility to be used as plasticizer, dispersant, etc. A comparison of lignosulphonates with kraft

lignin is shown in Table 2.6.

Table 2.6. Properties of lignosulfonate and kraft lignin[61].

Property	Lignosulfonates	Kraft Lignin
Sulfur Amount [wt%]	3.5-8.0	1.0-3.0
	5	1-2
	4-8	1-1.5
	3-8	1-2
	5..3-7.7	0.23
	3.56	-
Sulfonated Content [mmolg^{-1}]	1.25-2.5	0
	0.7-1.9	0
	1.38	-
	1.68	-
	1.38	-
	2.34	-
	-	0
	-	0
Water Solubility [g L^{-1}]	-	1.8
	10	0
	-	0
Charge Density [meq g^{-1}]	0.9	-
	-	0.01
	-	0
MW [g mol^{-1}]	1000-150000	1500-25000
	20000-50000	2000-3000
	1000-50000	-
	2400-140000	-
	-	2950-5000

2.4. Application of CNFs in Bioplastics

The incorporation of CNFs significantly increased the mechanical properties and humidity resistance of thermoplastic starch films[13]. Modified cellulose including cellulose acetate and ethyl cellulose were blended with zein and electrospun into nanofibers[65,66]. The resultant composite nanofibers showed better thermal stability, higher glass transition

temperatures, and improved water resistance compared to the pure zein nanofibers. Most recently, lignin-containing cellulose nanofibrils (LCNF) were used to reinforce thermoplastic starch. At 15% LCNF content, the tensile strength and modulus were increased by 319% and 800%, respectively. The thermal stability and water barrier property were also improved substantially after the incorporation of the nanofibrils. These improvements were mainly attributed to lignin's chemical characteristics[11].

2.5. Application of Lignin in Bioplastics

Lignin has found applications in polymer composites in recent years. Its functional groups, including phenolic and aliphatic hydroxyl, carbonyl, carboxylic, and methoxyl groups, can interact with many polymer matrixes and lead to improved material properties[9,10,11]. The mechanical properties of thermoplastic zein was improved after incorporating lignin because the strong hydrogen bonding between lignin and zein disrupted the secondary structures of the protein[67]. Lignin was found to increase the mechanical properties and water resistant of thermoplastic starch under certain conditions[12]. Lignin was also shown to increase water resistance of urea-crosslinked starch film[68]. The tensile strength, modulus, and impact strength of PLA were increased when 15% lignin was incorporated[69]. The mechanical properties of a acrylonitrile-butadiene rubber containing 50% lignin were significantly improved after $ZnCl_2$ was added to induce interfacial crosslinking between the two phases[10].

2.5.1. Starch-lignin composites

Starch, the second largest component of biomass produced, is one of the most studied natural polymers[21]. Thermoplastic starch (TPS) can be processed in injection, extrusion, and blow molding, similar to most conventional synthetic thermoplastic polymers. However, TPS is rarely used alone because of its poor mechanical properties and moisture resistance. The

19

incorporation of lignin provides the possibility to interact with many polymers and lead to improved material characteristics.

Shi et al. (2016) prepared corn starch based composites using a casting method[70]. Sodium lignosulfonate used as reinforcement and sorbitol used as a plasticizer were added at different concentrations. The peaks of stretching vibrations of C-O and S=O were shifted to lower frequencies in the starch/lignosulfonate blend which indicated the interaction (e.g. hydrogen bonding) between the components. The XRD pattern also indicated that the addition of lignosulfonate influenced the microstructures of the starch because it prevented starch from recrystallization. Viscosity was increased after the addition of lignin and caused bubbles/voids in the blends because degassing was more difficult at higher viscosities. With an increase in the lignosulfonate content, the ultimate stress decreased. The best mechanical properties were achieved at 66 wt% lignin (based on starch weight) with a failure strain of 321.76% and a strength of 2.53 MPa. Composites' water resistance was also increased.

To increase the interfacial bonding between starch and lignin, Iuliana Spiridon et al. (2011) prepared adipic acid (AA) modified starch as a filler for the composites system through a casting process[24]. The AA groups on the adipic acid modified starch (AASM) chains led to formation of highly cross-linked starch. FTIR testing results showed an increase in the number of oscillation modes, which may be ascribed to different types of hydrogen bonding interactions. The bands attributed to the stretching vibration of C–O in C–O–H groups indicated that new hydrogen bonds were formed between hydroxyl, carbonyl groups in starch and carbonyl, hydroxyl, ether groups in lignin. Compared to un-modified starch film, the AA modified starch film showed a larger water contact angle and a lower water absorption. With an addition of

lignin, the composites presented a higher tensile strength, modulus but lower elongation capacity. The incorporation of lignin increased the thermal stability of starch/lignin composites.

Meryem Aqlil et al (2017) investigated the potential of using graphene oxide (GO) to reinforce starch/lignin composites[71]. The composites were prepared by a solution casting method. FTIR results showed strong interfacial bonding between lignin and starch molecules due to hydrogen bonding. The incorporation of GO in the starch/lignin matrix led to interconnected network due to the oxygen group of GO. Figure 2.9 showed the structure of GO incorporated starch/lignin composites film and possible interactions between these three components. Due to these interactions, mechanical properties of the composites have significant improved. The water swelling, moisture absorption, water vapor permeability, and thermal stability of the composites were also increased.
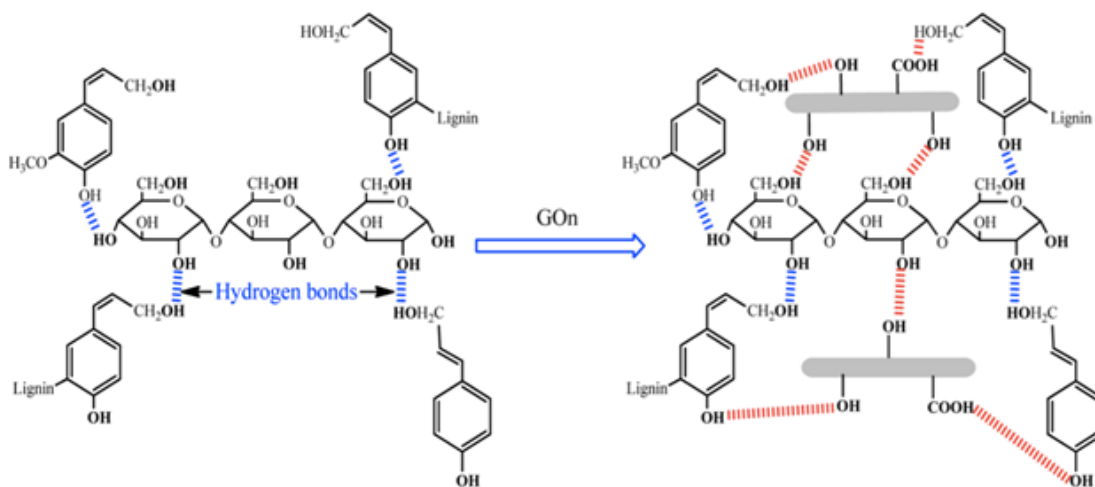
Figure 2.9. Structure of the starch/lignin blend, starch/lignin-GO bionanocomposite film and the possible interactions between starch, lignin, and GO nanosheets[71].

Besides lignin content, molecular weight of lignin also plays a very important role in the properties of a composite system. A study of Baumberger et al. (1998b) showed that low molecular lignin can act as plasticizer while high molecular weight of lignin can be used to increase the mechanical properties of composites[72]. The composites were prepared by casting

and extrusion process. Content of lignin was varied from 0 to 30% to study its influence on composites mechanical properties. Composites with 30% of lignin showed the lowest elongation value at high water content.

Kraft lignin can also be used to reduce starch biodegradation. A research of urea crosslinked starch reinforced with lignin was reported by Zahid Majeed et al (2018)[73]. Composites were prepared by casting method. With an addiction of lignin, FTIR peals of composites showed a fast diminution in the biodegradability of urea crosslinked starch, which indicated that lignin slowed down the biodegradability of starch. The decomposition temperature of lignin increased at 5% weight loss and maximum weight loss. The addition of lignin effectively inhibited the dimer, trimer and oligomer in the membrane. Optical microscope successfully proved the protective effect of lignin on starch particle morphology in the process of biodegradation, and the control effect of lignin on expansion, rupture, damage and other events in the process of biodegradation.

Chuan-wei Zhang et al. (2020) prepared lignin-containing, cellulose nanofibrils reinforced thermoplastic starch films[74]. TPS/LCNF composite films were prepared using solution casting and then compressed with hot press. Compared to the control sample (neat TPS), composites with LCNF shows better tensile strength (increased 319%) and modulus (increased 800%) but lower elongation break rate. Composites with 5wt% of LCNF showed the best toughness. The improved mechanical properties were found to be due to increased crystallization and strong interaction between TPS and LCNF. The thermal stability of the composite films improved with the addition of LCNF as lignin plays an important role in the thermal stability of the composites. The addition of LCNF to the composite films also significantly decreased water absorption and transmission because the permeation of molecules was reduced. The weakened

hydroxyl group stretching vibration and the formation of new hydrogen bonds observed from IR testing showed the increased compatibility between TPS and LCNF.

2.5.2. Protein-lignin composites

An interesting alternative is to blend starch with zein because of its film-forming ability and its hydrophobicity. Maria Oliviero et al. (2011) investigated the effect of lignin on the structure of thermoplastic zein (TPZ) while using polyethylene glycol as a plasticizer[67]. Two kinds of lignin were selected for this research: alkaline lignin (AL) and sodium lignosulfonate (LSS). Composites were prepared by using a melt mixing method. Content of lignin were varied from 0 to 10 wt% of the zein and PEG system. The XRD and FTIR results showed that with low percentages of both types of lignin (3 wt%), the interhelix packing of zein was re-arranged (Figure 2.10). This arrangement could be induced by the formation of the hydrogen bonding zein and lignin molecule. The amino acids of zein (C=O, OH, RNH) could bond with the functional groups (OH, SH) of lignin fragments and generate hydrogen bonding. At 1wt% of AL, the d0-spacing was decrease, indicating that the modification of α-helix backbone only occurred at low concentrations of AL. This phenomenon was cause by the strong hydrogen bonding between the amino acids of zein and the SH groups present in AL. This suggested that similar bonding could not happen in LSS incorporated composites because the absence of -SH in LSS. The modification and destruction of the α-helix, β-sheet, and β-turn structure also influenced the thermomechanical properties and water uptake of TPZ.

Elham Mohammad Zadeh et al. (2018) investigated the effect of lignin on the properties of the enzymatically modified soy protein isolate (SPI)[75]. Different content of alkali lignin and lignosulfonates were incorporated into the composites. The composites were prepared by casting method. Compared to commercial butylated hydroxytoluene, alkali lignin and lignosulfonates

have higher radical scavenging activity, especially lignosulfonates. Lignosulfonates showed higher compatibility with enzymatically modified soy protein isolate. Alkali lignin incorporated composites showed strong UV-blocking ability due to its nature color. With the AL content increased, the UV-blocking ability of the composites increased. Compared to the neat composites film (without lignin), films with lignin showed better mechanical properties and thermostability.
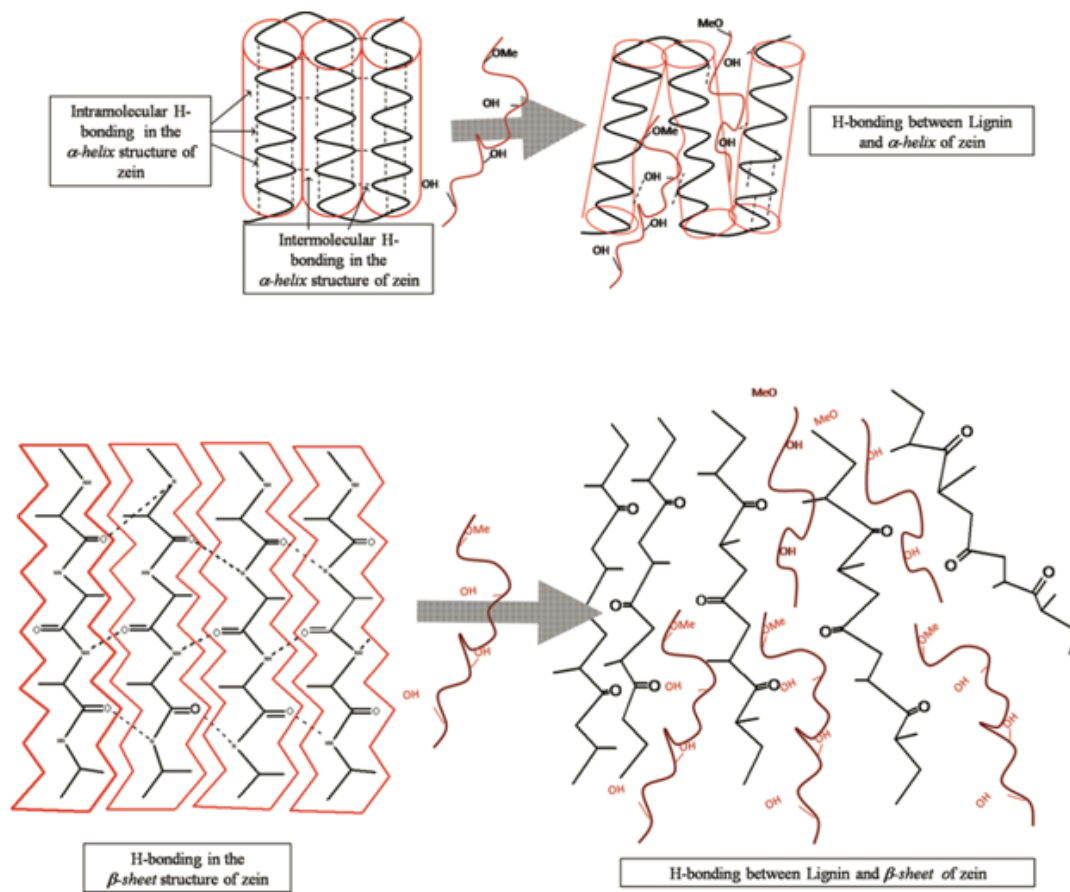
Figure 2.10. Proposed mechanism of interaction between lignin and different secondary structures of zein: (a, top) R-helix; (b, bottom) β-sheet[67].

A study of Antoine Duval et al. (2013) showed that kraft lignin (KL) and lignosulfonates (LS) have complementary effects on the mechanical properties of the composites[76]. With the addition of kraft lignin, wheat gluten/KL composites become stiffer and showed less water sensitivity and better thermal stability compared to neat WG films. Its Young's modulus was increased with not much change on elongation at break. However, wheat gluten/LS composites

showed an increase in elongation at break and deceases in tensile strength and Young's modulus as well as negligible changes on the water sensitivity and glass transition temperature compared to neat wheat gluten films. The distinct behaviors observed in this study may be due to the structural difference between kraft lignin and lignosulfonates.

Warren J. Grigsby et al. (2020) investigated kraft lignin/keratin bio-composites using a green chemistry method to conjugate keratin protein with polyphenolic lignin[77]. The blends were prepared by melting process. A new method of complexing lignin with protein was used to form copolymer and enhance keratin crosslinking. The optimum ratio of keratin to lignin was found to be 4:1. Based on the results, the protein complexation was primarily induced by the amides group of protein and aryl hydroxyls group of lignin. The extruded FDM filaments could be formed at about 130 °C with a plasticizer. The keratin-lignin hydrogel was successfully used to for 3D printing.

2.5.3. Others

Lignin has also been studied as a functional additive in non-protein/starch systems. Iuliana Spiridon et al. (2018) studied the influence of lignin on the PLA/lignin composites[69]. Two kinds of lignin, Organosolv lignin (LO) and Lignoboost® lignin (LB), were used in this research. Composites were prepared by melting process. PLA/lignin composites showed higher modulus, lower tensile strength and water absorption at 7wt% lignin content. The tensile strength was found to increase in the 7 - 15wt% lignin content range. After immersing PLA/LO and PLA/LB in simulated body fluid (SBF) for 30 days, both lignin reinforced composites showed good mechanical resistance and dimensional stability. PLA/LO composites showed better mechanical properties than PLA/LB.

Min Yu et al. (2019) evaluated the durability of alkali lignin reinforced wheat straw/recycled polypropylene blends[79]. Composites were prepared by melting process. Compared to the control sample, the composites with lignin showed improved mechanical properties. The corporation of lignin improve the compatibility between wheat straw fiber and recycled polypropylene. The oxidation induction time was also reduced for the reinforced blends, which may be due to the anti-oxidation function and the dark color of lignin. Lignin could act as a radical scavenger because of its phenolic groups while the dark color of lignin composites would play a role in blocking the UV light.

Phosphorylated kraft lignin (KLP)/polyester composites could be used as a fireproof material in rocket propellant thermal protection systems. Jelena Rusmirović et al. (2019) evaluated the effects of surface functionalization of industrial sulfate lignin (KL) on the mechanical and thermal properties of unsaturated polyester (UPe) composites[80]. The composites were prepared through melting process. KL with methyl terminal groups was firstly prepared by a phosphorylation method. Compared to the neat UPe matrix, UPe/KL (1 wt% KL) showed a higher tensile strength (31 %). However, the incorporation of KLP decreased the tensile strength and elongation at break of composites. With an addiction of modified lignin, fire resistance properties of UPe composites were increased. With 5 wt.% KLP, UPe/KL composites achieved V-1 category flame resistance.

The incorporation of lignin nanoparticles could also enhance antioxidant and antibacterial properties of polyvinyl alcohol/chitosan hydrogels. Different content (1wt% and 3wt%) of lignin nanoparticles (LNPs) were prepared through a freezing-thaw procedure by W. Yang et al. (2018)[81]. A low content of LNPs led to large increases in the thermal and mechanical properties of PVA/Ch hydrogels. This phenomenon was due to the agglomeration present in the higher

LNP content hydrogels. Swelling studies revealed that the strong interaction between PVA/Ch molecules and LNPs prevented PVA molecules from moving and dissolving into water, thus promoting the cross-linking effect. Moreover, a synergic effect on antioxidative response of chitosan and LNPs (as releasing agent) was observed in PVA/Ch.

The literature review above shows that although starch, zein, lignin, and CNFs have been used in polymer systems for their different functions and purposes, their synergy has not been explored in a system where their complementary properties are expected to lead to enhanced performance of the material. This master thesis research is designed to study the synergy and eventually develop a new class of corn-based thermoplastic resin.

3. IMPROVING MECHANICAL PROPERTIES OF THERMOPLASTIC STARCH-ZEIN COMPOSITES THROUGH INCORPORATING KRAFT LIGNIN AND CELLULOSE NANOFIBERS

3.1. Introduction

In recent years, there has been an increased interest in producing renewable materials due to the significant environmental impacts of producing and disposing of petroleum-based polymers.[17] Corn-derived materials including starch, zein, and polylactic acid (PLA), can be attractive materials for applications such as food packaging, mulch, plant pots, utensils, and other household and industrial items. Their potential to replace some petroleum-based polymers has been recognized and has been widely studied[18,19,20,21,22,23,24].

Starch, the second largest biomass produced, is one of the most studied and used natural polymers. It has major applications in food industry, packaging, adhesives, paper, and biocomposites because of its renewability, sustainability and low-cost[26,27,28,29,30]. In its natural state, semi-crystalline starch exists in a granular form and shows poor processability[17,21,43]. However, in the presence of plasticizers including water, glycerol, and ethylene glycol, the crystalline structure of starch granules can be ruptured under heat and shear due to the formation of the hydrogen bonds between the plasticizer and starch molecules[17,82,83]. As a result, starch behaves like a typical thermoplastic polymer after this plasticization process, allowing the material (termed thermoplastic starch or TPS) to be processed through injection molding, extrusion, and blow molding, in ways similar to conventional synthetic thermoplastic polymers[17,43,36]. However, TPS is rarely used alone because of its low mechanical properties and poor moisture resistance. It is often blended with hydrophobic thermoplastic polymers, such as

polyethylene, polypropylene, PLA, poly(ethylene-co-vinyl alcohol), and polyvinyl alcohol to improve its performance[21,44,45,46,47,48].

Zein is the major storage amphiphilic protein of corn and it belongs to the family of prolamins[5,53]. Zein is a completely amorphous polymer and can be processed as a thermoplastic material in the presence of plasticizers, such as glycerol, oleic acid, etc[21]. According to Habeych et al., thermoplastic starch–zein blends showed better water resistance than thermoplastic starch due to the insolubility of zein in water.[4] However, more recent studies demonstrated that starch–zein blends exhibited poor mechanical properties because of the incompatibility between the two phases, resulting in poor stability of the resulting material[5,84,7,50].

Lignin, an amorphous, amphiphilic, aromatic material, is one of the most abundant organic substances on earth. Currently, around 63 million tons of lignin is generated each year from the pulp and paper industry and most of the material is burned to generate electricity and heat. Only a very small portion (less than 2%) is used for producing value-added products such as chemicals used in dispersants, adhesives, and surfactants. Lignin has found applications in polymer composites in recent years. Its functional groups, including phenolic and aliphatic hydroxyl, carbonyl, carboxylic, and methoxyl groups, can interact with many polymer matrixes and lead to improved material properties[9,10,11]. The mechanical properties of thermoplastic zein was improved after incorporating lignin because the strong hydrogen bonding between lignin and zein disrupted the secondary structures of the protein[67]. Lignin was found to increase the mechanical properties and water resistant of thermoplastic starch under certain conditions[12]. Lignin was also shown to increase water resistance of urea-crosslinked starch film[68]. The tensile strength, modulus, and impact strength of PLA were increased when 15% lignin was incorporated[69]. The mechanical properties of a acrylonitrile-butadiene rubber containing 50%

lignin were significantly improved after $ZnCl_2$ was added to induce interfacial crosslinking between the two phases[10].

Cellulose is the most abundant natural polymer on earth. It is the main constituent of plant fibers. Cellulose nanofibers (CNFs), the elementary cellulose fibrils, are extracted from wood cell walls and have been extensively studied in recent years for many important applications including polymer nanocomposites[13]. Their high crystallinity, high aspect ratio, outstanding mechanical properties, low density, and surface functionalization have made them the most promising biobased nano-reinforcement materials[14,15]. The incorporation of CNFs significantly increased the mechanical properties and humidity resistance of thermoplastic starch films.[13] Modified cellulose including cellulose acetate and ethyl cellulose were blended with zein and electrospun into nanofibers[65,66]. The resultant composite nanofibers showed better thermal stability, higher glass transition temperatures, and improved water resistance compared to the pure zein nanofibers. Most recently, lignin containing cellulose nanofibrils (LCNF) were used to reinforce thermoplastic starch. At 15% LCNF content, the tensile strength and modulus were increased by 319% and 800%, respectively. The thermal stability and water barrier property were also improved substantially after the incorporation of the nanofibrils. These improvements were mainly attributed to lignin's chemical characteristics[74].

The goal of this part of study is to develop a corn-based thermoplastic with substantially improved mechanical properties and water resistance than traditional thermoplastic starch plastic. The main components of corn, i.e., starch and zein, are incompatible but offer complementary properties – hydrophobic zein is expected to increase water resistance of thermoplastic starch. The incorporation of amphiphilic and functional lignin and CNFs are hypothesized to improve the compatibility, refine the zein/starch phase structure, and therefore

increase the mechanical properties of the new corn thermoplastic. The synergy of these ingredients has not been explored in any prior studies and it can lead to a new class of materials with a good balance of sustainability, functionality, and performance. The new material can be readily processed into final products using existing techniques such as extrusion and injection molding, making an impact on the plastics industry.

3.2. Materials and Methods

3.2.1. Materials

Argo® pure corn starch was purchased from a local grocery store. Zein (W555025) and Kraft lignin (471003) were both purchased from Sigma-Aldrich. The zein had a protein concentration of ~ 92% and an ash content of < 2%. The other properties of zein were provided in Table A1 in the appendix. The lignin contained 4% sulfur and had an average Mw of ~10,000. Glycerol (99+%, 11443297) and ethylene glycol (BDH1125-1LP) were purchased from Alfa Aesar and VWR, respectively. CNF slurry with a CNF concentration of ~2.5 wt% was purchased from the Process Development Plant of University of Maine. The slurry was concentrated by centrifugation to increase the concentration to 10 wt% before use. All the chemicals and materials were used as received without further purification or modification.

3.2.2. Lignin solution preparation

Glycerol and ethylene glycol were used as the plasticizers in the corn-based thermoplastic in this study. Lignin was incorporated into the material in the form of either dry powder or solutions (in glycerol or ethylene glycol). To prepare the solutions, glycerol or ethylene glycol were first mixed with distilled water at a 1:1 weight ratio. Predetermined amounts of lignin powder were then added into the mixtures to obtain lignin/glycerol/water ratios of x/50/50 (w/w/w, x=0, 1, 2). Complete lignin dissolution was achieved after stirring the mixtures (500

rpm) for one hour under room temperature. The obtained lignin solutions were stored under

ambient conditions for future use and testing. Four lignin solutions were prepared in total and

their compositions and sample codes are listed in Table 3.1.

Table 3.1. Formulations of lignin solutions.

Sample Codes	Ingredients (All in parts)			
	Lignin	Glycerol	Ethylene Glycol	Distilled Water
EG-1	1	0	50	50
EG-2	2	0	50	50
G-1	1	50	0	50
G-2	2	50	0	50

3.2.3. Preparation of thermoplastic starch-zein composites

When lignin was incorporated into the composites in the form of dry powder, 80 parts of

corn starch, 20 parts of zein and x parts of lignin powder (x= 0, 1, 2) were manually mixed in a

beaker to achieve an even distribution. Glycerol/water (50 parts /50 parts) or ethylene

glycol/water (50/50) as the plasticizer was added to the premixed powder, manually mixed, and

then sealed in a plastic bag and stored for 24 hours to achieve equilibrium. The mixture was

compounded into a thermoplastic using a HAKKE internal mixer (Rheomix 600 Haake,

Germany) operating at 140°C and 100 rpm. The product was compressed into ~0.5mm thickness

sheets using a hot press (1200 N, 10 min) and cut into standard tensile test specimens for

mechanical property characterization. When lignin solutions were used, the liquids were mixed

with the corn starch and zein powder in the beaker and a reduced amount of plasticizer was

added to maintain a constant content of the plasticizer. To prepare the composites containing

CNFs, the concentrated nanofiber slurry was first dispersed in the plasticizer solutions through

sonication. The premixed starch/zein/lignin powder was slowly added to the solutions under

continuous stirring, and the mixture was sealed in a plastic bag for 24h before compounding.

A flow chart of the sample preparation process is shown in Figure 3.1. All the prepared samples are listed in Table 3.2 with their sample codes and respective compositions. In the sample codes, G and EG denote the glycerol and ethylene glycol plasticizers, respectively. P and S denote the lignin in powder and solution forms, respectively. The number after the dash indicates the part number of the lignin. CNF and the number after it indicate the presence of CNFs in the composites and its part number. For instance, GP-2-CNF4 means that the composite contains 2 parts lignin powder and 4 parts CNF and has glycerol as the plasticizer. Letter C in the sample codes indicates the denoted samples are control samples, containting no lignin and CNFs.
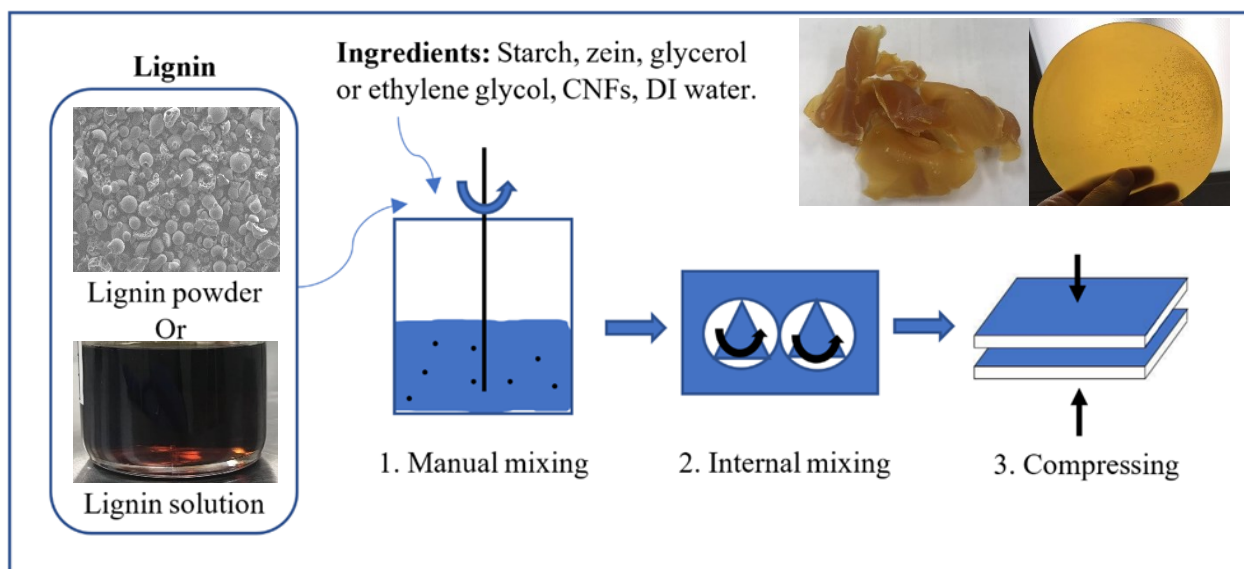
Figure 3.1. Flowchart of the corn-based thermoplastic sample preparation process. The photos on the top right corner of the figure shows the resin after internal mixing and hot press. The micrograph on the top left corner shows lignin powder.

Table 3.2. Formulations of corn-based thermoplastic composites.

Sample Codes	Ingredients (All in parts)						
	Corn Starch	Zein	Lignin	Cellulose Nanofiber	Glycerol	Ethylene Glycol	Distill Water
EGC	80	20	0	0	/	50	50
EGP-1	80	20	1	0	/	50	50
EGP-2	80	20	2	0	/	50	50
EGS-1	80	20	1	0	/	50	50
EGS-2	80	20	2	0	/	50	50
GC	80	20	0	0	50	/	50
GP-1	80	20	1	0	50	/	50
GP-2	80	20	2	0	50	/	50
GS-1	80	20	1	0	50	/	50
GS-2	80	20	2	0	50	/	50
G(S)P-2*	100	0	2	0	50	/	50
G(Z)P-2*	0	100	2	0	50	/	50
GP-2-CNF2	80	20	2	2	50	/	50
GP-2-CNF4	80	20	2	4	50	/	50
GP-2-CNF6	80	20	2	6	50	/	50
GC-CNF2	80	20	0	2	50	/	50
GC-CNF4	80	20	0	4	50	/	50
GC-CNF6	80	20	0	6	50	/	50

*G(S)P-2 is sample using starch only as the matrix and incorporated with 2 parts of lignin powder. G(Z)P-2 is sample using zein only as the matrix and incorporated with 2 parts of lignin powder. The plasticizer of these two composites were glycerol.

3.2.4. Sample characterization

Dynamic light scattering (DLS) (Nicomp 380, Particle Sizing Systems, Santa barbara, CA, USA) was used to characterize the particle size of lignin in glycerol or ethylene glycol solutions. The tests were carried out at 20°C using the following parameters: 5.922 cP and 2.800 cP for the viscosities of the glycerol and ethylene glycol solutions, respectively, and 1.398 and 1.383 for their refractive indexes. Three repeats were tested to obtain the average particle sizes.

Tensile properties of the composites were characterized using the dumbbell test bars cut from the hot-pressed sheets. The tests were performed under ambient conditions (~ 23 °C) on an

MTS Insight test system equipped with a 5 kN electronic load cell at a crosshead speed of 50 mm/min.

Scanning electron microscopy (SEM) was used to study the morphology of lignin powder and the microstructure of the composites. Lignin powder sample was placed on carbon adhesive tabs on aluminum mounts and the excess material was blown off with a forceful stream of dry nitrogen gas. Composites samples were cooled in liquid nitrogen and fractured. The fractured samples were attached to aluminum mounts with silver paint to view the fracture surfaces. The surfaces were coated with conductive carbon using a Cressington 208c carbon coater (Ted Pella Inc., Redding, California) before imaging. Images were obtained with a JEOL JSM-7600F scanning electron microscope (JEOL USA Inc., Peabody, Massachusetts) operating at 2 kV. Energy dispersive spectroscopy (EDS) was used to determine the elemental concentrations of sulfur and sodium in the different phases of the composites. The two elements were brought into the composites through lignin and their distributions could be used to determine the distribution of the lignin in the composites. EDS information was acquired at an accelerating voltage of 8 kV using an UltraDry silicon drift X-ray detector and NSS-212e NORAN System 7 X-ray Microanalysis System (Thermo Fisher Scientific, Madison, Wisconsin).

Thermogravimetric analysis (TGA, TA Instruments Q500) was performed to determine the thermal stability of the composites and the constituents. All sample were tested between room temperature and 600°C with a heating rate of 10°C/min under a continuous air flow (60 ml/min).

3.3. Results and Discussion

3.3.1. Lignin particle size in solution

Table 3.3 shows lignin particle size and size distribution in glycerol/water (1:1) and ethylene glycol/water (1:1) solutions. Most of the lignin particles (> 98%) had a particle size of ~ 7.27 nm in the glycerol solution and ~ 6.10 nm in the ethylene glycol. The particle sizes increased (roughly doubled) after additional 24h storage. In term of ease of dissolution, the kraft lignin was water soluble and could be dissolved in water within half of an hour. It took about one hour to dissolve the same amount of lignin in pure ethylene glycol and about 5 days in pure glycerol. Since the polarity of glycerol is higher than that of ethylene glycol, the slow dissolution in glycerol may be attributed to glycerol's much higher viscosity than ethylene glycol (5.9 cP vs 2.8 cP), which makes the diffusion of the solvent much slower. This higher viscosity can also contribute to the larger lignin particle size in glycerol. The increases in the particle sizes with increasing storage time is due to weak electrostatic repulsion between the lignin particles.[85] The impurities in lignin solution could further speed up the formation and growth of aggregates.[86]

Table 3.3. Lignin particle size and size distribution in glycerol/water (G) and ethylene glycol/water (EG) solutions. Two parts of lignin were dissolved in each sample.

Sample	Storage time	Peak 1 (nm / %)	Peak 2 (nm / %)	Peak 3 (nm / %)
G-2	24h	7.27 / 99.30	79.6 / 0.50	406.1 / 0.20
G-2	72h	14.6 / 97.60	180.7 / 1.20	594.3 / 1.90
EG-2	24h	6.1 / 98.7	26.9 / 1.20	371.8 / 0.10
EG-2	72h	11 / 98.50	101.1 / 8.30	725.8 / 0.70

3.3.2. Tensile properties

Tensile test results for all the formulations listed in Table 3.2 are compared in Figures 3.2 and 3.3. The representative tensile stress-strain curves are provided in the Appendix (Figure A1 and Figure A2). Figure 3.2a compares the results from the samples using ethylene glycol as the

plasticizer while Figure 3.2b compares those using glycerol. For the first system (Figure 3.2a), in general the strength and modulus of the samples increased with the content of the lignin, regardless of being incorporated in the form of powder or solution. While the strength and modulus being improved, the ultimate (fracture) strain and toughness of the samples were generally decreased as the samples became increasingly rigid. The lignin incorporated in powder form at two parts led to the best overall mechanical properties among all the formulations.

For the glycerol system (Figure 3.2b), a similar property trend was observed: a higher lignin content led to higher mechanical properties for both lignin forms. It was still the powder lignin at 2 parts that produced the highest overall composite properties. Specifically, in the glycerol system the modulus and strength of the control sample (GC) were increased by 297.3% and 129.5% respectively after two parts of powder lignin was incorporated, whereas in the ethylene glycol system the increases were much smaller at 198.8% and 72.7%, respectively. The percentage changes of the properties for all the composites are summarized in Table 3.4.

Table 3.4 shows that lignin offered stronger reinforcement in the glycerol system than in the ethylene glycol system based on the percentage increases in the sample modulus and strength. Moreover, significant increases in toughness were simultaneously incurred by the lignin in the glycerol system, whereas in the ethylene glycol system the toughness was similar or even slightly decreased. The results in Table 3.4 do not suggest any clear advantages of using lignin solutions over lignin powder. Since the as-received lignin powder can dissolve in the water/plasticizer mixture (during the formulation and equilibrium stage and the internal mixer blending process), pre-dissolving the lignin powder before formulation appears unnecessary for achieving homogeneous dispersion of the lignin. Indeed, for both ethylene glycol and glycerol

systems, the formulations containing two parts of powder lignin showed the best overall

mechanical properties.
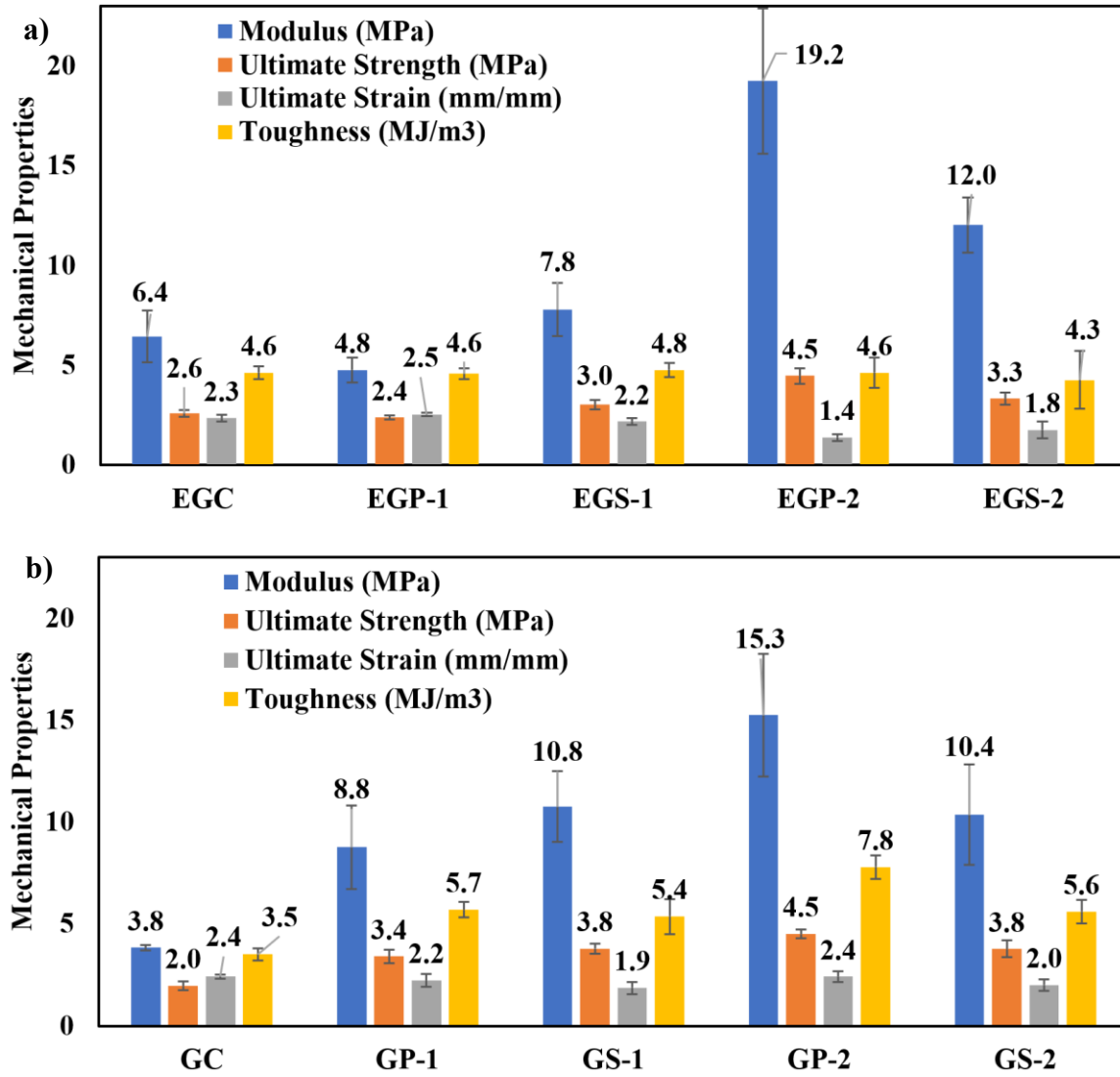
Figure 3.2. Tensile test results of the corn-based thermoplastics using a) ethylene glycol and b) glycerol as the plasticizers.

Table 3.4. Percentage changes in tensile properties of the composites.

	Modulus	Ultimate Strength	Ultimate Strain	Toughness
GC	0.0%	0.0%	0.0%	0.0%
GP-1	128.3%	73.5%	-7.9%	61.9%
GS-1	180.2%	92.8%	-22.7%	52.6%
GP-2	297.3%	129.5%	0.1%	121.3%
GS-2	170.0%	92.1%	-17.0%	59.2%
EGC	0.0%	0.0%	0.0%	0.0%
EGP-1	-26.1%	-7.6%	7.5%	-1.0%
EGS-1	20.9%	17.1%	-7.4%	2.9%
EGP-2	198.8%	72.7%	-41.1%	0.2%
EGS-2	86.9%	28.7%	-25.0%	-7.8%

It is also worth noting that the control samples of both systems, i.e., EGC and GC, showed markedly different properties. EGC exhibited a higher modulus and strength but a lower ultimate strain than GC. The viscosity of ethylene glycol was about half of that of glycerol and the former was expected to show a stronger plasticizing effect than the latter, leading to a lower composite modulus and strength. The unexpected high modulus and strength of EGC is believed to be caused by the much lower boiling point of ethylene glycol compared to glycerol (197 ℃ vs 290 ℃). The incorporation of lignin further reduced the boiling temperature of ethylene glycol to around 160°C, which was caused by reduced hydrogen bonding between ethylene glycol molecules after the addition of lignin.[87,88] It was noticed during the melt blending process that steam (due to volatilization of water and the plasticizers) was released from the internal mixer. With a lower boiling point, the loss of ethylene glycol is expected to be heavier than that of glycerol, resulting in less residual plasticizer in the composites and hence more rigid materials.

Based on the above discussion, GP-2 was selected for further reinforcement using CNFs. Figure 3.3 compares the mechanical properties of GP-2 after incorporating 2, 4, or 6 parts of CNFs. The representative stress-strain curves of the samples are compared in Figure A-2

(Appendix). The results for the composites containing CNFs but no lignin, i.e. GC-CNF2, GC-CNF4, and GC-CNF6, are also shown for comparison. First, the reinforcement effect of the CNFs in the last three composites could be clearly observed. Especially, at 6 parts of CNFs, the modulus and strength of the composite were 5 and 2.4 times, respectively, those of the control sample GC. The reinforcement of CNFs to polymer matrixes is well known and have been observed in many polymer nanocomposites. Second, when comparing these three composites with the composites containing both CNFs and lignin, i.e. GP-2-CNF2, GP-2-CNF4, and GP-2-CNF6, the latter exhibited significantly higher modulus and strength than the former at the same CNF contents, as shown in both Figure 3.3 and Table 3.5. This result clearly showed the synergy between the lignin and CNFs in reinforcing the corn-based plastics. It should also be pointed out that the composites containing CNFs exhibited reduced toughness compared to the control sample (GC) and the sample containing only lignin (GP-2), as shown in Table 3.5. This is likely due to the constrained mobility of the polymer chains, which is caused by the interactions between CNFs and the matrix polymers.
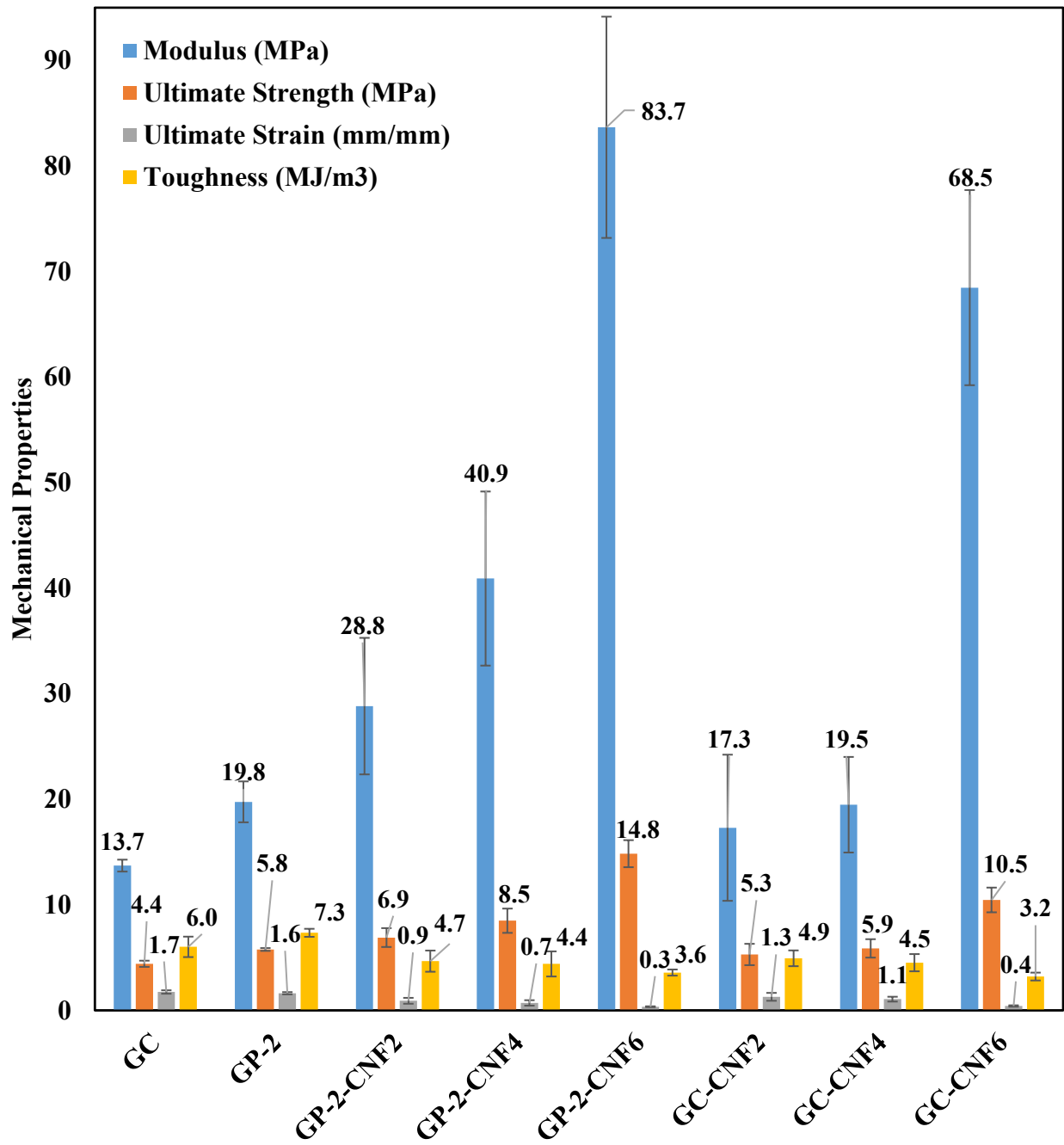
Figure 3.3. Tensile test results of glycerol group composites.

Table 3.5. Percentage changes in tensile properties of the composites.

	Modulus	Ultimate Strength	Ultimate Strain	Toughness
GC	0.0%	0.0%	0.0%	0.0%
GP-2	44.1%	30.7%	-6.7%	22.1%
GP-2-CNF2	110.2%	56.3%	-48.0%	-22.5%
GP-2-CNF4	198.3%	92.4%	-59.5%	-26.9%
GP-2-CNF6	510.1%	236.4%	-80.4%	-40.5%
GC-CNF2	26.2%	19.9%	-26.3%	-18.0%
GC-CNF4	42.1%	33.0%	-39.0%	-24.9%
GC-CNF6	399.4%	137.0%	-76.4%	-46.8%

3.3.3. SEM analysis

The microstructure of the composites was studied using SEM and the results were correlated to their mechanical properties. Figure 3.4 shows the cross-sections of the G(S)P-2 (containing starch and 2 parts powder lignin) and G(Z)P-2 (containing zein and 2 parts powder lignin) composites. They are shown and discussed first to lay the foundation for the discussion about the composites containing both starch and zein. G(S)P-2 showed a very smooth cross-section and lignin particles between 0.5-4 μm could be clearly observed on the facture surface (Figures 3.4a-b). During internal mixing, starch granules were destructed by the mechanical forces with the assistance of plasticizer and heat, and the material appeared and flew like a molten thermoplastic. This led to a homogeneous thermoplastic starch product as shown in the figure.

By contrast, the cross-section of G(Z)P-2 was not as smooth because it contained many cavities (Figures 3.4c-e). These cavities were formed by trapped air during the internal mixing. It was observed that during the mixing G(Z)P-2 formed a porous, paste-like material which contained insufficiently plasticized zein aggregates. These aggregates imparted high resistance to material flow during the mixing and resulted in a much higher mixing torque of G(Z)P-2 than G(S)P-2 (22.8 Nm vs 7 Nm). Many of the pores in the mixed material were transformed into the

cavities shown in the micrographs after the material was compressed into a sheet. The insufficient plasticization of zein in the presence of glycerol may be ascribed to the incompatibility of the two materials. The incompatibility led to separation of glycerol from the zein matrix, which resulted in the presence of the spheres (i.e. glycerol droplets) shown in Figure 3.4d. Glycerol can also be observed from the optical photograph shown in Figure 3.4f, where the liquid plasticizer leached out from the matrix and adhered to the facture surface[5]. The presence of the cavities and glycerol droplets made the identification and size determination of the lignin particles difficult. Nevertheless, it can be estimated from comparing Figures 3.4d and 3.4e that the average particle size of the lignin in zein was smaller than that in starch. The lignin particles in the two composites were estimated to vary between 0.5 - 4 μm. Stevens et al. found the size of lignin in starch/Kraft lignin/glycerol blends was 0.1 to 1 μm[89]. which is similar to our findings.
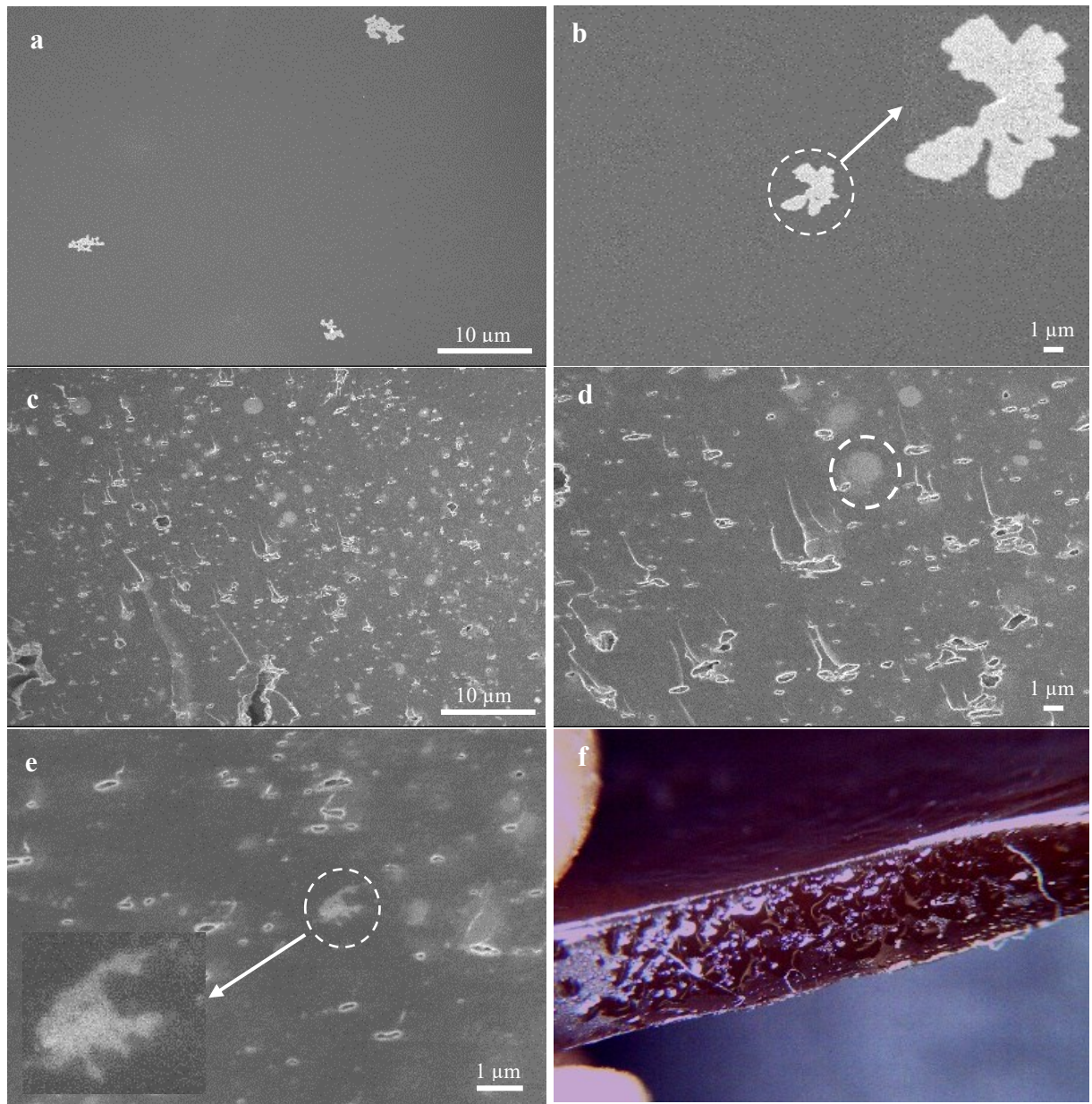
Figure 3.4. SEM micrographs of G(S)P-2 (a and b) and G(Z)P-2 composites (c, d, and e) taken under different magnifications. An optical photograph of the cross section of G(Z)P-2 is shown in f. The circles in b and e indicate the lignin particles. The circle in d indicates the glycerol droplet.

Figure 3.5 shows SEM images of the cross-sections of the composites containing both starch and zein. In the control sample GC (Figure 3.5a1-3), a typical sea-island phase structure could be identified with the sea and island being the starch and zein phases, respectively. The interface between the two phases was obvious. The incorporation of the solution lignin led to a

smaller domain size of zein in GS-2 (Figures 3.5b1-3) and the incorporation of the powder lignin produced the most refined phase structure in GP-2 among the three composites (Figures 3.5c1-3). GP-2 exhibited the smallest domain size of zein and the least distinguishable interface between the starch and zein phases. This evolution of the composite phase structure indicates improved compatibility and strengthened interfacial bonding between the two phases after the incorporation of the lignin, which, based on the composite mechanics theory, contributed to the increases in mechanical properties of the composites containing lignin. It is also worth noting that cavities were still present in the zein phase of the composites. The strong compatibility between glycerol and starch suggests that most of the plasticizer would be distributed in the starch phase in the composites containing both starch and zein.

Figure 3.5. SEM micrographs of GC (a1, a2, & a3), GS-2 (b1, b2, & b3) and GP-2 (c1, c2, & c3) taken under different magnifications. Both composites were mixed in an internal mixer operating at 140 °C and 100 rpm for 15 min.

The reduced domain size of zein and the more compatible interface can be attributed to two possible reasons. One is the increased shear stress during internal mixing. It was observed that the mixing torque was higher for the formulations containing lignin. The higher torque was due to the higher shear stress that was applied on the lignin-containing formulations during mixing. The higher stress promoted breakup of the dispersed zein domains and let to refined phase structure. The second reason is due to the multifunctional lignin, which contains groups including hydroxyl, methoxyl, carbonyl, and carboxyl groups. These groups can interact with the functional groups on starch and zein physically or chemically, and therefore compatibilize the two phases to a certain degree[90,91]. The nano/micro-sized lignin particles dispersed at the starch/zein interface can increase interfacial adhesion between the two phases and therefore hinders agglomeration of the zein domains[92].

Figure 3.6 compares the morphology of two composites containing cellulose nanofibrils. GC-CNF4 contained starch, zein, and four parts CNF whereas GP-2-CNF4 contained additional two parts lignin powder. Besides the sea-island structure, some new observations can be made from these two composites. First, GP-2-CNF4 composite has the smallest zein domain size among the GP-2, GC-CNF4 and GP-2-CNF4 samples. The further reduction in the domain size after the incorporation of CNFs can be ascribed to the increased shear stress in the samples containing CNFs. The mixing torques for GP-2, GC-CNF4 and GP-2-CNF4 were 6 Nm, 9 Nm, and 11 Nm, respectively, indicating the increased shear stress after the CNF incorporation. Second, comparing GC (Figures 3.5a1-3) with GC-CNF4 (Figures 3.6a1-3), the latter showed more distinguishable edges of the zein domains. At the edges of some of the domains, ribbon-like objects, which were hypothesized to be CNF bundles, were pulled out from the surface. In GP-2-CNF4 (Figures 3.6b1-3), CNF bundles could be seen in larger numbers and longer lengths on the surface. The exact reason for this enhanced visibility of CNFs is still unknown, but we hypothesize that it is related to the added lignin in GP-2-CNF4, which can interact with zein, starch, and CNFs during the mixing process and therefore change the phase morphology of the composites.
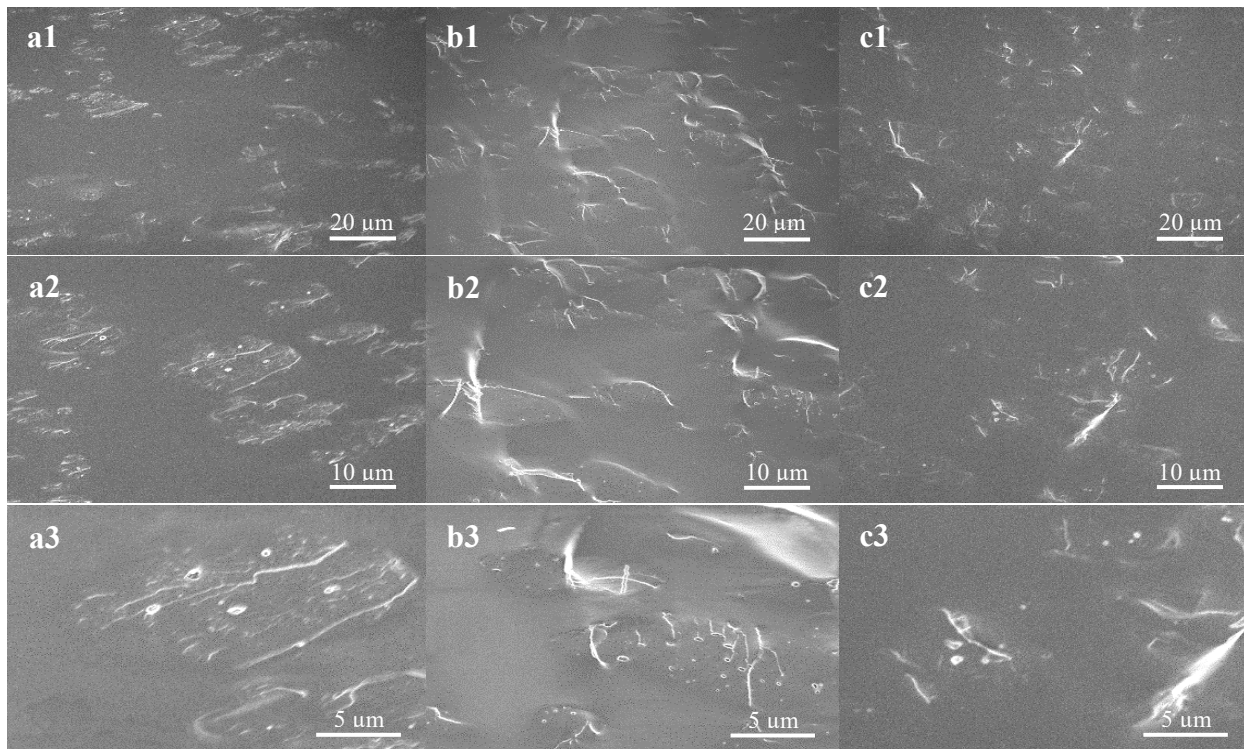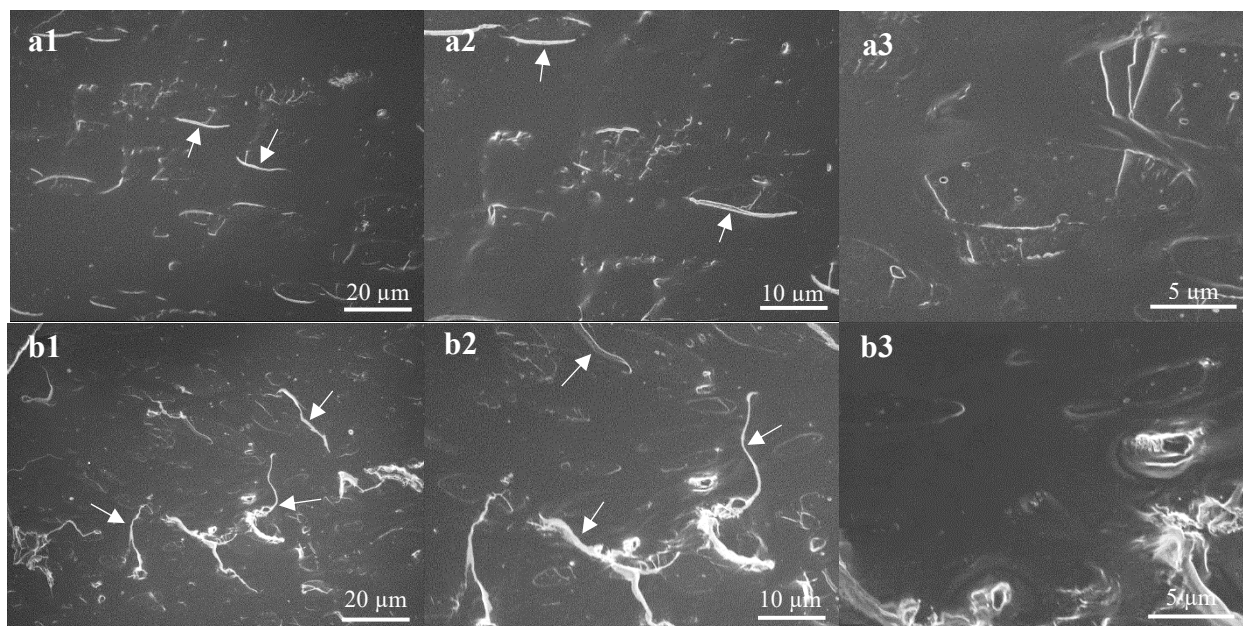
Figure 3.6. SEM micrographs of GC-CNF4 (a1, a2, & a3) and GP-2-CNF4 (b1, b2, & b3) taken under different magnifications. Both composites were mixed in an internal mixer operating at 140 °C and 100 rpm for 15 min. Arrows indicate CNFs.

3.3.4. Energy dispersive spectroscopy (EDS)

To understand the distribution of lignin in the composites, EDS was performed at four spots on the cross section of the composites (spots 1 & 2 on the zein domain and spots 3 & 4 on the starch domain) to analyze their elemental contents, as shown in Figure 3.7. The elemental composition of lignin powder was also analyzed using EDS as a reference. The sodium (Na) and sulfur (S) contents for the lignin and the three composites GC, GS-2, and GP-2 are summarized in Table 3.6 for comparison. The contents of Na and S in the lignin powder were 5.28% and 3.35%, respectively. These two elements originated from the Kraft lignin production process where NaOH and Na_2S were used to dissolve the material. GC as the control sample contained no lignin and the contents of Na and S were very low. The relatively high content of S (0.48%) in the zein domain can be attributed to the -SH and -SS- groups of the protein. After the incorporation of either lignin solution (GS-2) or lignin powder (GP-2), the contents of Na and S were increased in both zein and starch domains of the composites (Table 3.6), indicating that

48

lignin were dispersed in both domains. The increases in the content of Na appeared to be much greater than the increases of S for both domains and composites. For instance, in the starch domain, the content of Na increased from 0.15% (GC) to 0.67% (GS-2) and 0.96% (GP-2), whereas the content of S increased from 0.04% to 0.06% and 0.08% under the same condition. The greater increases in Na might be due to its higher mobility in the composites: dissolved in glycerol/water as ions, the element could be uniformed dispersed throughout the composites during the mixing. Therefore, strong Na signals could be detected by EDS at any spot on the cross-sectional surface. By contrast, S is covalently connected to lignin molecules and its distribution depends on the distribution of lignin. As shown in Figure 3.4, lignin particles were scattered on the surface, suggesting ununiform distribution of S. In addition, the original content of S in the lignin powder was lower than that of Na (3.35% vs 5.28%). These two factors together result in relatively low detection rate of S in the composites.
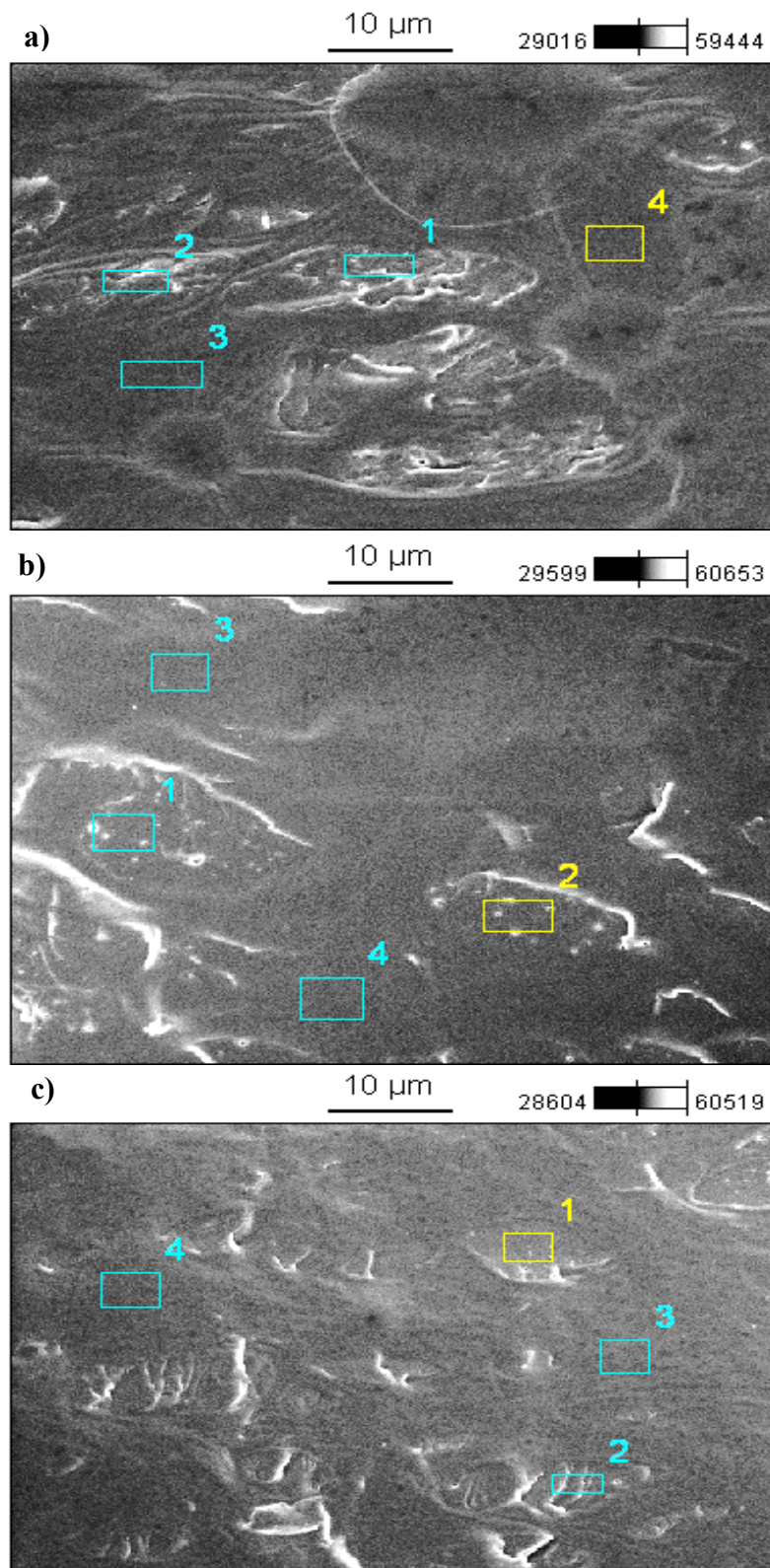
Figure 3.7. SEM images showing the areas where the EDS analysis was conducted. (a) GC, (b) GS-2, and (c) GP-2. In every image, areas 1 and 2 represent the zein phase and areas 3 and 4 represent the starch phase.

Table 3.6. Contents of sulfur and sodium in the zein and starch phases of the composites from EDS analysis.

	Lignin powder	GC		GS-2		GP-2	
		Zein	Starch	Zein	Starch	Zein	Starch
Na-K (atom%)	5.28	0.02	0.15	0.1	0.67	0.37	0.96
S-K (atom%)	3.35	0.48	0.04	0.52	0.06	0.5	0.08

3.3.5. Thermogravimetric analysis (TGA)

TGA was performed on the composites and their ingredients to determine the thermal stability of the composites. TGA curves of all the samples and their first derivative (DTG) curves are compared in Figure 8. Based on Figures 3.8a and 3.8b, the two plasticizers showed the lowest decomposition temperatures (173°C and 233°C) among all the ingredients. A simple one-step decomposition process was demonstrated by both materials. By contrast, all the three biobased ingredients, i.e., starch, zein, and lignin, exhibited more complicated decomposition behaviors due to their complex structures. Starch and zein showed mild weight losses below 100°C due to the removal of moisture. A major rapid decomposition event occurred for all the three materials with a peak decomposition temperature at ~ 300°C, followed by relatively slow further decomposition at higher temperatures.

In Figure 3.8b, starch showed the highest weight loss rate among the three biobased ingredients at ~ 300°C, which can be attributed to its relatively simple pyrolysis mechanism. Elimination of the hydroxyl groups, scission of the glycosidic and other covalent bonds, and possible transglucosidation occurs at this temperature range. The degradation peak at 495°C corresponds to the oxidation of the material's carbonaceous residue[93–95].

The weight loss rate of zein at ~300°C was much lower than that of starch and the peak width was also widened to a range between ~ 225°C and ~ 375°C. The process involved two overlapping thermal processes, which likely corresponded to volatilization of impurities and

thermal degradation of zein, with their peak temperatures at 260 and 300 °C, respectively[96]. At temperatures higher than 420 °C the degradation residue of zein is oxidized[96–98]. The peak at around 530 °C may be due to the degradation of impurity included in the product[99].

Among the three natural biopolymers, lignin showed the highest thermal stability, featuring the lowest weight loss rate at ~ 300ºC and the highest residual weight of ~ 56% at 600°C. The thermal degradation of lignin in air consisted of three main steps and resulted in a weight loss over a broad range of temperatures (25–600 °C). The weight loss below 125 °C was due to moisture evaporation and scission of the side chains which led to the release of CO, CO_2, and other volatile products[100]. Between 200 and 400 °C, the inter-unit bonds were fractured and thereby monomer phenol was released in the vapor phase[101]. Above 400 °C, the sample mass loss was related to the decomposition or condensation reactions of aromatic rings and the oxidation of the degradation products. The large amount of char residue at 600°C (~ 56%) can be attributed to the high aromatic content of lignin. Similar observations have been reported by other researchers[93,96,101–105].
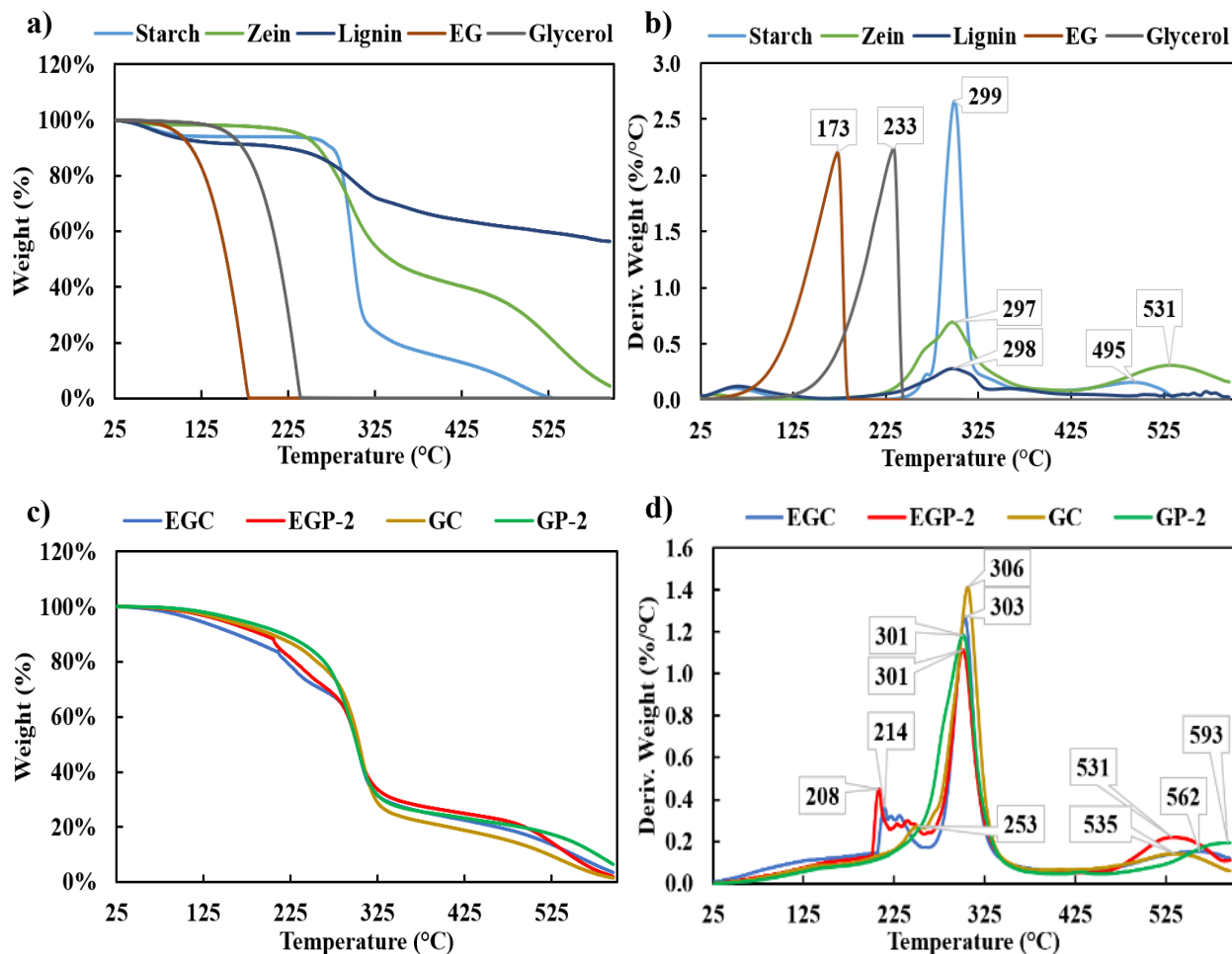
Figure 3.8. TGA and DTG curves for starch, zein, lignin, glycerol and ethylene glycol (a and b) and their composites (c and d).

The decomposition of the composites was largely controlled by that of the ingredients. From Figures 3.8d, the peak degradation temperature of ethylene glycol in the composites (EGC and EGP-2) was increased to 208-214°C, significantly higher than that of the free plasticizer (173°C). The peak temperature for starch and zein was also increased to ~ 305°C from less than 300°C. These increases can be partially attributed to the different forms of the materials: free liquid or loose powder as the neat ingredients versus compact solid pieces of the composites. The latter exhibit stronger resistance to mass and heat transfer than the former and therefore show lower weight loss rates. Another reason for ethylene glycol's much higher degradation

53

temperature in the composites than its free form is that the plasticizer likely forms hydrogen bonds with starch and zein, leading to a higher energy requirement for its degradation. Moreover, instead of one sharp decomposition peak for the free-form ethylene glycol, the decomposition of the bond ethylene glycol occurred over a ~ 50°C range starting from the peak temperature, indicating again the slowed degradation and improved thermal stability.

Figure 3.8d also shows that the decomposition peak temperature of glycerol was increased to 253°C in the composites (GC and GP-2). Its weight loss rate was much lower than that of ethylene glycol in the composites, which is likely due to glycerol's higher polarity and stronger bonding to starch and lignin. The main decomposition peaks of the composites range from 301°C to 306°C, as shown in Figure 3.8d. These peaks correspond to the degradation peaks of starch, zein, and lignin within the temperature range 297°C - 299°C in Figure 3.8b, suggesting slight improvements in thermal resistance of the ingredients.

Focusing on the weight loss of the composites (Figure 3.8c), the composites containing glycerol as their plasticizer (i.e. GC & GP-2) showed a lower weight loss below 275°C compared to the composites containing ethylene glycol (e.g. EGC & EGP-2). This is due to the higher thermal stability of glycerol than ethylene glycol as discussed previously. The composites containing lignin (i.e. EGP-2 & GP-2) also showed a slightly lower weight loss than the composites without lignin (i.e. EGC & GC) over most of the test temperature range. The difference can be attributed to the high thermal stability of lignin.

3.4. Conclusion

Glycerol-plasticized and ethylene plasticized composites were prepared using internal mixer. The incorporation of lignin particles can significantly improve the mechanical properties of starch-zein blend regardless of the plasticizer types as demonstrated by tensile test and

scanning electron microcopy (SEM) micrographs, especially the incorporation of the powder lignin which appears to lead to higher overall mechanical properties and smaller domain size of zein phase in the blends than incorporation of lignin nanoparticle solutions. With the increasing lignin content, the mechanical properties of blends increased, which indicated better interfacial bonding between starch and zein, especially for GP-2. Compared to control sample (GC sample), the modulus and tensile strength of the GP-2 sample were increased by ~300% and ~130%, respectively. The introduced of cellulose nanofibrils (CNFs) were further enhanced the modulus and strength of the blends. Compared to control sample (GC sample), the modulus and strength of GC-CNF6 sample were increased by ~400% and ~140%, respectively. The GP-2-CNF6 exhibited the largest increases in modulus (~510%) and strength (~240%), suggesting strong synergy between lignin and CNFs in reinforcing the corn-based thermoplastic. However, the thermogravimetric analysis showed that the thermal stability of the blends was only slightly improved with the incorporation of lignin.

4. USE OF CITRIC ACID AS A PROCESSING AID FOR THERMOPLASTIC STARCH-ZEIN COMPOSITES

4.1. Introduction

Citric acid has been reported to be able to significantly reduce the shear viscosity of thermoplastic starch (TPS) and improve its processability. This is because citric acid can cause fragmentation and dissolution of starch granules and weaken the interaction between starch molecules, facilitating inter-molecule movement[106,107]. The reduction in TPS viscosity improved the blending of TPS with other thermoplastics including polyethylene (PE) and polylactic acid (PLA)[37,106,107]. As a polar reactive chemical, citric acid can form strong bonds with starch and is reported to improve the thermal stability and water resistance of TPS and protect starch from retrogradation and re-crystallization[108,107]. However, high content of citric acid in TPS can cause a substantial decrease in tensile strength of the material due to severe starch degradation.

In this chapter, citric acid is used to replace water as the processing aid and compatibilizer/crosslinker in the composite formulations studied in Chapter 3. The incorporation of citric acid is hypothesized to improve the processability of native starch, improve the thermostability of the composites and improve the compatibility between starch and zein, and therefore increased the mechanical properties of the new thermoplastic. With the combination of lignin and cellulose nanofibrils, the mechanical properties of the citric acid included starch-zein thermoplastic should be further increased. The synergy of these ingredients has not been explored in any prior studies and it can lead to a new class of materials with a good balance of sustainability, functionality, and performance. The new material can be readily processed into final products using existing techniques such as extrusion and injection molding, making an impact on the plastics industry.

4.2. Materials and Methods

4.2.1. Materials

Argo® pure corn starch (10% moisture) was purchased from a local grocery store. Zein (F4400C-FG, properties provided in Table A2 in the appendix.) and glycerol (99+%) were purchased from Flo Chemical and Alfa Aesar, respectively. Kraft lignin and citric acid monohydrate were purchased from Sigma-Aldrich. The lignin contained 4% sulfur and had an average Mw of ~10,000. CNF slurry (CNFs dispersed in water) with a CNF concentration of ~2.5 wt% was purchased from the Process Development Plant of the University of Maine. All the chemicals and materials were used as received without further purification or modification.

4.2.2. Methods

4.2.2.1. Preparation of thermoplastic composites

4.2.2.1.1. CNFs/glycerol/citric acid mixture preparation

Citric acid (CA) and glycerol were used as the crosslinker and plasticizer in the product, respectively. To prepare the CNFs/glycerol/CA mixtures, CA was dissolved in glycerol (CA : glycerol = 0.5 : 35 by weight) by stirring with a high-speed homogenizer (IKA® T25 digital ULTRA-TURRAX®) at 3600 rpm for 10min. The received CNF slurry was concentrated using a centrifuge (Eppendorf® Centrifuge 5804) to increase the concentration to ~12 wt%. Next, predetermined amounts of the concentrated CNF slurry were added into the CA/glycerol solution to obtain CNF/glycerol/CA mixtures with the ratios of the three components at x/35/0.5 (w/w/w, x=2, 4, 6). The mixtures were sonicated (Sonicators® 3000) in an ice bath to break apart CNF agglomerates and achieve stable, homogeneous CNF suspensions in CA/glycerol. Finally, the sonicated suspensions were placed in a Lab-Line vacuum oven (Thermo Fisher Scientific) at 90°C and 80 inHg to remove the water (brought into the mixtures by the CNF slurry). The paste-

like water-free mixtures were sealed and stored under ambient conditions for future use. The

formulations and sample codes of the obtained CNF mixtures are listed in Table 4.1.

Table 4.1. Formulations of water-free CNFs/glycerol/CA mixtures.

Sample Code	Ingredients (All in parts)		
	Glycerol	Citric Acid	Cellulose Nanofiber
CNF2	35	0.5	2
CNF4	35	0.5	4
CNF6	35	0.5	6

4.2.2.1.2. Preparation of thermoplastic starch-zein and cornmeal composites

Starch, zein, and lignin were all in dry powder format. They were weighted and manually

mixed in a beaker following the formulations listed in Table 4.2. The powder mixtures were then

blended with the prepared CNFs/glycerol/CA mixtures in a kitchen blender and then sealed in a

plastic bag and stored overnight to achieve equilibrium. In the sample codes of Table 4.2, SZ

denotes the starch/zein mixture, which were the matrix materials of the composites. LP denotes

the lignin powder. The numbers after the LP and CNF indicate the number of grams for the

lignin and CNFs (dry weight). For instance, SZ-LP6-CNF6 means that the composite contains 6

grams of lignin powder and 6 grams of CNFs. Letter C in the sample codes of SZC indicates that

the denoted sample is control a sample containing no lignin and CNFs.

Table 4.2. Formulations of corn-based thermoplastic composites. Starch contains ~ 10% moisture.

Sample Code	Ingredients (All in parts)					
	Starch	Zein	Glycerol	CA	Lignin	CNF
SZC	88.89	20	35	0.5	0	0
SZ-CNF4	88.89	20	35	0.5	4	0
SZ-CNF6	88.89	20	35	0.5	6	0
SZ-CNF10	88.89	20	35	0.5	10	0
SZ-LP4	88.89	20	35	0.5	0	4
SZ-LP6	88.89	20	35	0.5	0	6
SZ-LP10	88.89	20	35	0.5	0	10
SZ-LP4-CNF4	88.89	20	35	0.5	4	4
SZ-LP6-CNF6	88.89	20	35	0.5	6	6

The equilibrated composite formulations were compounded into thermoplastics using a co-rotating HAAKE twin-screw extruder (Rheomex™ PTW16 OS, screw diameter d = 16 mm, screw L/D ratio = 40:1, Germany) operating at 100 rpm. The extruder temperatures were set to 90°C, 120°C, 140°C, 140°C, 140°C, 140°C, 140°C, 140°C, and 140°C from the feed zone to the die. The thermoplastics were extruded through a slit die with a 25 mm x 0.5 mm rectangular opening (Thermo Electron) to produce ribbon-like extrudates, which were sealed in plastic bags immediately after extrusion and were transferred into a desiccator (~ 45% relative humidity at 20°C) and stored for 24h before testing. The flow chart of the sample preparation process is shown in Figure 4.1.
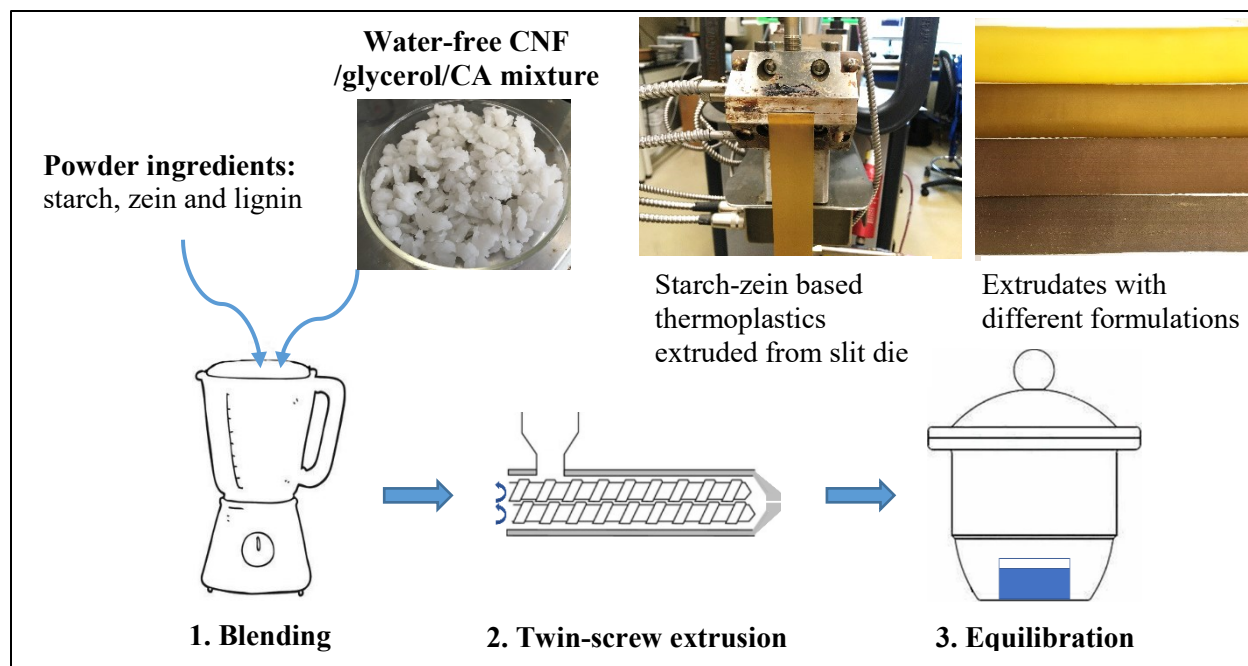
Figure 4.1. Flowchart of the starch-zein-based thermoplastic sample preparation process.

4.2.2.2. Mechanical properties of the starch-zein-based thermoplastics

Dumbbell shaped tensile test bars were cut from the extruded ribbons. Tensile tests were performed under ambient conditions (~ 23 °C) on an MTS Insight test system equipped with a 5 kN electronic load cell at a crosshead speed of 50 mm/min.

4.2.2.3. Scanning electron microscopy (SEM)

Scanning electron microscopy (SEM) was used to study the morphology of the microstructure of the composites. Samples were frozen and fractured in liquid nitrogen to produce a clean cross section. They were attached to aluminum mounts with colloidal silver paste (Structure Probe Inc., West Chester PA, USA) for view of the fractured surface and then coated with a conductive layer of gold using a Cressington 108auto sputter coater (Ted Pella Inc., Redding CA, USA). Images were obtained at an accelerating voltage of 15 kV using a JEOL JSM-6490LV scanning electron microscope (JEOL USA, Peabody MA, USA).

4.2.2.4. X-ray diffraction

X-ray diffraction (XRD, Bruker D8 Discover X-ray diffractometer) measurements were operating at 40 kV and 40 mA with Cu Kα source ($\lambda = 0.154$ nm). The scanning rate is 2°/min. The 2θ range was 3–58°.

4.2.2.5. Fourier transform infrared spectrometry (FTIR)

Fourier-transform infrared spectroscopy (FTIR, Thermo Scientific Nicolet 8700 FTIR spectrometer) was used to characterize the chemical bonds of native ingredients (starch, zein, lignin, CNF) and their film composite samples. FTIR spectra (4000–650 cm^{-1}) were collected using an ATR accessory for both powder and film composite samples.

4.2.2.6. Thermogravimetric analysis (TGA)

Thermogravimetric analysis (TGA, TA Instruments Q500) was performed to determine the thermal stability of the composites and the constituents. All sample were tested between room temperature and 600°C with a heating rate of 10°C/min under a continuous air flow (60 ml/min).

4.3. Results and Discussion

4.3.1. Mechanical properties

Tensile test results for all the formulations listed in Table 4.2 are compared in Figure 4.2. The stress-strain curve for each formulation is provided in Figure A3 in the appendix. The composites reinforced by lignin and the composites reinforced by CNF showed a similar property trend (except for SZ-CNF10): a higher reinforcement content (lignin or CNF) led to higher strength and modulus of the samples. The composites containing both lignin and CNF exhibited the highest strength and modulus. While the strength and modulus were improved, the ultimate strain and toughness of the samples were decreased as the samples became increasingly

rigid. The incorporation of six grams of lignin and six grams of CNFs led to the best overall mechanical properties among all the formulations. Table 4.3 summarizes the percentage changes of the properties for all the composites compared to those of the control sample SZC. The decreases in strength and modulus for the SZ-CNF10 sample may be attributed to poor dispersion of CNFs and other defects in the composites. It was noticed that the extrusion became very difficult (high torque, overheating, etc.) at the high CNF content due to the high viscosity of the material, which could cause a series sample defects including inhomogeneous blending, material thermal degradation, etc.
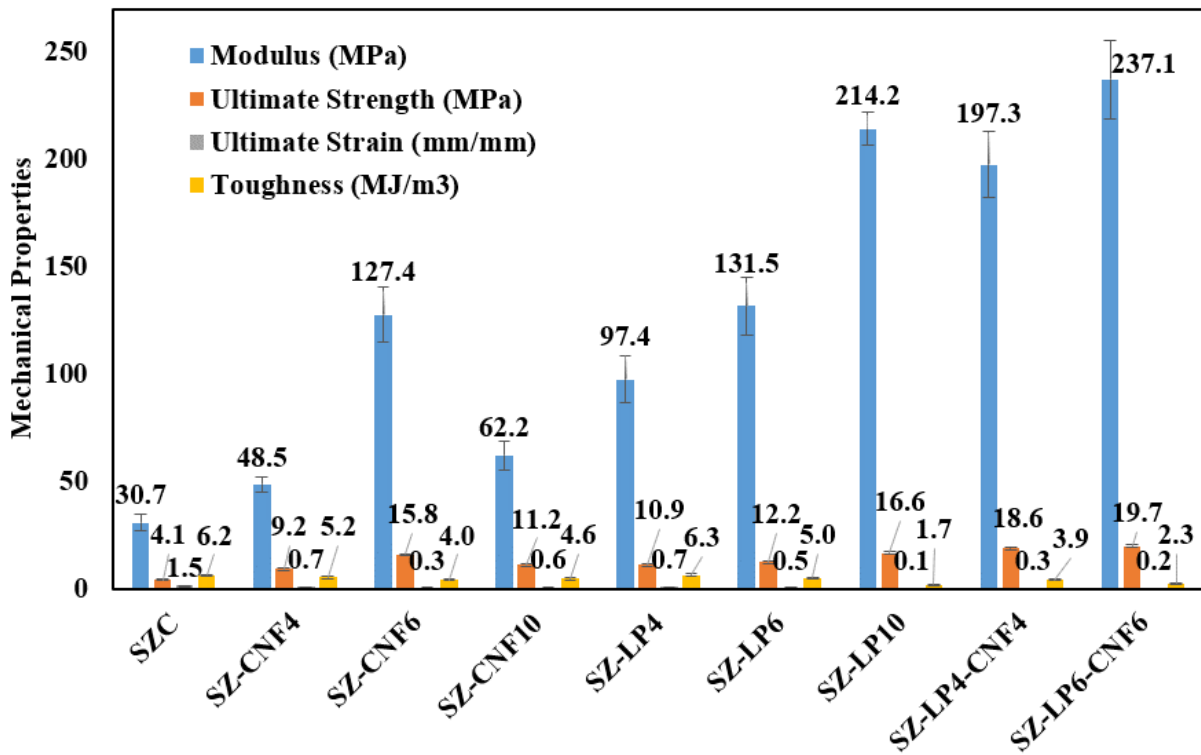

Figure 4.2. Tensile test results of the corn-based thermoplastics based on starch/zein mixture.

Table 4.3. Percentage changes in tensile properties of the composites.

	Modulus	Ultimate Strength	Ultimate Strain	Toughness
SZC	0.0%	0.0%	-0.3%	-0.1%
SZ-CNF4	57.7%	127.7%	-49.1%	-16.2%
SZ-CNF6	314.8%	290.8%	-76.2%	-35.0%
SZ-CNF10	102.3%	176.2%	-59.7%	-24.8%
SZ-LP4	217.0%	169.3%	-54.3%	2.0%
SZ-LP6	328.1%	201.0%	-67.2%	-18.2%
SZ-LP10	597.1%	310.8%	-90.0%	-73.1%
SZ-LP4-CNF4	542.1%	360.0%	-80.4%	-36.3%
SZ-LP6-CNF6	671.7%	386.4%	-88.8%	-63.5%

For the composites containing both lignin and CNFs, they all exhibited much higher moduli and strengths compared to the composites containing only lignin or CNFs, see Figure 4.2 and Table 4.3. The modulus of SZ-LP4-CNF4 was 2.0 and 4.1 times that of SZ-LP4 and SZ-CNF4, respectively, whereas the strength of SZ-LP4-CNF4 was 1.7 and 2.0 times that of the two single-reinforcement composites. For SZ-LP6-CNF6, its modulus was 1.8 and 1.9 times that of SZ-LP6 and SZ-CNF6, respectively; its strength was 1.6 and 1.2 times that of the two composites. The increases in mechanical properties of the dual-reinforcement composites were even more significant when compared with the control sample (SZC). For example, the moduli of SZ-LP4-CNF4 and SZ-LP6-CNF6 were increased by 542.2% and 671.8%, respectively, while their strengths were increased by 360.0% and 386.4%. It should be pointed out that the composites containing both lignin and CNFs exhibited reduced ultimate strain and toughness compared to the control sample and the samples containing only lignin or CNF. The increases in the modulus and strength and the reduction in the strain can be both attributed to the synergetic reinforcement effect of the lignin and CNFs on the corn-based thermoplastic. Lignin nanoparticles in the starch-zein blend have been shown to refine the phase structure of the blend and increase the compatibility of the two phases, leading to improved mechanical properties.

CNFs as a nanofibrous material is known to significantly reinforce polymers at low fiber concentrations. The interactions between the nanomaterials and the polymer chains reduced the mobility of the chains and resulted in decreased strain and toughness.

4.3.2. SEM

The fracture surface of the control sample SZC was flat and smooth as shown in Figure 4.3a. Compared with the SEM images of the samples (containing no citric acid) in Chapter 3, no "sea-island" phase structure was observed on the fracture surface of SZC (Figure 4.3a), indicating that the compatibilizing effect of CA on starch and zein[84,109]. Under high shear and high temperature conditions, glycerol and citric acid will be able to disrupt intermolecular and intramolecular hydrogen bonds and plasticize native starch[107]. Besides, citric acid can obviously decrease the shear viscosity and improve the processability of TPS by promoting the fragmentation and dissolution of cornstarch granules[107].

The surface of the composites containing lignin (Figure 4.3c) was similar to that of the control sample, demonstrating lignin's good compatibility with the system. The fracture face of the sample containing CNFs (Figure 4.3b) is however rougher compared with the first two samples. The rough surface can be an indication of CNF agglomeration in the composite. During its sample preparation, concentrated CNF slurry was mixed with glycerol/CA solution using a sonicator and then dried in the oven to achieve a water-free condition. The resulting mixture was a highly viscous, paste-like material, which caused high torque and overheating in the subsequent twin-screw extrusion. The difficulties experienced in processing the sample contributed to the ununiform phase structure and further to the relatively low mechanical properties of the SZ-CNF10 sample as found from the tensile test in the previous section.
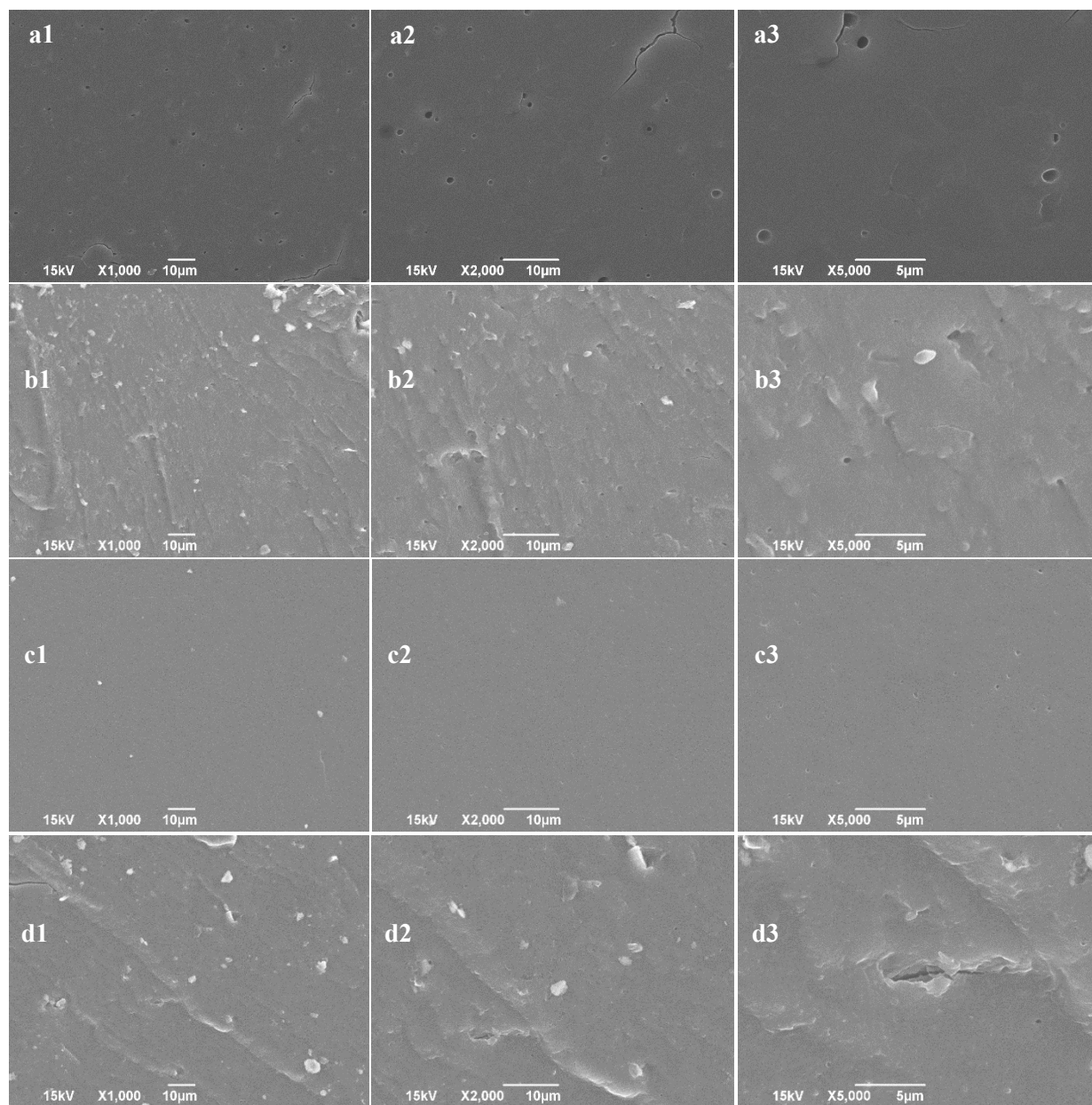
Figure 4.3. SEM micrographs of SZC (a1, a2, and a3), SZ-CNF6 (b1, b2, and b3), SZ-LP6 (c1, c2, and c3), SZ-LP6-CNF6 (d1, d2, and d3) taken under different magnifications.

4.3.3. XRD

XRD was used to investigate the crystalline structure of the samples. Figure 4.4 exhibits the XRD patterns of the CNF, SZC, SZ-LP6 and SZ-CNF6. CNFs showed diffraction peaks at 2θ 34.4°, 22.7°, 15.1° and 16.4°, which are the characteristic diffraction patterns of cellulose I crystals[110]. The diffraction peaks at ~9.5°and 29° may be due to impurities in the sample.

Thermoplastic starch is almost amorphous right after extrusion because starch crystals are disrupted/melted under the shear and heat. However, starch can recrystallize if aged above its glass transition temperature. The short outer chains of amylopectin crystallize into the B-type structure, with a characteristic peak at 16.8°[84]. The crystallization of amylose involving glycerol can form V-type crystalline structure, which can be further categorized into two subtypes, Va (anhydrous) and Vh (hydrated)[84]. Va shows XRD peak at 13.2° and 20.6°, while Vh has peaks at 12.6° and 19.4°. In this study the control sample SZC showed peaks at 13.1°, 18.8°, and 20.0°, indicating recrystallization of starch in the sample. These three peaks were shifted to higher angles in the SZ-LP6 and SZ-CNF6 composites, suggesting a reduction in the crystal cell size and the refining of the starch crystal structure in the presence of lignin or CNFs. The two peaks at 38.3° and 44.5° on the diffraction patterns of all the composite are due to CA[111]. Zein became completely amorphous after the extrusion and displayed no diffraction peaks in the Figure[84].
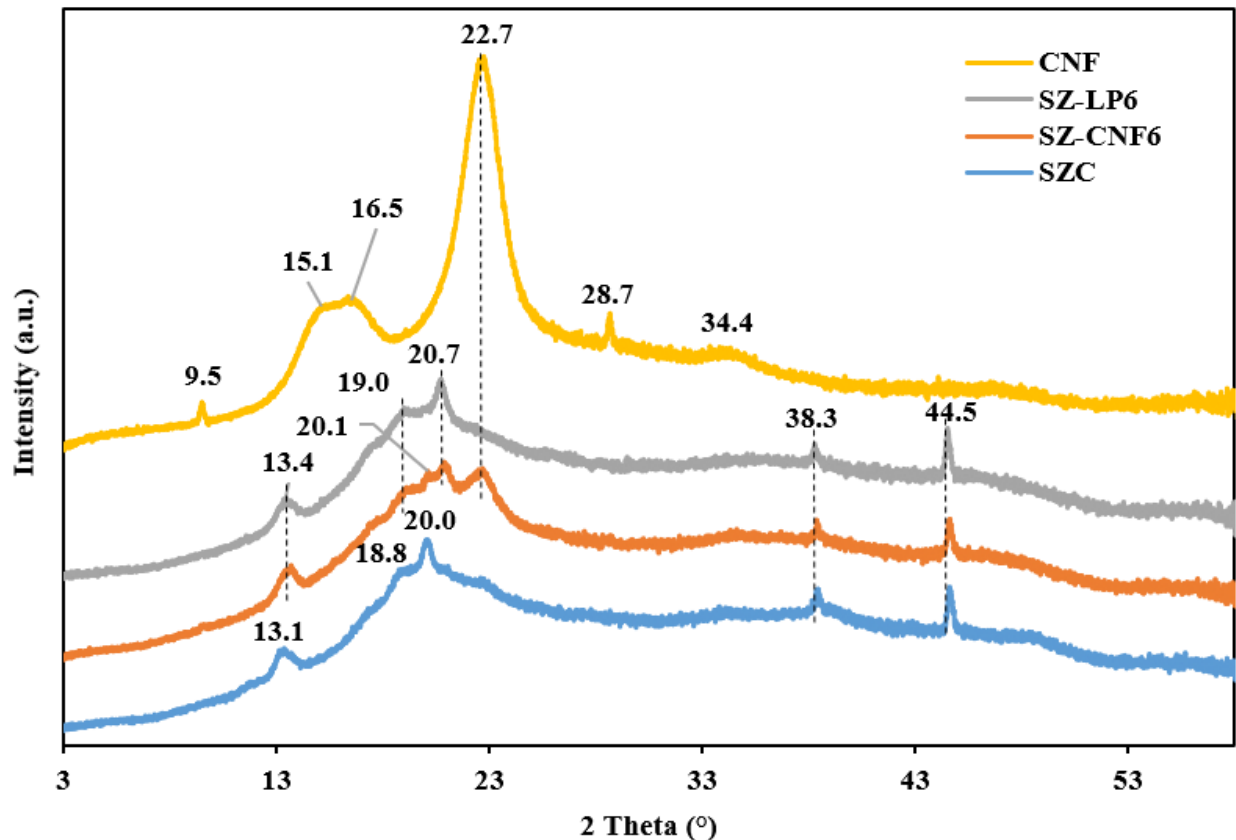
Figure 4.4. XRD patterns of the CNFs, SZC, SZ-LP6 and SZ-CNF6.

4.3.4. FTIR

The amorphous state of starch could be identified by the band at 1025 cm^{-1}, while the band at 1047 cm^{-1} was assigned to crystalline state of starch[112,113]. The signal around 1000 cm^{-1} may corresponded to water sensitive of sample which related to intramolecular hydrogen bonding of hydroxyl groups[112,113]. All extruded sample revealed two peaks at 1000 and 1025 cm^{-1} in the FTIR spectra, as shown in Figure 4.5. This may be related to the -OH and -COOH groups of citric acid form hydrogen bonding with both C-O-H and C-O-C groups in starch, C-O-H group in glycerol, as well as the -NH group from zein[107]. The results reveal that both amorphous phase and crystalline phase of starch were occurred in the extruded sample.

The band referring to C=O stretching of the amide group occurred at 1650 cm^{-1} in native zein, as well as starch-zein based composites[114]. The band at 1645 cm^{-1} was ascribed to the

bending vibration of H-O-H from water. The stretching vibrations band at 3324 cm^{-1} could be attributed to the oxidation in the ambient environment and adsorbed water[115]. The band at 2920 cm^{-1} may attribute to -CH_2 stretching vibration from starch[114,116]. Band at 1147 cm^{-1} and 1082 cm^{-1} may both corresponded to C–O–H stretching vibration[116]. The absorption band at 1460 cm^{−1} was attributed to the N-H bending and C-N stretching combination[117]. FTIR spectra showed no noticeable peak shifting.
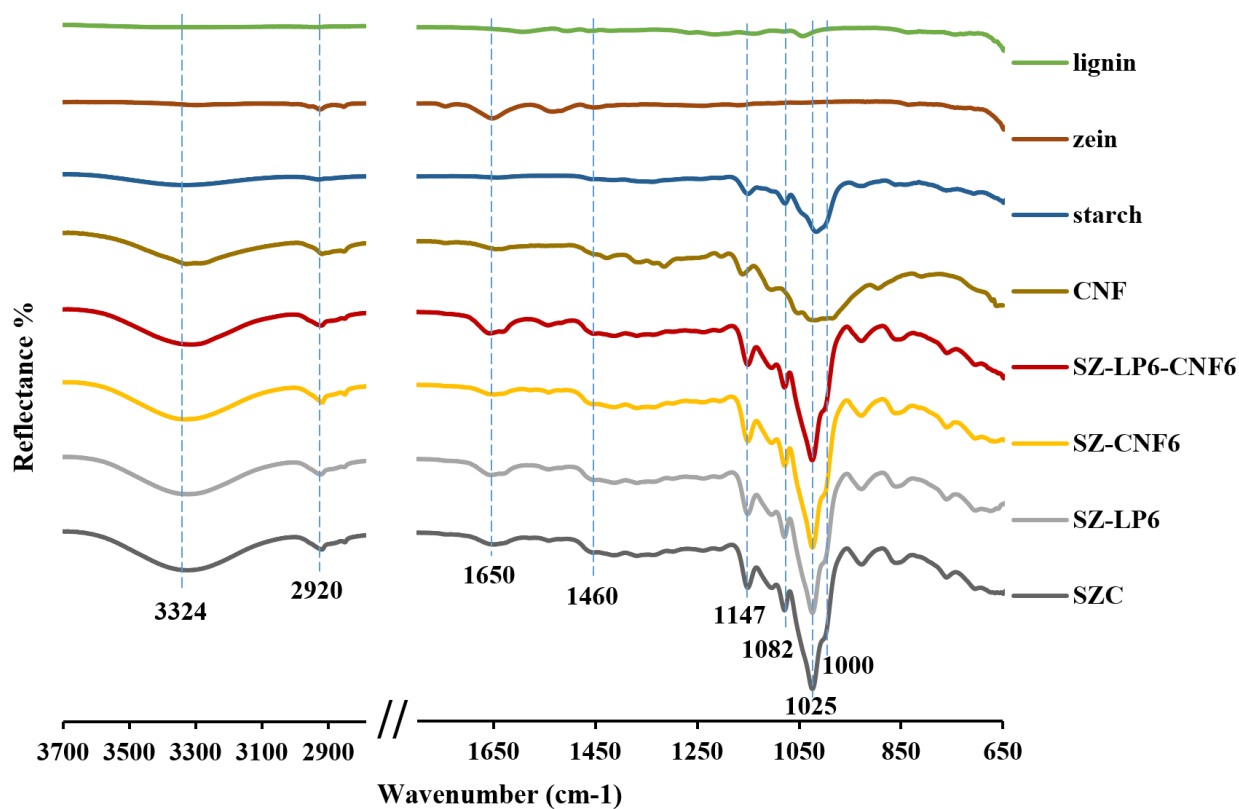
Figure 4.5. Fourier transform infrared spectroscopy (FTIR) spectra of neat lignin, zein, starch and CNFs and their composites including SZC, SZ-LP6, SZ-CNF6 and SZ-LP6-CNF6.

4.3.5. TGA

TGA study was conducted over a temperature range of 25-600 °C to identify the thermostability of the native ingredients and the extruded composites. Figure 4.6 presents the results of TGA and differential thermogravimetry (DTG) curves. The weight loss below 100°C was mainly ascribed to water loss. Overall, after heating the films to 600 °C, the lignin-

68

containing starch-zein blends showed a lower weight loss than the composites without lignin, which can be attributed to lignin's high thermal stability. As shown in Table 4.4, the residual weight of lignin was ~56% at 595.6 °C. Compared to SZC, the remaining weight of SZ-LP6 was 10% higher, suggesting that the incorporation of lignin could improve the thermal stability of the starch-zein blends.

Thermal degradation of starch involves the dehydration and main chain secession. The starch DTG curve has three peaks, 58.6 °C, 298.9 °C and 494.4 °C, respectively[118]. The first weight loss occurred between room 25 °C to 100 °C, which was due to the loss of the absorbed and bound water. The second degradation peak at around 300 °C is due to starch thermal decomposition[119]. The third weight loss observed at 495°C may be ascribed to the oxidation of the carbonaceous residues[120], during which CO_2 and CO are produced from oxygen-containing materials from 350 °C to 500 °C[118].

The DTG curve of zein had two major peaks with the first maximum at 297°C and the second one at 531°C. The first one appeared to include overlapping thermal processes which were likely caused by the volatilization of impurities and the pyrolysis of zein. The second peak may be due to the degradation of impurity included in the product[121,122,123].
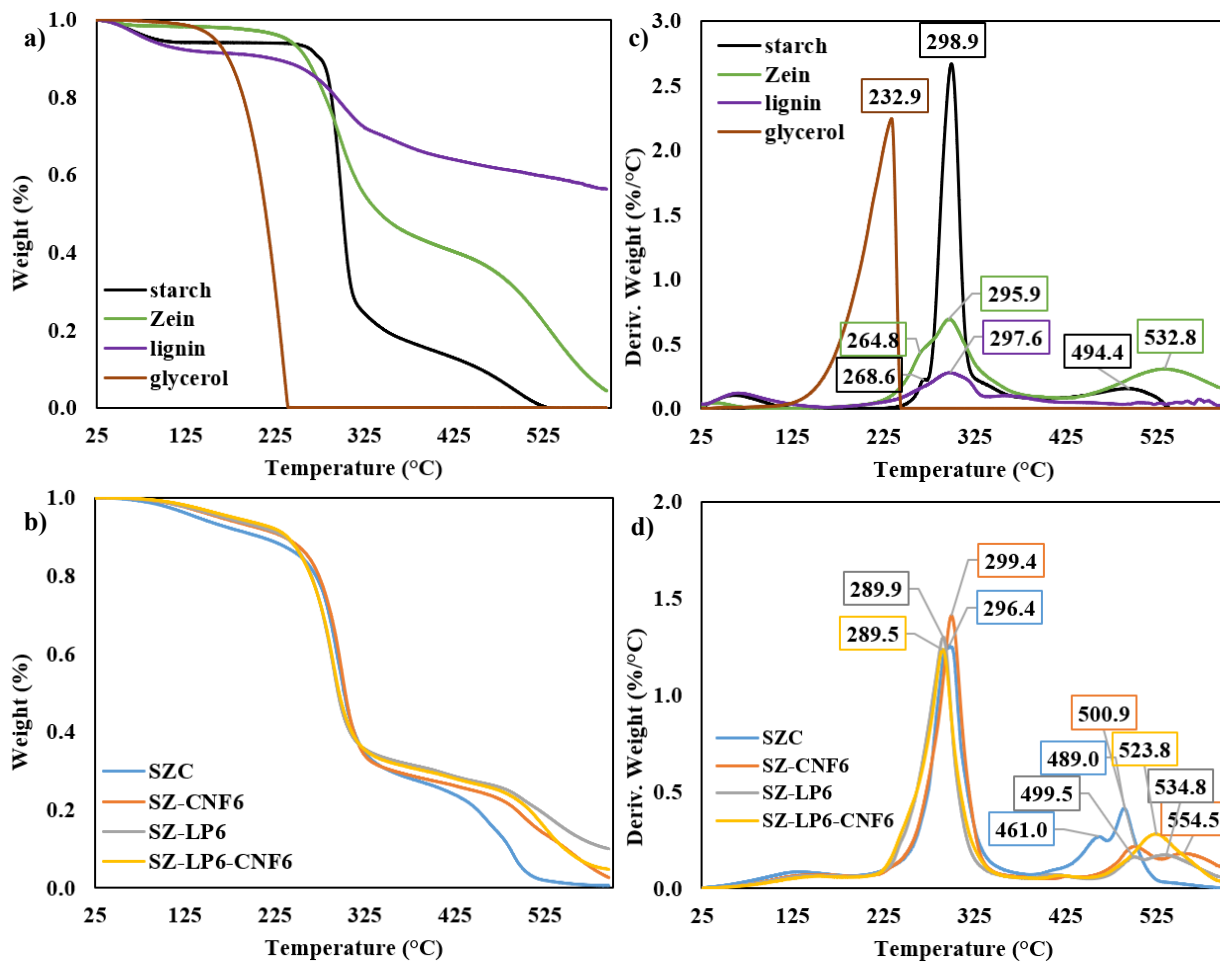
Figure 4.6. (a-b) TGA plot of starch, zein, lignin, glycerol and extruded composites. (c-d) weight loss derivative of starch, zein, lignin, glycerol and extruded composites.

Table 4.4. Native ingredients and composites' peak degradation temperature.

	Peak Degradation Temperature (°C)				80% Weight Loss Temperature (°C)	Remaining Weight at 595.6°C
	1st stage	2nd stage	3rd stage	4th stage		
Starch	58.6	298.9	494.4	-	347.1	0%
Zein	264.8	295.9	532.8	-	532.0	4.4%
Lignin	62.3	297.6	-	-	N/A*	56.4%
Glycerol	232.9	-	-	-	230.1	0%
SZC	130.9	296.4	461.0	489.0	449.5	0.6%
SZ-CNF6	140.9	299.4	500.9	554.5	492.6	2.6%
SZ-LP6	144.6	289.9	499.5	534.8	517.5	10%
SZ-LP6-CNF6	147.2	289.5	523.8	-	507.2	4.7%

* Not applicable.

70

As shown in Table 4.4, 80 % weight loss of the composites occurred was between native corn starch (347°C) and zein (532°C). temperature This indicated that the presence of citric acid increased the compatibility between starch and zein. Composites incorporated with only 6 parts of lignin and 6 parts of CNFs show two degradation peaks between the last degradation peak of starch and zein or even above, which confirmed the improvement of their thermal stability compared to pure starch and zein. In addition, by comparing Figure 4.6d with 4.6b, it could be easily noted that the third degradation peaks of SZ-LP6-CNF6 only exhibits one degradation peak between 494.4°C and 532.8 °C, in other word, this composite showed the best compatibility between ingredients. The exception of SZC may be due to the possibly acidolysis of starch occurred in the system as a side reaction. So, although the addition of citric acid can improve the thermal stability of the composite, the possibly side reaction could decrease the thermal stability of thermoplastic starch[107]. In conclusion, the incorporation of both lignin and CNFs enhanced the compatibility between starch and zein the most. This may be contributed to the highest shear rate caused by the addition of both reinforcement agents.

4.4. Conclusion

Corn-based thermoplastics with high mechanical properties were developed from this research. Lignin and CNFs, two biobased materials derived from plants, were the critical ingredients that provided significant reinforcement to the corn plastics. The purified starch/zein mixture could be used as the main feedstock to produce the plastics. However, the cornmeal had a great cost advantage over the starch/zein mixture while offering similar product properties. With the increasing lignin and cellulose nanofibrils content, the mechanical properties of blends increased, except SZ-CNF10 sample. The extrusive may due to the dispersion status of CNF. With relatively low plasticizer content, more cellulose granular structures were found from the

SEM image which decreased blends modulus and strength on the contrary compared to SZ-CNF6 sample. SZ-LP6-CNF6 exhibited the largest increases in modulus and strength, 671.7% and 386.4% respectively, compared to the control sample (SZC). The "sea-island" structure was no longer be found in the citric acid included blends, which may be ascribed to the better compatibility between starch and zein. Besides, the addition of citric acid improved thermal stability of composites compared to pure starch and zein, except for SZC. The exception was possibly ascribed to the acidolysis of starch occurred in the system as a side reaction.

5. THERMOPLASTIC COMPOSITES BASED ON CORNMEAL

5.1. Introduction

Zein was use as a hydrophobic ingredient in the previous chapter to increase the mechanical properties and water barrier properties of TPS. However, zein is an expensive material ($20-70 per kg) compared to other biopolymers due to the costly material separation and purification processes in zein production[118]. Thus, to find an economic substitute for zein becomes very important for large scale industrial applications of the corn plastic. Cornmeal is a low-cost material containing both starch and zein. It is produced by directly grinding corn kernel into a powdered material. Cornmeal contains around 72.9% of carbohydrate (out of which 84% is starch), 9.85% protein (mainly zein) and 5.88% fat[119].

In this chapter, it is hypothesized that the replacement of starch and zein with cornmeal is feasible because of the main ingredients of cornmeal being starch and zein. The goal of this study is to evaluate the potential of using cornmeal as a substitute to the starch-zein matrix to decrease the cost of the product for large scale industrial. Lignin and CNFs will also be evaluated as the compatibilizer and reinforcement for the cornmeal-based thermoplastics.

5.2. Materials and Methods

5.2.1. Materials

Cornmeal (B07NZPQ2RM, Homestead Gristmill Stone Ground Yellow Cornmeal) was purchased from Amazon. The lignin contained 4% sulfur and had an average Mw of ~10,000. Glycerol (99+%, 11443297) was purchased from Alfa Aesar. CNF slurry with a CNF concentration of ~2.5 wt% was purchased from the Process Development Plant of University of Maine. The slurry was concentrated by centrifugation to 10 wt% before use. All the chemicals and materials were used as received without further purification or modification.

73

5.2.2. Methods

5.2.2.1. Preparation of thermoplastic composites

5.2.2.1.1. CNFs/glycerol/citric acid mixture preparation

Citric acid (CA) and glycerol were used as the crosslinker and plasticizer in the product, respectively. To prepare the CNFs/glycerol/CA mixtures, CA was dissolved in glycerol (CA : glycerol = 0.5 : 35 by weight) by stirring with a high-speed homogenizer (IKA® T25 digital ULTRA-TURRAX®) at 3600 rpm for 10min. The received CNF slurry was concentrated using a centrifuge (Eppendorf® Centrifuge 5804) to increase the concentration to ~12 wt%. Next, predetermined amounts of the concentrated CNF slurry were added into the CA/glycerol solution to obtain CNF/glycerol/CA mixtures with the ratios of the three components at x/35/0.5 (w/w/w, x=2, 4, 6). The mixtures were sonicated (Sonicators® 3000) in an ice bath to break apart CNF agglomerates and achieve stable, homogeneous CNF suspensions in CA/glycerol. Finally, the sonicated suspensions were placed in a Lab-Line vacuum oven (Thermo Fisher Scientific) at 90°C and 80 inHg to remove the water (brought into the mixtures by the CNF slurry). The water-free mixtures appeared like pastes and they were sealed and stored under ambient conditions for future use. The formulations and sample codes of the obtained CNF mixtures are listed in Table 5.1.

Table 5.1. Formulations of water-free CNFs/glycerol/CA mixtures.

Sample Code	Ingredients (All in parts)		
	Glycerol	Citric Acid	Cellulose Nanofiber
CNF2	35	0.5	2
CNF4	35	0.5	4
CNF6	35	0.5	6

5.2.2.1.2 Preparation of thermoplastic starch-zein and cornmeal composites

Cornmeal and lignin in dry powder form were weighted and manually mixed in a beaker following the formulations listed in Table 5.2. The powder mixtures were then blended with the prepared CNFs/glycerol/CA mixtures in a kitchen blender and then sealed in a plastic bag and stored overnight to achieve equilibrium. In the sample codes of Table 5.2, SZ and CM denote the starch/zein mixture and cornmeal, respectively, which were the two matrix materials of the composites. LP denotes the lignin powder. The numbers after the LP and CNF indicate the number of grams for the lignin and CNFs (dry weight). For instance, CM-LP6-CNF6 means that the composite contains 6 grams of lignin powder and 6 grams of CNFs. Letter C in the sample codes of CMC indicates that the denoted samples are control samples containing no lignin and CNFs.

Table 5.2. Formulations of cornmeal-based thermoplastic composites. Cornmeal contains ~ 10% moisture.

Sample Code	Ingredients (All in parts)				
	Cornmeal	Glycerol	CA	Lignin	CNFs
CMC	108.89	35	0.5	0	0
CM-LP2-CNF2	108.89	35	0.5	2	2
CM-LP4-CNF4	108.89	35	0.5	4	4
CM-LP6-CNF6	108.89	35	0.5	6	6

The equilibrated composite formulations were compounded into thermoplastics using a corotating HAAKE twin-screw extruder (Rheomex™ PTW16 OS, screw diameter d = 16 mm, screw L/D ratio = 40:1) operating at 100 rpm. The extruder temperatures were set to 90°C, 120°C, 140°C, 140°C, 140°C, 140°C, 140°C, 140°C, and 140°C from the feed zone to the die. The thermoplastics were extruded through a slit die with a 25 mm x 0.5 mm rectangular opening (Thermo Electron) to produce ribbon-like extrudates, which were sealed in plastic bags immediately after extrusion and were transferred into a desiccator (~ 45% relative humidity at

20°C) and stored for 24h before testing. The flow chart of the sample preparation process is shown in Figure 5.1.
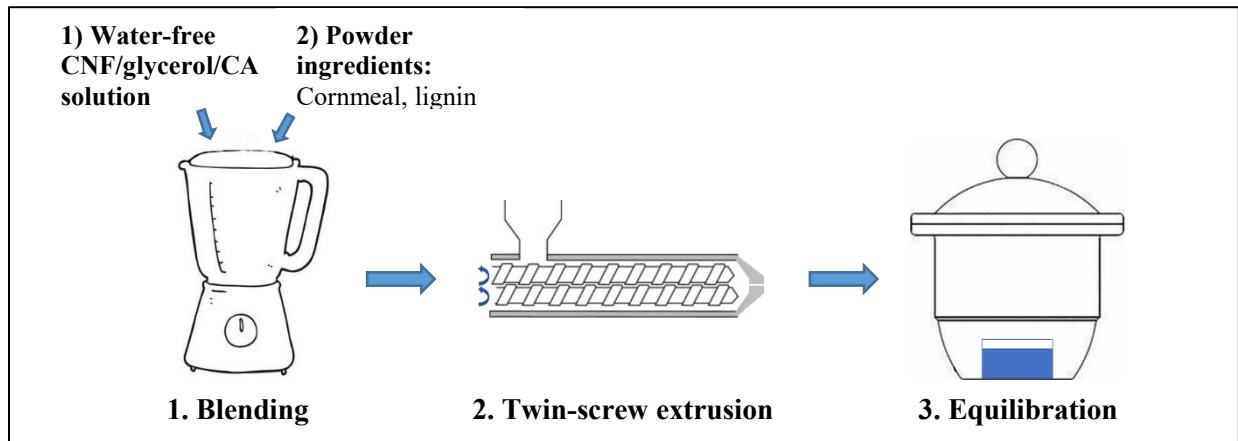

Figure 5.1. Flowchart of the cornmeal-based thermoplastic sample preparation process.

5.2.2.2. Mechanical properties of the corn-based thermoplastics

Dumbbell shaped tensile test bars were cut from the extruded ribbons. Tensile tests were performed under ambient conditions (~ 23 °C) on an MTS Insight test system equipped with a 5 kN electronic load cell at a crosshead speed of 50 mm/min.

5.2.2.3. Scanning electron microscopy (SEM)

Scanning electron microscopy (SEM) was used to study the morphology of the microstructure of the composites. Samples were frozen and fractured in liquid nitrogen to produce a clean cross section. They were attached to aluminum mounts with colloidal silver paste (Structure Probe Inc., West Chester PA, USA) for view of the fractured surface and then coated with a conductive layer of gold using a Cressington 108auto sputter coater (Ted Pella Inc., Redding CA, USA). Images were obtained at an accelerating voltage of 15 kV using a JEOL JSM-6490LV scanning electron microscope (JEOL USA, Peabody MA, USA).

5.2.2.4. Fourier transform infrared spectrometry (FTIR)

Fourier-transform infrared spectroscopy (FTIR, Thermo Scientific Nicolet 8700 FTIR spectrometer) was used to characterize the chemical bonds of native ingredients (starch, zein, lignin, CNF) and their film composite samples. Both powder and film composite samples were characterized using ATR accessory (4000–650 cm^{-1}) to collect their FTIR spectra.

5.3. Results and Discussion

5.3.1. Mechanical properties

Tensile test results for all the formulations listed in Table 5.2 are compared in Figures 5.2. The composites incorporated with both lignin and CNF exhibited the highest strength and modulus. While the strength and modulus being improved, the ultimate strain and toughness of the samples were decreased as the samples became increasingly rigid. The incorporation of six grams of lignin and six grams of CNFs led to the best overall mechanical properties.

The control sample based on cornmeal (CMC) showed a lower modulus and strength than those of the control sample based on the starch/zein mixture. This may be attributed to the fact that the cornmeal contained 4.14% fat, which can function as a plasticizer to soften the material (Table 5.3). By comparing CM-LP2-CNF2, CM-LP4-CNF4, and CM-LP6-CNF6 with the control sample (Table 5.4), the moduli of the composites were increased by 466%, 1061.1%, and 1340.2%, respectively, while the strengths were increased by 176.1%, 352%, and 410.2%, respectively. Indeed, the cornmeal-based composites exhibited a property trend similar to that of the starch/zein based composites. The percentage increases in the properties were even larger for the former than for the latter. The moduli and strengths of CM-LP4-CNF4 and CM-LP6-CNF6 were comparable to those of SZ-LP4-CNF4 and SZ-LP6-CNF6 (Chapter 4), whereas the ultimate strain/toughness of the former (cornmeal-based composites) was lower. This may be

due to the presence of pericarp (skin of corn kernel) in the composites, which can cause

premature sample fracture due to its relatively large size. The above results confirm that low-cost

cornmeal can be reliably used to replace the expensive starch/zein mixture to produce corn

plastics with similar properties.

Table 5.3. Nutrition analysis of cornmeal.

Sample	Ash (%)	CP (%)	N (%)	Fat (%)	Starch (%)	NDF (%)	ADF (%)	ADL (%)	Ca (%)	Phos (%)
Stoneground Cornmeal	1.38	7.58	1.21	4.14	75.34	11.90	2.60	0.56	0.01	0.34

CP: Crude protein; ADF: Acid detergent fiber; ADL: Acid detergent lignin; NDF: Acid detergent fiber; Phos: Phosphorus

Table 5.4. Percentage changes in tensile properties of the composites.

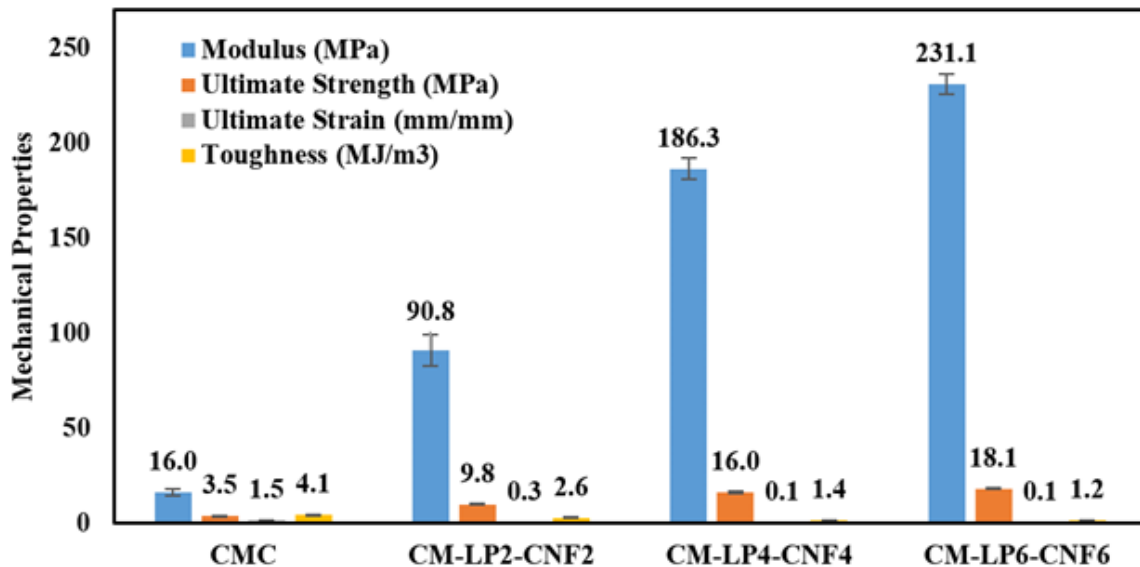|	Modulus	Ultimate Strength	Ultimate Strain	Toughness
CMC	0.0%	0.0%	-0.3%	-0.1%
CM-LP2-CNF2	466.0%	127.7%	-49.1%	-16.2%
CM-LP4-CNF4	1061.1%	290.8%	-76.2%	-35.0%
CM-LP6-CNF6	1340.2%	176.2%	-59.7%	-24.8%

Figure 5.2. Tensile test results of the corn-based thermoplastics based on cornmeal.
Representative stress-strain curves for the samples are presented in Figure A4 in the appendix.

5.3.2. SEM

Figure 5.3 exhibits the SEM micrographs of cornmeal control sample (CMC) and the

cornmeal sample incorporated with 6 parts of lignin powder and 6 parts of cellulose nanofibrils

(CM-LP6-CNF6). Compared to the fracture surface of CMC (Figure 5.3a), the facture surface of

CM-LP6-CNF6 was significantly rougher. There are visible pores or cracks showed on the

surface of the fractured cross-section. The pores may be due to the possibility degradation of

cornmeal at high temperature processing. The other reason would be the incorporation of citric

acid may react with the moisture (~10%) in the cornmeal and generate bubble in the sample as a

result. The cracks showed on Figure 5.3b may be ascribed to the relatively rigid property of the

sample after the addition of lignin and cellulose nanofibrils. There are some bonds found in the

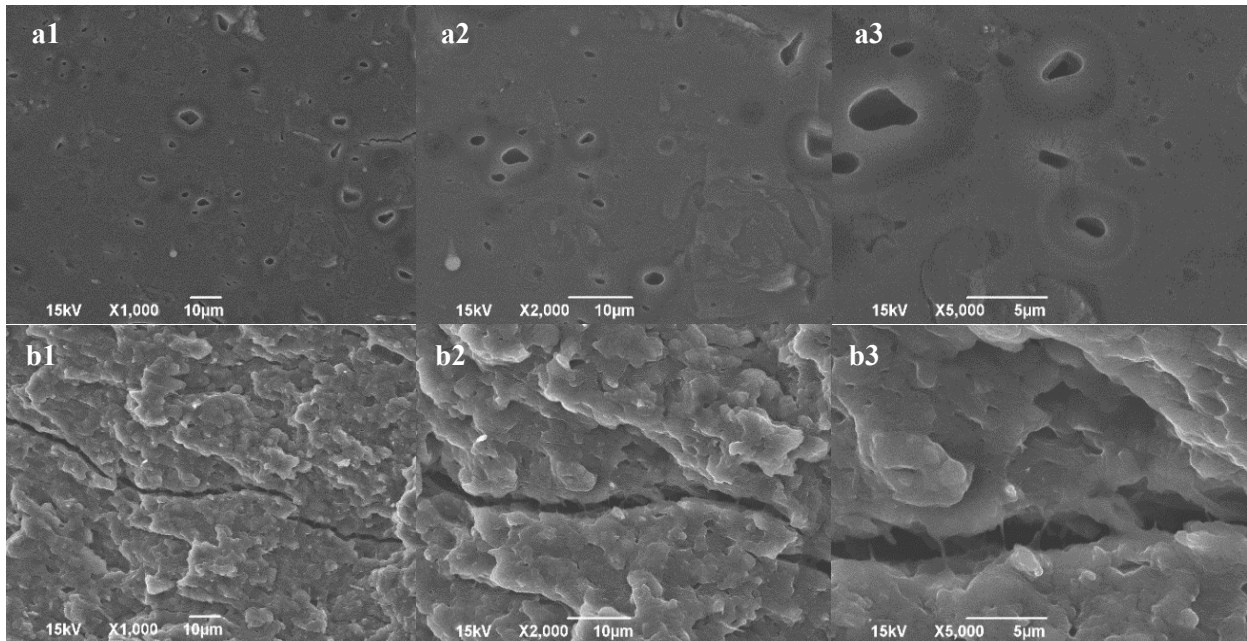crack, which may be due to the incorporation of nanofibrils.

Figure 5.3. SEM micrographs of CMC (a1, a2, and a3) and CM-LP6-CNF6 (b1, b2, and b3)
taken under different magnifications.

5.3.3. FTIR

Figure 5.4 shows the Fourier transform infrared spectroscopy (FTIR) spectra of lignin, CNF, CMC and CM-LP6-CNF6. The stretching vibrations band at 3324 cm^{-1} could be attributed to the oxidation in the ambient environment and adsorbed water[115]. The band at 2920 cm^{-1} is attributed to -CH$_2$ stretching vibration from starch ingredient in cornmeal[114],[116]. The bands at 1147 cm^{-1} and 1082 cm^{-1} can be ascribed to C–O–H stretching vibration[116]. The band at 1650 cm^{-1} is due to C=O stretching of the amide group[124]. The absorption band at 1460 cm^{-1} was attributed to N-H bending and C-N stretching from the protein ingredient in cornmeal[117]. However, there's not much different found between CMC and CM-LP6-CNF6 from the FTIR spectra.
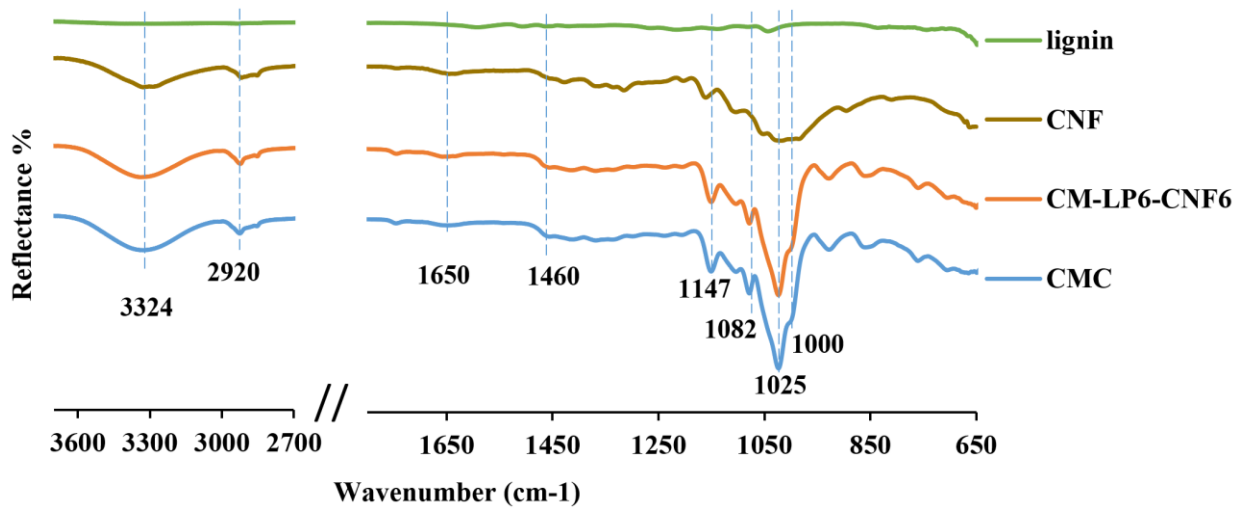
Figure 5.4. Fourier transform infrared spectroscopy (FTIR) spectra of lignin, CNF, CMC and CM-LP6-CNF6.

5.4. Conclusion

The composites incorporated with both lignin and CNF exhibited the highest strength and modulus for the cornmeal-based thermoplastic. While the strength and modulus being improved, the ultimate strain and toughness of the samples were decreased as the samples became increasingly rigid. The incorporation of six grams of lignin and six grams of CNFs led to the best

overall mechanical properties. Compared to the cornmeal-based control sample (CMC), the modulus of CM-LP6-CNF6 was increased by 1340.2%.

In short, with proper plasticizer, temperature and shear, cornmeal could be used as a substitute material for starch-zein based thermoplastic. The incorporation of lignin and cellulose nanofibrils shows similar trend of improvement in cornmeal-based thermoplastic as well, which mean lignin and cellulose nanofibrils are both efficient reinforcement for corn-based thermoplastic.

6. SUMMARY AND FUTURE WORK

6.1. Summary

In this dissertation, lignin and cellulose nanofibrils reinforced corn-based thermoplastic was developed. The contents of lignin and cellulose nanofibrils were varied from 0 part to 6 parts to study their influence on the properties of the composites. Two types of plasticizers (ethylene glycol and glycerol) and two forms of lignin (lignin solution and as-received lignin powder) were also tested for their effects. An internal mixer was first used to explore the processing conditions and twin-screw extrusion was subsequently employed to produce a larger quantity of samples with better processing control and improved dispersion of the reinforcement.

In the first part of this research (Chapter 3), glycerol-plasticized and ethylene glycol plasticized starch-zein composites were prepared using an internal mixer. The incorporation of lignin particles significantly improved the mechanical properties and phase structure of starch-zein blend regardless of the plasticizer type. The mechanical properties of the composites increased with the increasing lignin content and the incorporation of CNFs further enhanced the modulus and strength of the blends, suggesting strong synergy between lignin and CNFs in reinforcing the corn-based thermoplastic. This study demonstrated the potentials of using lignin and cellulose nanofibrils as reinforcement to increase starch-zein based composites.

Based on the results from the first part, citric acid (CA) was used to replace water in Chapter 4 with the aim of improving the processability, reducing the content of glycerol, and increasing interfacial bonding of the starch-zein composites. With CA, composites processability was significant increased and therefore the glycerol content was decreased from 50 parts to 35 parts to increase the mechanical properties and water resistance of final samples. The mechanical properties of CA-containing composites exhibited trends similar to those in Chapter 3: higher

contents of lignin and CNFs led to higher mechanical properties. With CA, the "sea-island" two phase structure found in the composites in Chapter 3 disappeared due to improved compatibility between the components. The addition of CA also improved thermal stability of the composites.

The third part of the research was focus on low-cost substitute for zein to enable large scale use of corn-based thermoplastics. While using starch and zein as separate ingredients allows the study of their individual contributions to the properties of the corn thermoplastics, commercially available zein is an expensive material and therefore render the corn plastics cost-prohibitive. Cornmeal, which is a low-cost raw material and contains mainly starch and zein, was therefore used in Chapter 5 to show that this low-cost replacement for the starch-zein blend can also be processed into thermoplastic with similar properties using the same method. Four kinds of sample have been studied, including CMC, CM-LP2-CNF2, CM-LP4-CNF4 and CM-LP6-CNF6 samples. Compared to the cornmeal control sample (CMC), the modulus CM-LP2-CNF2, CM-LP4-CNF4 and CM-LP6-CNF6 samples were improved 466.0%, 1061.1% and 1340.2%, respectively. This discovery confirmed the possibility of using lignin and cellulose to enhance the mechanical properties of the cornmeal-based thermoplastics.

The corn-based composites developed in this research can be molded into different forms of articles such as sheets, films, rods, and laminates. The products can find applications in packaging, household items, plant pots, controlled release chemical delivery tools (for fertilizers and pesticides etc.), and other fields.

6.2. Future Work

6.2.1. 3D printing

The composites extruded from a thread die were trialed for 3D printing. The extruded corn-based filament (**Figure 6.1**) was printed at 150°C nozzle temperature. However, the

materials' printability was poor due to its low flowability and poor adhesion between the layers. Increasing the glycerol content of the filament improved the flexibility and potentially increased the inter-layer adhesion of the filaments but still could not fully overcome the difficulty. In future studies, we can consider adding a preheat instrument in the 3D printer, which may provide the filament better flexibility and processability. Replacing glycerol with a higher molecular weight plasticizer (e.g., hyperbranched polyols/esters) at a higher content is another option because they can provide good flowability without causing leaching and moisture absorption issues.

Figure 6.1. Extruded filament for 3D printing.

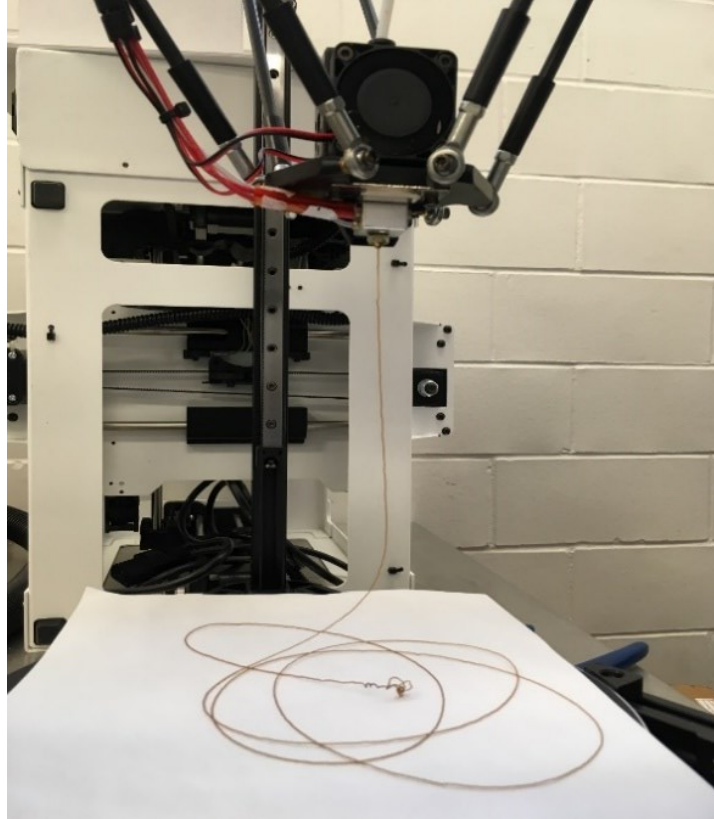Figure 6.2. Filament being extruded from the nozzle of a 3D printer.

6.2.2. Water resistance improvement

Poly (ethylene oxide) (PEO) can be considered to replace part of the glycerol in the composites to improve their water resistance. Preliminary results show improved strength and modulus and improved moisture absorption as shown in Figure 6.3 and Table 6.1. Further exploration in this direction is needed.
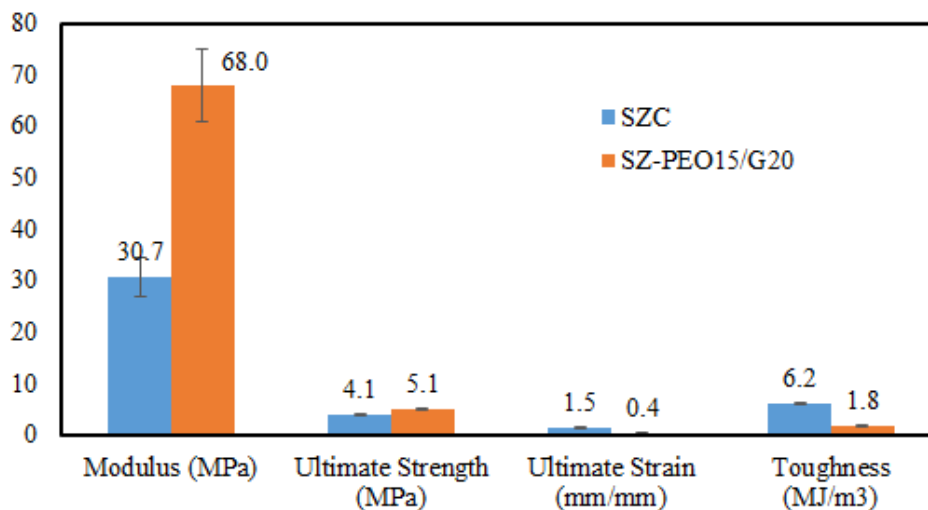
Figure 6.3. Comparison of SZC and SZ-PEO15/G20 tensile properties.

Table 6.1. Composites water absorption at different humidity conditions.

	56% RH	79% RH
SZ-PEO15/G20	6.7%	18.0%
SZC or SZ-G35	11.9%	20.4%

Note: SZC is incorporated with 35 parts of glycerol, so it was named as SZ-G35 as well.

6.2.3. Thermal stability improvement

The content of citric acid needs to be optimized. Starch acidolysis will be severe when citric acid content is high. This side reaction can greatly decrease the thermal stability of thermoplastic starch. An optimal CA content that facilitates processing and promotes composite compatibility without causing severe acidolysis is desired.

REFERENCES

(1)   Doebley, J.; Stec, A.; Hubbard, L. The Evolution of Apical Dominance in Maize. Nature 1997, 386 (6624), 485–488. https://doi.org/10.1038/386485a0.

(2)   USDA - National Agricultural Statistics Service - Charts and Maps - Corn: Production by Year, US https://www.nass.usda.gov/Charts_and_Maps/Field_Crops/cornprod.php (accessed 2021 -06 -21).

(3)   Production of Corn | Iowa Corn https://www.iowacorn.org/corn-production/production/ (accessed 2021 -06 -21).

(4)   Habeych, E.; van der Goot, A. J.; Boom, R. In Situ Compatibilization of Starch–Zein Blends under Shear Flow. Chem. Eng. Sci. 2009, 64 (15), 3516–3524. https://doi.org/10.1016/j.ces.2009.04.034.

(5)   Chanvrier, H.; Colonna, P.; Della Valle, G.; Lourdin, D. Structure and Mechanical Behaviour of Corn Flour and Starch–Zein Based Materials in the Glassy State. Carbohydr. Polym. 2005, 59 (1), 109–119. https://doi.org/10.1016/j.carbpol.2004.09.005.

(6)   Corradini, E.; Carvalho, A. J. F. de; Curvelo, A. A. da S.; Agnelli, J. A. M.; Mattoso, L. H. C. Preparation and Characterization of Thermoplastic Starch/Zein Blends. Mater. Res. 2007, 10, 227–231. https://doi.org/10.1590/S1516-14392007000300002.

(7)   Habeych, E.; Dekkers, B.; van der Goot, A. J.; Boom, R. Starch–Zein Blends Formed by Shear Flow. Chem. Eng. Sci. 2008, 63 (21), 5229–5238. https://doi.org/10.1016/j.ces.2008.07.008.

(8)   Zeng, M.; Huang, Y.; Lu, L.; Fan, L.; Lourdin, D. Effects of Filler-Matrix Morphology on Mechanical Properties of Corn Starch–Zein Thermo-Moulded Films. Carbohydr. Polym. 2011, 84 (1), 323–328. https://doi.org/10.1016/j.carbpol.2010.11.038.

(9)   Doherty, W. O. S.; Mousavioun, P.; Fellows, C. M. Value-Adding to Cellulosic Ethanol:
        Lignin Polymers. Ind. Crops Prod. 2011, 33 (2), 259–276.
        https://doi.org/10.1016/j.indcrop.2010.10.022.

(10)   An Ionomeric Renewable Thermoplastic from Lignin-Reinforced Rubber - Barnes - 2019
        - Macromolecular Rapid Communications - Wiley Online Library
        https://onlinelibrary.wiley.com/doi/full/10.1002/marc.201900059 (accessed 2021 -06 -
        21).

(11)   Bajwa, D. S.; Pourhashem, G.; Ullah, A. H.; Bajwa, S. G. A Concise Review of Current
        Lignin Production, Applications, Products and Their Environmental Impact. Ind. Crops
        Prod. 2019, 139, 111526. https://doi.org/10.1016/j.indcrop.2019.111526.

(12)   Stevens, E. S.; Willett, J. L.; Shogren, R. L. Thermoplastic Starch-Kraft Lignin-Glycerol
        Blends. J. Biobased Mater. Bioenergy 2007, 1 (3), 351–359.
        https://doi.org/10.1166/jbmb.2007.009.

(13)   Nasri-Nasrabadi, B.; Behzad, T.; Bagheri, R. Preparation and Characterization of
        Cellulose Nanofiber Reinforced Thermoplastic Starch Composites. Fibers Polym. 2014,
        15 (2), 347–354. https://doi.org/10.1007/s12221-014-0347-0.

(14)   Ferreira, F. V.; Dufresne, A.; Pinheiro, I. F.; Souza, D. H. S.; Gouveia, R. F.; Mei, L. H.
        I.; Lona, L. M. F. How Do Cellulose Nanocrystals Affect the Overall Properties of
        Biodegradable Polymer Nanocomposites: A Comprehensive Review. Eur. Polym. J.
        2018, 108, 274–285. https://doi.org/10.1016/j.eurpolymj.2018.08.045.

(15)   Kargarzadeh, H.; Mariano, M.; Huang, J.; Lin, N.; Ahmad, I.; Dufresne, A.; Thomas, S.
        Recent Developments on Nanocellulose Reinforced Polymer Nanocomposites: A
        Review. Polymer 2017, 132, 368–393. https://doi.org/10.1016/j.polymer.2017.09.043.

(16)   Avérous, L. Biodegradable Multiphase Systems Based on Plasticized Starch: A Review. J. Macromol. Sci. Part C 2004, 44 (3), 231–274. https://doi.org/10.1081/MC-200029326.

(17)   Schmitt, H.; Guidez, A.; Prashantha, K.; Soulestin, J.; Lacrampe, M. F.; Krawczak, P. Studies on the Effect of Storage Time and Plasticizers on the Structural Variations in Thermoplastic Starch. Carbohydr. Polym. 2015, 115, 364–372. https://doi.org/10.1016/j.carbpol.2014.09.004.

(18)   Chandra, R.; Rustgi, R. Biodegradable Polymers. Progress in Polymer Science, 1998, 23(7): 1273-1335. http://dx.doi.org/10.1016/S0079-6700(97)00039-7.

(19)   Degradable Polymers: Principles and Applications; Scott, G., Gilead, D., Eds.; Springer Netherlands, 1995. https://doi.org/10.1007/978-94-011-0571-2.

(20)   Hablot, E.; Dewasthale, S.; Zhao, Y.; Zhiguan, Y.; Shi, X.; Graiver, D.; Narayan, R. Reactive Extrusion of Glycerylated Starch and Starch–Polyester Graft Copolymers. Eur. Polym. J. 2013, 49 (4), 873–881. https://doi.org/10.1016/j.eurpolymj.2012.12.005.

(21)   Corradini, E.; Medeiros, E. S. de; Carvalho, A. J. F.; Curvelo, A. A. S.; Mattoso, L. H. C. Mechanical and Morphological Characterization of Starch/Zein Blends Plasticized with Glycerol. J. Appl. Polym. Sci. 2006, 101 (6), 4133–4139. https://doi.org/10.1002/app.23570.

(22)   Trujillo-de Santiago, G.; Rojas-de Gante, C.; García-Lara, S.; Verdolotti, L.; Di Maio, E.; Iannace, S. Strategies to Produce Thermoplastic Starch–Zein Blends: Effect on Compatibilization. J. Polym. Environ. 2014, 22 (4), 508–524. https://doi.org/10.1007/s10924-014-0685-4.

(23)   Ojogbo, E.; Ogunsona, E. O.; Mekonnen, T. H. Chemical and Physical Modifications of Starch for Renewable Polymeric Materials. Mater. Today Sustain. 2020, 7–8, 100028. https://doi.org/10.1016/j.mtsust.2019.100028.

(24)   Spiridon, I.; Teaca, C.-A.; Bodirlau, R. Preparation and Characterization of Adipic Acid-Modified Starch Microparticles/Plasticized Starch Composite Films Reinforced by Lignin. J. Mater. Sci. 2011, 46 (10), 3241–3251. https://doi.org/10.1007/s10853-010-5210-0.

(25)   Shukla, R.; Cheryan, M. Zein: The Industrial Protein from Corn. Ind. Crops Prod. 2001, 13 (3), 171–192. https://doi.org/10.1016/S0926-6690(00)00064-9.

(26)   Zhang, K.; Cheng, F.; Lin, Y.; Zhou, M.; Zhu, P. Effect of Hyperbranched Poly(Trimellitic Glyceride) with Different Molecular Weight on Starch Plasticization and Compatibility with Polyester. Carbohydr. Polym. 2018, 195, 107–113. https://doi.org/10.1016/j.carbpol.2018.04.080.

(27)   Zdanowicz, M.; Johansson, C. Mechanical and Barrier Properties of Starch-Based Films Plasticized with Two- or Three Component Deep Eutectic Solvents. Carbohydr. Polym. 2016, 151, 103–112. https://doi.org/10.1016/j.carbpol.2016.05.061.

(28)   Averous, L.; Boquillon, N. Biocomposites Based on Plasticized Starch: Thermal and Mechanical Behaviours. Carbohydr. Polym. 2004, 56 (2), 111–122. https://doi.org/10.1016/j.carbpol.2003.11.015.

(29)   Wang, Z.; Li, Z.; Gu, Z.; Hong, Y.; Cheng, L. Preparation, Characterization and Properties of Starch-Based Wood Adhesive. Carbohydr. Polym. 2012, 88 (2), 699–706. https://doi.org/10.1016/j.carbpol.2012.01.023.

(30)   López, O. V.; Lecot, C. J.; Zaritzky, N. E.; García, M. A. Biodegradable Packages

         Development from Starch Based Heat Sealable Films. J. Food Eng. 2011, 105 (2), 254–

         263. https://doi.org/10.1016/j.jfoodeng.2011.02.029.

(31)   Le Corre, D.; Bras, J.; Dufresne, A. Starch Nanoparticles: A Review. Biomacromolecules

         2010, 11 (5), 1139–1153. https://doi.org/10.1021/bm901428y.

(32)   Marichelvam, M. K.; Jawaid, M.; Asim, M. Corn and Rice Starch-Based Bio-Plastics as

         Alternative Packaging Materials. Fibers 2019, 7 (4), 32.

         https://doi.org/10.3390/fib7040032.

(33)   Buléon, A.; Colonna, P.; Planchot, V.; Ball, S. Starch Granules: Structure and

         Biosynthesis. Int. J. Biol. Macromol. 1998, 23 (2), 85–112.

         https://doi.org/10.1016/S0141-8130(98)00040-3.

(34)   Kadokawa, J.-I. Preparation and Applications of Amylose Supramolecules by Means of

         Phosphorylase-Catalyzed Enzymatic Polymerization. Polymers 2012, 4.

         https://doi.org/10.3390/polym4010116.

(35)   Sjöö, M.; Nilsson, L. Starch in Food: Structure, Function and Applications; Woodhead

         Publishing, 2017. https://doi.org/10.1016/C2015-0-01896-2.

(36)   Fishman, M. L.; Coffin, D. R.; Konstance, R. P.; Onwulata, C. I. Extrusion of

         Pectin/Starch Blends Plasticized with Glycerol. Carbohydr. Polym. 2000, 41 (4), 317–

         325. https://doi.org/10.1016/S0144-8617(99)00117-4.

(37)   Martin, O.; Schwach, E.; Av?rous, L.; Couturier, Y. Properties of Biodegradable

         Multilayer Films Based on Plasticized Wheat Starch. Starch - Stärke 2001, 53 (8), 372–

         380. https://doi.org/10.1002/1521-379X(200108)53:8<372::AID-STAR372>3.0.CO;2-F.

(38)   Structure Evolution in Amylopectin/Ethylene Glycol Mixtures by H-bond Formation and Phase Separation Studied with Dielectric Relaxation Spectroscopy | The Journal of Physical Chemistry B https://pubs.acs.org/doi/abs/10.1021/jp003289f (accessed 2021 -06 -22).

(39)   Wang, L.; Shogren, R. L.; Carriere, C. Preparation and Properties of Thermoplastic Starch-Polyester Laminate Sheets by Coextrusion. Polym. Eng. Sci. 2000, 40 (2), 499–506. https://doi.org/10.1002/pen.11182.

(40)   Ma, X.; Yu, J. The Effects of Plasticizers Containing Amide Groups on the Properties of Thermoplastic Starch. Starch - Stärke 2004, 56 (11), 545–551. https://doi.org/10.1002/star.200300256.

(41)   Ma, X.; Yu, J. Formamide as the Plasticizer for Thermoplastic Starch. J. Appl. Polym. Sci. 2004, 93 (4), 1769–1773. https://doi.org/10.1002/app.20628.

(42)   Ma, X. F.; Yu, J. G.; Ma, Y. B. Urea and Formamide as a Mixed Plasticizer for Thermoplastic Wheat Flour. Carbohydr. Polym. 2005, 60 (1), 111–116. https://doi.org/10.1016/j.carbpol.2004.11.029.

(43)   Jiang, L.; Liu, B.; Zhang, J. Novel High-Strength Thermoplastic Starch Reinforced by in Situ Poly(Lactic Acid) Fibrillation. Macromol. Mater. Eng. 2009, 294 (5), 301–305. https://doi.org/10.1002/mame.200900018.

(44)   Yun, Y.-H.; Wee, Y.-J.; Byun, H.-S.; Yoon, S.-D. Biodegradability of Chemically Modified Starch (RS4)/PVA Blend Films: Part 2. J. Polym. Environ. 2008, 16 (1), 12–18. https://doi.org/10.1007/s10924-008-0084-9.

(45)   Thakore, I. M.; Desai, S.; Sarawade, B. D.; Devi, S. Studies on Biodegradability, Morphology and Thermo-Mechanical Properties of LDPE/Modified Starch Blends. Eur. Polym. J. 2001, 37 (1), 151–160. https://doi.org/10.1016/S0014-3057(00)00086-0.

(46)   Huneault, M. A.; Li, H. Morphology and Properties of Compatibilized Polylactide/Thermoplastic Starch Blends. Polymer 2007, 48 (1), 270–280. https://doi.org/10.1016/j.polymer.2006.11.023.

(47)   St-Pierre, N.; Favis, B. D.; Ramsay, B. A.; Ramsay, J. A.; Verhoogt, H. Processing and Characterization of Thermoplastic Starch/Polyethylene Blends. Polymer 1997, 38 (3), 647–655. https://doi.org/10.1016/S0032-3861(97)81176-7.

(48)   Martins, A. B.; Santana, R. M. C. Effect of Carboxylic Acids as Compatibilizer Agent on Mechanical Properties of Thermoplastic Starch and Polypropylene Blends. Carbohydr. Polym. 2016, 135, 79–85. https://doi.org/10.1016/j.carbpol.2015.08.074.

(49)   Palanisamy, C. P.; Cui, B.; Zhang, H.; Jayaraman, S.; Kodiveri Muthukaliannan, G. A Comprehensive Review on Corn Starch-Based Nanomaterials: Properties, Simulations, and Applications. Polymers 2020, 12 (9), 2161. https://doi.org/10.3390/polym12092161.

(50)   López Córdoba, A.; Deladino, L.; Martino, M. Effect of Starch Filler on Calcium-Alginate Hydrogels Loaded with Yerba Mate Antioxidants. Carbohydr. Polym. 2013, 95 (1), 315–323. https://doi.org/10.1016/j.carbpol.2013.03.019.

(51)   Lv, S.; Gu, J.; Cao, J.; Tan, H.; Zhang, Y. Effect of Annealing on the Thermal Properties of Poly (Lactic Acid)/Starch Blends. Int. J. Biol. Macromol. 2015, 74, 297–303. https://doi.org/10.1016/j.ijbiomac.2014.12.022.

(52)   Lawton, J. W. Zein: A History of Processing and Use. Cereal Chem. 2002, 79 (1), 1–18. https://doi.org/10.1094/CCHEM.2002.79.1.1.

(53)   Corradini, E.; Curti, P.; Meniqueti, A.; Martins, A.; Rubira, A.; Muniz, E. Recent
         Advances in Food-Packing, Pharmaceutical and Biomedical Applications of Zein and
         Zein-Based Materials. Int. J. Mol. Sci. 2014, 15 (12), 22438–22470.
         https://doi.org/10.3390/ijms151222438.

(54)   Zhang, Y.; Cui, L.; Li, F.; Shi, N.-Q.; Li, C.; Yu, X.; Chen, Y.; Kong, W. Design,
         Fabrication and Biomedical Applications of Zein-Based Nano/Micro-Carrier Systems.
         Int. J. Pharm. 2016, 513. https://doi.org/10.1016/j.ijpharm.2016.09.023.

(55)   Zini, E.; Scandola, M. Green Composites: An Overview. Polym. Compos. 2011, 32 (12),
         1905–1915. https://doi.org/10.1002/pc.21224.

(56)   Terzopoulou, Z. N.; Papageorgiou, G. Z.; Papadopoulou, E.; Athanassiadou, E.;
         Alexopoulou, E.; Bikiaris, D. N. Green Composites Prepared from Aliphatic Polyesters
         and Bast Fibers. Ind. Crops Prod. 2015, 68, 60–79.
         https://doi.org/10.1016/j.indcrop.2014.08.034.

(57)   Yang, J.; Ching, Y. C.; Chuah, C. H. Applications of Lignocellulosic Fibers and Lignin in
         Bioplastics: A Review. Polymers 2019, 11 (5), 751.
         https://doi.org/10.3390/polym11050751.

(58)   Bamdad, H.; Hawboldt, K.; MacQuarrie, S. A Review on Common Adsorbents for Acid
         Gases Removal: Focus on Biochar. Renew. Sustain. Energy Rev. 2017, 81.
         https://doi.org/10.1016/j.rser.2017.05.261. DOI: 10.15376/biores.10.2.3364-3377

(59)   Ching, Y. C.; Rahman, A.; Ching, K. Y.; Sukiman, N. L.; Cheng, H. C. Preparation and
         Characterization of Polyvinyl Alcohol-Based Composite Reinforced with Nanocellulose
         and Nanosilica. BioResources 2015, 10 (2), 3364–3377.

https://bioresources.cnr.ncsu.edu/resources/preparation-and-characterization-of-polyvinyl-alcohol-based-composite-reinforced-with-nanocellulose-and-nanosilica/.

(60)   Lignin as Renewable Raw Material - Calvo-Flores - 2010 - ChemSusChem - Wiley Online Library https://chemistry-europe.onlinelibrary.wiley.com/doi/full/10.1002/cssc.201000157 (accessed 2021 -06 - 22).

(61)   Aro, T.; Fatehi, P. Production and Application of Lignosulfonates and Sulfonated Lignin. ChemSusChem 2017, 10 (9), 1861–1877. https://doi.org/10.1002/cssc.201700082.

(62)   Ralph, J.; Lundquist, K.; Brunow, G.; Lu, F.; Kim, H.; Schatz, P. F.; Marita, J. M.; Hatfield, R. D.; Ralph, S. A.; Christensen, J. H.; Boerjan, W. Lignins: Natural Polymers from Oxidative Coupling of 4-Hydroxyphenyl- Propanoids. Phytochem. Rev. 2004, 3 (1), 29–60. https://doi.org/10.1023/B:PHYT.0000047809.65444.a4.

(63)   Vishtal, A. G.; Kraslawski, A. Challenges in Industrial Applications of Technical Lignins. BioResources 2011, 6 (3), 3547–3568. https://doi.org/10.15376/biores.6.3.3547-3568

(64)   Recent developments in polymers derived from industrial lignin - Ten - 2015 - Journal of Applied Polymer Science - Wiley Online Library https://onlinelibrary.wiley.com/doi/full/10.1002/app.42069 (accessed 2021 -06 -22).

(65)   Ali, S.; Khatri, Z.; Oh, K. W.; Kim, I.-S.; Kim, S. H. Zein/Cellulose Acetate Hybrid Nanofibers: Electrospinning and Characterization. Macromol. Res. 2014, 22 (9), 971–977. https://doi.org/10.1007/s13233-014-2136-4.

(66)   Niu, B.; Zhan, L.; Shao, P.; Xiang, N.; Sun, P.; Chen, H.; Gao, H. Electrospinning of Zein-Ethyl Cellulose Hybrid Nanofibers with Improved Water Resistance for Food

Preservation. Int. J. Biol. Macromol. 2020, 142, 592–599.
https://doi.org/10.1016/j.ijbiomac.2019.09.134.

(67)   Effect of Supramolecular Structures on Thermoplastic Zein–Lignin Bionanocomposites |
        Journal of Agricultural and Food Chemistry
        https://pubs.acs.org/doi/abs/10.1021/jf201728p (accessed 2021 -06 -22).

(68)   Sarwono, A.; Man, Z.; Bustam, M. A.; Azizli, K. A. Water Uptake Behavior of Lignin
        Modified Starch Film. Appl. Mech. Mater. 2015, 699, 204–209.
        https://doi.org/10.4028/www.scientific.net/AMM.699.204.

(69)   Spiridon, I.; Tanase, C. E. Design, Characterization and Preliminary Biological
        Evaluation of New Lignin-PLA Biocomposites. Int. J. Biol. Macromol. 2018, 114, 855–
        863. https://doi.org/10.1016/j.ijbiomac.2018.03.140.

(70)   Shi, R.; Li, B. Preparation and Characterization of Corn Starch and Lignosulfonate Blend
        Film with a High Content of Lignosulfonate. BioResources 2016, 11 (4), 8860–8874.
        https://bioresources.cnr.ncsu.edu/resources/preparation-and-characterization-of-corn-
        starch-and-lignosulfonate-blend-film-with-a-high-content-of-lignosulfonate/.

(71)   Graphene Oxide Filled Lignin/Starch Polymer Bionanocomposite: Structural, Physical,
        and Mechanical Studies | Journal of Agricultural and Food Chemistry
        https://pubs.acs.org/doi/abs/10.1021/acs.jafc.7b04155 (accessed 2021 -06 -22).

(72)   Baumberger, S.; Lapierre, C.; Monties, B.; Valle, G. D. Use of Kraft Lignin as Filler for
        Starch Films. Polym. Degrad. Stab. 1998, 59 (1), 273–277.
        https://doi.org/10.1016/S0141-3910(97)00193-6.

(73)   Majeed, Z.; Mansor, N.; Ajab, Z.; Man, Z.; Sarwono, A. Kraft Lignin Ameliorates
       Degradation Resistance of Starch in Urea Delivery Biocomposites. Polym. Test. 2018,
       65, 398–406. https://doi.org/10.1016/j.polymertesting.2017.12.011.

(74)   Zhang, C.; Nair, S. S.; Chen, H.; Yan, N.; Farnood, R.; Li, F. Thermally Stable,
       Enhanced Water Barrier, High Strength Starch Bio-Composite Reinforced with Lignin
       Containing Cellulose Nanofibrils. Carbohydr. Polym. 2020, 230, 115626.
       https://doi.org/10.1016/j.carbpol.2019.115626.

(75)   Utilization of Lignin in Biopolymeric Packaging Films | ACS Omega
       https://pubs.acs.org/doi/abs/10.1021/acsomega.7b01341 (accessed 2021 -06 -22).

(76)   Duval, A.; Molina-Boisseau, S.; Chirat, C. Comparison of Kraft Lignin and
       Lignosulfonates Addition to Wheat Gluten-Based Materials: Mechanical and Thermal
       Properties. Ind. Crops Prod. 2013, 49, 66–74.
       https://doi.org/10.1016/j.indcrop.2013.04.027.

(77)   Grigsby, W. J.; Scott, S. M.; Plowman-Holmes, M. I.; Middlewood, P. G.; Recabar, K.
       Combination and Processing Keratin with Lignin as Biocomposite Materials for Additive
       Manufacturing Technology. Acta Biomater. 2020, 104, 95–103.
       https://doi.org/10.1016/j.actbio.2019.12.026.

(78)   Li, J.; He, Y.; Inoue, Y. Thermal and Mechanical Properties of Biodegradable Blends of
       Poly(L-Lactic Acid) and Lignin. Polym. Int. 2003, 52 (6), 949–955.
       https://doi.org/10.1002/pi.1137.

(79)   Yu, M.; Wang, J.; Tian, P.; Sun, L.; Sun, K.; Ge, Z.; Huang, R. Evaluation of the
       Durability of Lignin-Reinforced Composites Based on Wheat Straw/Recycled
       Polypropylene Blends. BioResources 2019, 14 (3), 5683–5697.

https://bioresources.cnr.ncsu.edu/resources/evaluation-of-the-durability-of-lignin-reinforced-composites-based-on-wheat-straw-recycled-polypropylene-blends/.

(80) Rusmirović, J.; Lukić, V.; Kovačević, T.; Bogosavljević, M.; Brzić, S.; Marinković, A.; Stevanović, T. Fireproof Phosphorylated Kraft Lignin/Polyester Based Composites: Green Material for Rocket Propellant Thermal Protection Systems. Sci. Tech. Rev. 2019, 69 (1), 16–22. https://doi.org/10.5937/str1901016R.

(81) Yang, W.; Fortunati, E.; Bertoglio, F.; Owczarek, J. S.; Bruni, G.; Kozanecki, M.; Kenny, J. M.; Torre, L.; Visai, L.; Puglia, D. Polyvinyl Alcohol/Chitosan Hydrogels with Enhanced Antioxidant and Antibacterial Properties Induced by Lignin Nanoparticles. Carbohydr. Polym. 2018, 181, 275–284. https://doi.org/10.1016/j.carbpol.2017.10.084.

(82) Jiping, P.; Shujun, W.; Jinglin, Y.; Hongyan, L.; Jiugao, Y.; Wenyuan, G. Comparative Studies on Morphological and Crystalline Properties of B-Type and C-Type Starches by Acid Hydrolysis. Food Chem. 2007, 105 (3), 989–995. https://doi.org/10.1016/j.foodchem.2007.04.053.

(83) An efficient and stable star-shaped plasticizer for starch: cyclic phosphazene with hydrogen bonding aminoethoxy ethanol side chains - Green Chemistry (RSC Publishing) DOI:10.1039/C4GC00794H https://pubs.rsc.org/en/content/articlehtml/2014/gc/c4gc00794h (accessed 2021 -06 -22).

(84) Corradini, E.; Carvalho, A. J. F. de; Curvelo, A. A. da S.; Agnelli, J. A. M.; Mattoso, L. H. C. Preparation and Characterization of Thermoplastic Starch/Zein Blends. Mater. Res. 2007, 10, 227–231. https://doi.org/10.1590/S1516-14392007000300002.

(85) Vainio, U.; Maximova, N.; Hortling, B.; Laine, J.; Stenius, P.; Simola, L. K.; Gravitis, J.; Serimaa, R. Morphology of Dry Lignins and Size and Shape of Dissolved Kraft Lignin

Particles by X-Ray Scattering. Langmuir 2004, 20 (22), 9736–9744.

https://doi.org/10.1021/la048407v.

(86)   Norgren, M.; Edlund, H.; Wågberg, L. Aggregation of Lignin Derivatives under Alkaline

Conditions. Kinetics and Aggregate Structure. Langmuir 2002, 18 (7), 2859–2865.

https://doi.org/10.1021/la011627d.

(87)   Mu, L.; Shi, Y.; Wang, H.; Zhu, J. Lignin in Ethylene Glycol and Poly (Ethylene Glycol):

Fortified Lubricants with Internal Hydrogen Bonding. ACS Sustain. Chem. Eng. 2016, 4

(3), 1840–1849. https://doi.org/10.1021/acssuschemeng.6b00049.

(88)   Mu, L.; Wu, J.; Matsakas, L.; Chen, M.; Vahidi, A.; Grahn, M.; Rova, U.;

Christakopoulos, P.; Zhu, J.; Shi, Y. Lignin from Hardwood and Softwood Biomass as a

Lubricating Additive to Ethylene Glycol. Molecules 2018, 23 (3), 537.

https://doi.org/10.3390/molecules23030537.

(89)   Stevens, E.; Willett, J.; Shogren, R. Thermoplastic Starch-Kraft Lignin-Glycerol Blends.

J. Biobased Mater. Bioenergy 2007, 1 (3), 351–359.

https://doi.org/10.1166/jbmb.2007.009.

(90)   Zhang, C.; Nair, S. S.; Chen, H.; Yan, N.; Farnood, R.; Li, F. Thermally Stable,

Enhanced Water Barrier, High Strength Starch Bio-Composite Reinforced with Lignin

Containing Cellulose Nanofibrils. Carbohydr. Polym. 2020, 230, 115626.

https://doi.org/10.1016/j.carbpol.2019.115626.

(91)   Oliviero, M.; Verdolotti, L.; Di Maio, E.; Aurilia, M.; Iannace, S. Effect of

Supramolecular Structures on Thermoplastic Zein–Lignin Bionanocomposites. J. Agric.

Food Chem. 2011, 59 (18), 10062–10070. https://doi.org/10.1021/jf201728p.

(92)   Salzano de Luna, M.; Filippone, G. Effects of Nanoparticles on the Morphology of

Immiscible Polymer Blends – Challenges and Opportunities. Eur. Polym. J. 2016, 79,

198–218. https://doi.org/10.1016/j.eurpolymj.2016.02.023.

(93)   Qiao, Y.; Wang, B.; Ji, Y.; Xu, F.; Zong, P.; Zhang, J.; Tian, Y. Thermal Decomposition

of Castor Oil, Corn Starch, Soy Protein, Lignin, Xylan, and Cellulose during Fast

Pyrolysis. Bioresour. Technol. 2019, 278, 287–295.

https://doi.org/10.1016/j.biortech.2019.01.102.

(94)   Liu, X.; Yu, L.; Xie, F.; Li, M.; Chen, L.; Li, X. Kinetics and Mechanism of Thermal

Decomposition of Cornstarches with Different Amylose/Amylopectin Ratios. Starch ‐

Stärke 2010, 62 (3-4), 139–146. https://doi.org/10.1002/star.200900202.

(95)   Aggarwal, P.; Dollimore, D. A Thermal Analysis Investigation of Partially Hydrolyzed

Starch. Thermochim. Acta 1998, 319 (1–2), 17–25. https://doi.org/10.1016/S0040-

6031(98)00355-4.

(96)   Verdolotti, L.; Oliviero, M.; Lavorgna, M.; Iannace, S.; Camino, G.; Vollaro, P.; Frache,

A. On Revealing the Effect of Alkaline Lignin and Ammonium Polyphosphate Additives

on Fire Retardant Properties of Sustainable Zein-Based Composites. Polym. Degrad.

Stab. 2016, 134, 115–125. https://doi.org/10.1016/j.polymdegradstab.2016.10.001.

(97)   Sessa, D. J.; Selling, G. W.; Biswas, A. Reaction of Zein with Methylenediphenyl

Diisocyanate in the Melt State: Thermal, Mechanical, and Physical Properties. Ind. Eng.

Chem. Res. 2012, 51 (27), 9199–9203. https://doi.org/10.1021/ie201501s.

(98)   Neo, Y. P.; Ray, S.; Jin, J.; Gizdavic-Nikolaidis, M.; Nieuwoudt, M. K.; Liu, D.; Quek, S.

Y. Encapsulation of Food Grade Antioxidant in Natural Biopolymer by Electrospinning

Technique: A Physicochemical Study Based on Zein–Gallic Acid System. Food Chem. 2013, 136 (2), 1013–1021. https://doi.org/10.1016/j.foodchem.2012.09.010.

(99)　Oh, M.; Ma, Q.; Simsek, S.; Bajwa, D.; Jiang, L. Comparative Study of Zein-and Gluten-Based Wood Adhesives Containing Cellulose Nanofibers and Crosslinking Agent for Improved Bond Strength. Int. J. Adhes. Adhes. 2019, 92, 44–57. https://doi.org/10.1016/j.ijadhadh.2019.04.004.

(100)　Faris, A. H.; Ibrahim, M. N. M.; Rahim, A.; Hussin, M. H.; Brosse, N. Preparation and Characterization of Lignin Polyols from the Residues of Oil Palm Empty Fruit Bunch. BioResources 2015, 10 (4), 7339–7352. https://bioresources.cnr.ncsu.edu/resources/preparation-and-characterization-of-lignin-polyols-from-the-residues-of-oil-palm-empty-fruit-bunch/.

(101)　Alriols, M. G.; Tejado, A.; Blanco, M. al; Mondragon, I.; Labidi, J. Agricultural Palm Oil Tree Residues as Raw Material for Cellulose, Lignin and Hemicelluloses Production by Ethylene Glycol Pulping Process. Chem. Eng. J. 2009, 148 (1), 106–114. https://doi.org/10.1016/j.cej.2008.08.008.

(102)　El Mansouri, N.-E.; Yuan, Q.; Huang, F. Study of Chemical Modification of Alkaline Lignin by the Glyoxalation Reaction. BioResources 2011, 6 (4), 4523–4536. https://www.semanticscholar.org/paper/Study-of-chemical-modification-of-alkaline-lignin-Mansouri-Yuan/1f77ca5c0a430efe2e09d0b6d16023c5b0f05450.

(103)　Sarwono, A.; Man, Z.; Bustam, M. A.; Subbarao, D.; Idris, A.; Muhammad, N.; Khan, A. S.; Ullah, Z. Swelling Mechanism of Urea Cross-Linked Starch–Lignin Films in Water. Environ. Technol. 2018, 39 (12), 1522–1532. https://doi.org/10.1080/09593330.2017.1332108.

(104)   Li, J.; Li, B.; Zhang, X. Comparative Studies of Thermal Degradation between Larch

Lignin and Manchurian Ash Lignin. Polym. Degrad. Stab. 2002, 78 (2), 279–285.

https://doi.org/10.1016/S0141-3910(02)00172-6.

(105)   Yang, H.; Yan, R.; Chen, H.; Lee, D. H.; Zheng, C. Characteristics of Hemicellulose,

Cellulose and Lignin Pyrolysis. Fuel 2007, 86 (12–13), 1781–1788.

https://doi.org/10.1016/j.fuel.2006.12.013.

(106)   Ning, W.; Jiugao, Y.; Xiaofei, M.; Ying, W. The Influence of Citric Acid on the

Properties of Thermoplastic Starch/Linear Low-Density Polyethylene Blends. Carbohydr.

Polym. 2007, 67 (3), 446–453. https://doi.org/10.1016/j.carbpol.2006.06.014.

(107)   Jiugao, Y.; Ning, W.; Xiaofei, M. The Effects of Citric Acid on the Properties of

Thermoplastic Starch Plasticized by Glycerol. Starch - Stärke 2005, 57 (10), 494–504.

https://doi.org/10.1002/star.200500423.

(108)   van Soest, J. J. G.; Vliegenthart, J. F. G. Crystallinity in Starch Plastics: Consequences

for Material Properties. Trends Biotechnol. 1997, 15 (6), 208–213.

https://doi.org/10.1016/S0167-7799(97)01021-4.

(109)   Wang, N.; Yu, J.; Chang, P. R.; Ma, X. Influence of Citric Acid on the Properties of

Glycerol-Plasticized Dry Starch (DTPS) and DTPS/Poly(Lactic Acid) Blends. Starch -

Stärke 2007, 59 (9), 409–417. https://doi.org/10.1002/star.200700617.

(110)   Cheng, G.; Zhou, M.; Wei, Y.-J.; Cheng, F.; Zhu, P.-X. Comparison of Mechanical

Reinforcement Effects of Cellulose Nanocrystal, Cellulose Nanofiber, and

Microfibrillated Cellulose in Starch Composites. Polym. Compos. 2019, 40 (S1), E365–

E372. https://doi.org/10.1002/pc.24685.

(111) Shi, R.; Zhang, Z.; Liu, Q.; Han, Y.; Zhang, L.; Chen, D.; Tian, W. Characterization of Citric Acid/Glycerol Co-Plasticized Thermoplastic Starch Prepared by Melt Blending. Carbohydr. Polym. 2007, 69 (4), 748–755. https://doi.org/10.1016/j.carbpol.2007.02.010.

(112) Capron, I.; Robert, P.; Colonna, P.; Brogly, M.; Planchot, V. Starch in Rubbery and Glassy States by FTIR Spectroscopy. Carbohydr. Polym. 2007, 68 (2), 249–259. https://doi.org/10.1016/j.carbpol.2006.12.015.

(113) van Soest, J. J. G.; Tournois, H.; de Wit, D.; Vliegenthart, J. F. G. Short-Range Structure in (Partially) Crystalline Potato Starch Determined with Attenuated Total Reflectance Fourier-Transform IR Spectroscopy. Carbohydr. Res. 1995, 279, 201–214. https://doi.org/10.1016/0008-6215(95)00270-7.

(114) Pavoni, J. M. F.; Luchese, C. L.; Tessaro, I. C. Impact of Acid Type for Chitosan Dissolution on the Characteristics and Biodegradability of Cornstarch/Chitosan Based Films. Int. J. Biol. Macromol. 2019, 138, 693–703. https://doi.org/10.1016/j.ijbiomac.2019.07.089.

(115) Kiadehi, A. D.; Jahanshahi, M.; Rahimpour, A.; Ghoreyshi, S. A. A. The Effect of Functionalized Carbon Nano-Fiber (CNF) on Gas Separation Performance of Polysulfone (PSf) Membranes. Chem. Eng. Process. Process Intensif. 2015, 90, 41–48. https://doi.org/10.1016/j.cep.2015.02.005.

(116) Dai, L.; Zhang, J.; Cheng, F. Effects of Starches from Different Botanical Sources and Modification Methods on Physicochemical Properties of Starch-Based Edible Films. Int. J. Biol. Macromol. 2019, 132, 897–905. https://doi.org/10.1016/j.ijbiomac.2019.03.197.

(117) Deng, L.; Li, Y.; Feng, F.; Zhang, H. Study on Wettability, Mechanical Property and Biocompatibility of Electrospun Gelatin/Zein Nanofibers Cross-Linked by Glucose. Food Hydrocoll. 2019, 87, 1–10. https://doi.org/10.1016/j.foodhyd.2018.07.042.

(118) Šimkovic, I.; Jakab, E. Thermogravimetry/Mass Spectrometry Study of Weakly Basic Starch-Based Ion Exchanger. Carbohydr. Polym. 2001, 45 (1), 53–59. https://doi.org/10.1016/S0144-8617(00)00230-7.

(119) Thermal degradation and stability of starch under different processing conditions - Liu - 2013 - Starch - Stärke - Wiley Online Library https://onlinelibrary.wiley.com/doi/10.1002/star.201200198 (accessed 2021 -06 -23).

(120) Aggarwal, P.; Dollimore, D. A Thermal Analysis Investigation of Partially Hydrolyzed Starch. Thermochim. Acta 1998, 319 (1), 17–25. https://doi.org/10.1016/S0040-6031(98)00355-4.

(121) Oh, M.; Ma, Q.; Simsek, S.; Bajwa, D.; Jiang, L. Comparative Study of Zein- and Gluten-Based Wood Adhesives Containing Cellulose Nanofibers and Crosslinking Agent for Improved Bond Strength. Int. J. Adhes. Adhes. 2019, 92, 44–57. https://doi.org/10.1016/j.ijadhadh.2019.04.004.

(122) Verdolotti, L.; Oliviero, M.; Lavorgna, M.; Iannace, S.; Camino, G.; Vollaro, P.; Frache, A. On Revealing the Effect of Alkaline Lignin and Ammonium Polyphosphate Additives on Fire Retardant Properties of Sustainable Zein-Based Composites. Polym. Degrad. Stab. 2016, 134, 115–125. https://doi.org/10.1016/j.polymdegradstab.2016.10.001.

(123) Mariotti, C.; Ramos-Rivera, L.; Conti, B.; Boccaccini, A. Zein-Based Electrospun Fibers Containing Bioactive Glass with Antibacterial Capabilities. Macromol. Biosci. 2020, 20. https://doi.org/10.1002/mabi.202000059.

(124) Ojogbo, E.; Blanchard, R.; Mekonnen, T. Hydrophobic and Melt Processable Starch-

Laurate Esters: Synthesis, Structure–Property Correlations. J. Polym. Sci. Part Polym.

Chem. 2018, 56 (23), 2611–2622. https://doi.org/10.1002/pola.29237.

APPENDIX

Table A1. Properties of zein purchased from Sigma (W555025).

Test	Specification
Appearance (Color)	Yellow to Gold
Appearance (Form)	Powder
Solubility	Insoluble in water
Melting point/freezing point	266 - 283 °C (511 - 541 °F)
Incompatible materials	Oxidizing agents
Nitrogen	14.04 - 15.36 %
Residue on ignition (Ash)	< 2.0 %
Protein Concentration	88 - 96 %
Loss on Drying	< 8.0 %
Salmonella (Negative)	Pass
E. Coli (Negative)	Pass
Size (20 Mesh - 100%)	Pass
Arsenic (As)	< 3 ppm
Cadmium (Cd)	< 1 ppm
Mercury (Hg)	< 1 ppm
Lead (Pb)	< 2 ppm

Table A2. Properties of zein purchased from FloZein Products (F4400C- FOOD GRADE).

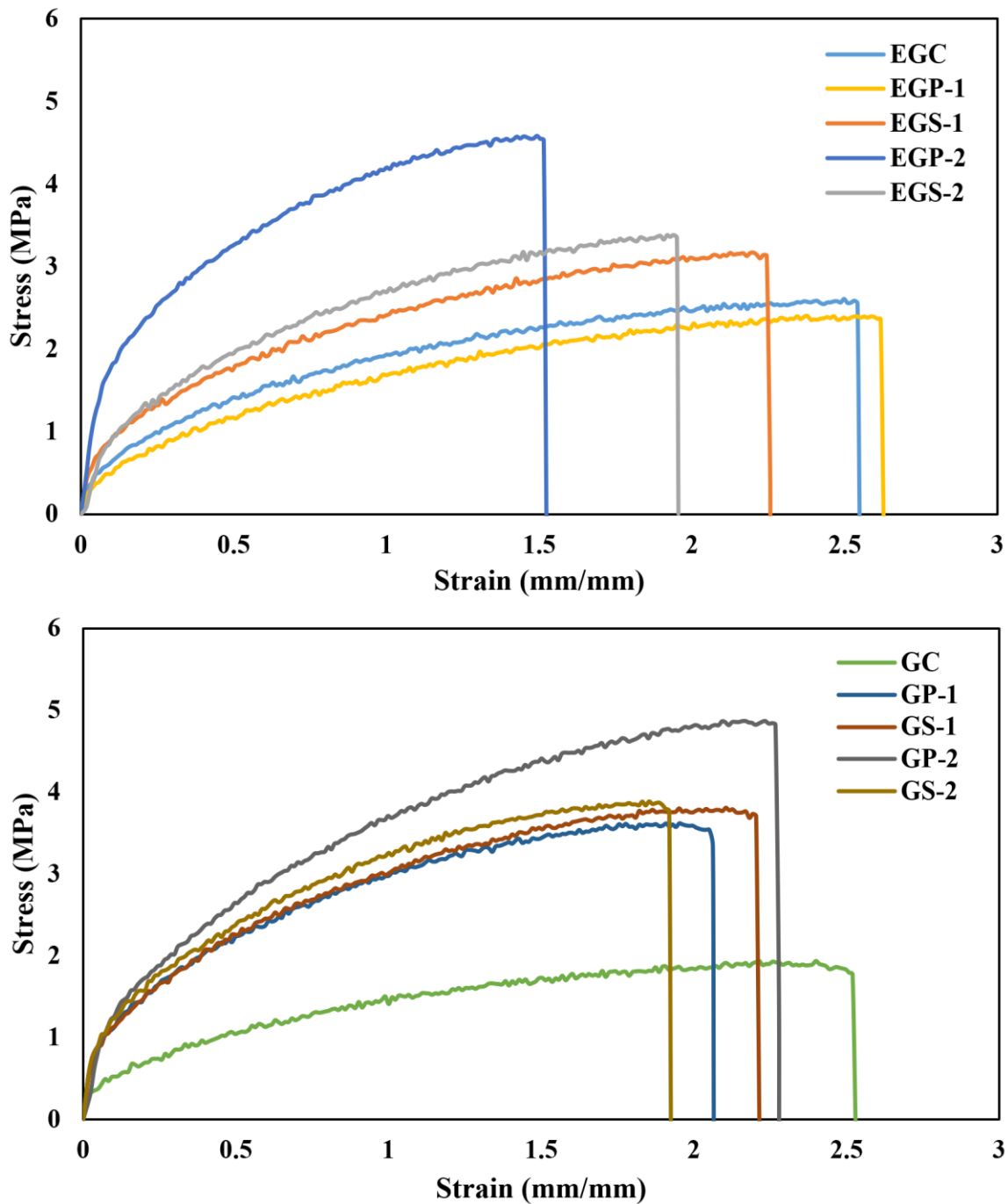| Test	Specification
Appearance (Color)	Straw to yellow
Appearance (Form)	Granular powder
Solubility	Insoluble in water
Melting point/freezing point	266 - 283 °C (511 - 541 °F)
Flash point	4˚C (57˚F), closed cup
Incompatible materials	Oxidizing agents
pH	4-7
Residue on Ignition	< 2.0 %
Loss on Drying	6.20%
Protein	87.06% calculated on dry basis

Figure A1.   Representative stress-strain curves of the corn-based thermoplastics using a) ethylene glycol and b) glycerol as the plasticizer.
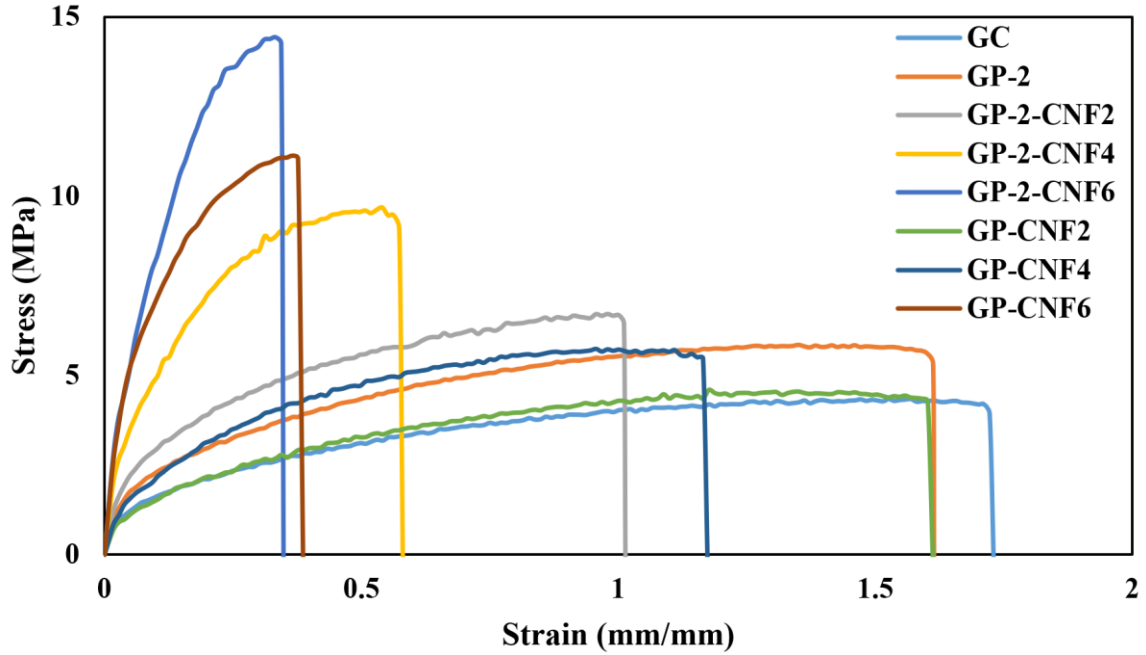Note: Samples were produced by internal mixing for 10 min.

Figure A2. Representative stress-strain curves of the composites using glycerol as the plasticizer.
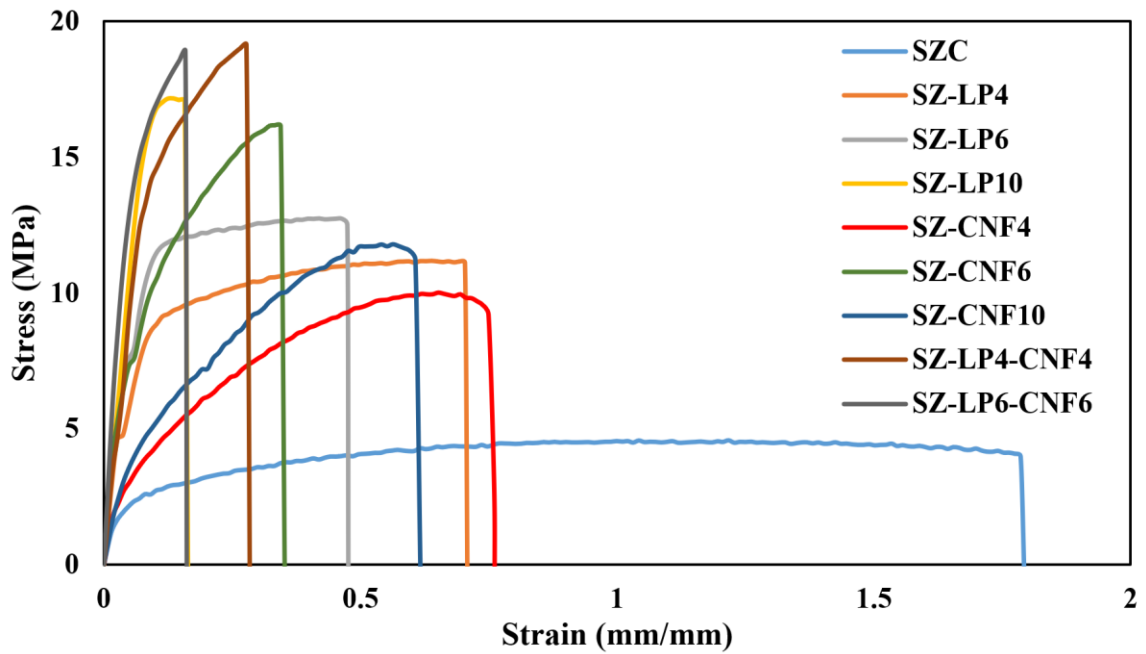Note: Samples were produced by internal mixing for 15 min.

Figure A3. Representative stress-strain curves of the corn-based thermoplastics based on starch/zein mixture.
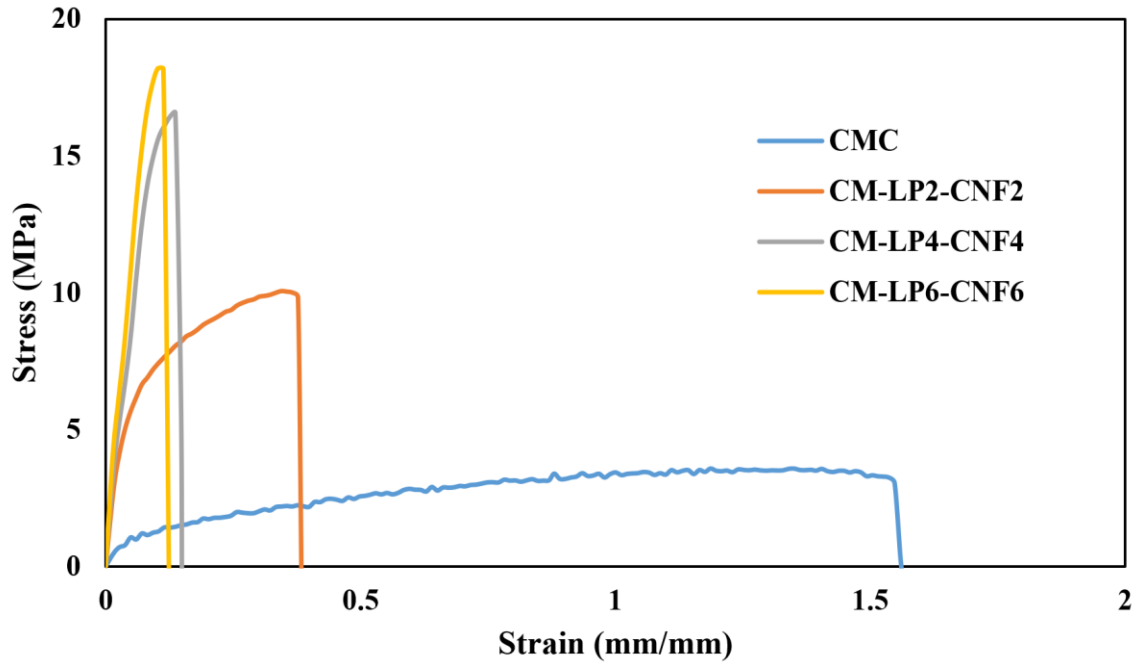
Figure A4. Representative stress-strain curves of the corn-based thermoplastics based on cornmeal.